Hillslope Evolution by Diffusive Processes: The Problem of Equilibrium and the Effects of Climatic and Tectonic Changes

by

Nelson Ferreira Fernandes

B.S. (Universidade Federal do Rio de Janeiro) 1984
M.S. (Universidade Federal do Rio de Janeiro) 1990

A dissertation submitted in partial satisfaction of the
requirements for the degree of
Doctor of Philosophy
in
Geology
in the
GRADUATE DIVISION
of the
UNIVERSITY OF CALIFORNIA at BERKELEY

Committee in charge:

Professor William E. Dietrich, Chair
Professor David L. Jones
Professor James K. Mitchell

1994

The dissertation of Nelson Ferreira Fernandes is aproved:

University of California at Berkeley

1994

Hillslope Evolution by Diffusive Processess: The Problem of Equilibrium and the Effects of Climatic and Tectonic Changes

ABSTRACT

by

Nelson Ferreira Fernandes

The convex hilltops of soil-mantled landscapes have been attributed to the action of diffusive (slope-dependent) processes like creep, rainsplash, and biogenic activity. Although many models based on the diffusion equation have been proposed, little is known about the effects of climatic and tectonic oscillations on the convex form. Such oscillations are expected to impose changes on the transport rates and/or the incision rates at the base of the hillslopes. I specifically focus on how equilibrium convex hillslope profiles respond, both in terms of form and sediment flux, to one-step and cyclic oscillations in the diffusion coefficient or incision rate.

Numerical and analytical solutions of the one-dimensional diffusion-type equation are obtained for initially convex hillslopes evolving under diffusion coefficient and incision rate values derived from field measurements. One-step changes, either in the diffusion coefficient or in the downcutting rate, are then imposed and the time required for the new equilibrium condition to be attained (relaxation time) is estimated. By characterizing the time-scale of morphological adjustments of these convex hillslopes, and consequently their relaxation times, we can determine whether the hilltop convexities that we observe in the field today represent equilibrium or relict forms. In addition, the effects of climatic and tectonic oscillations on diffusive hillslopes are modeled by imposing cyclic changes, in either the diffusion coefficient or in the incision rate, in the form of steps, sine waves, and ^{18}O-constrained oscillations.

Two-fold step changes in the diffusion coefficient or in the downcutting rate result in relaxation times of approximately 70 thousand years and one million years,

for 25 m and 100 m long hillslopes, respectively. The time-scale of such morphological adjustments varies depending on whether the hillslope profile is tending to increase or decrease its curvature through time. The new equilibrium condition is first developed at the base of the hillslope and then propagates upslope. A dimensionless graph is presented which allows the estimation of the relaxation time of convex hillslopes from estimates of diffusion coefficient, incision rate, magnitude of change, and hillslope length. Such a graph could be used in field studies. Step and sine oscillations in the diffusion coefficient cause the sediment flux from the hillslope to eventually oscillate around the initial equilibrium value, which is set by the downcutting rate. When these oscillations happen in the downcutting rate, the sediment flux oscillates around a new equilibrium value located mid-way between the lower and upper equilibrium values, associated with the minimum and maximum imposed downcutting rates, respectively. The sediment flux is shown to be in phase with ^{18}O-based oscillations in the diffusion coefficient while cumulative effects are observed when these oscillations take place in the incision rate.

Because the relaxation times estimated here are much longer than the frequency of the climatic oscillations observed in the last few million years, I argue that most of the convex hilltops of soil-mantled landscapes are likely to represent forms that are far from being truly time-independent morphologies. The results also suggest that these convex hilltops represent forms that, once formed, are difficult to be perturbed with modest, but reasonable, variations in the diffusion coefficient or in the incision rate. Consequently, these convex hilltops may represent, at least for the case of long hillslopes, forms that developed before the climatic and tectonic oscillations that took place during the Quaternary.

Hillslope Evolution by Diffusive Processes: The Problem of Equilibrium and the Effects of Climatic and Tectonic Changes

by

Nelson Ferreira Fernandes

Table of Contents

List of Figures

Chapter 1.

Chapter 2.

List of Tables

Chapter 1.

Acknowledgments

I would like to thanks Bill Dietrich for all his encouragement, guidance and many hours of discussion during the last four years. I really enjoyed and appreciated your friendship. I also would like to thanks David Jones and James Mitchell for their many suggestions and insightful discussions.

I am extremely grateful to Conselho Nacional de Desenvolvimento Científico e Tecnológico (CNPq) and to Federal University of Rio de Janeiro for their financial support during this period.

Thanks to Rob Reiss, Roland Gritto and Juan Somoano for helping me with my programming, and to Peter Alexander, Yuri Burlakov and Paulo Ney de Souza for helping me with the analytical solutions. I also thanks Jim Kirchner for our discussions on dimensional analysis. The conversations with Michele Seidl, Fred Booker, Jim McKean, David Montgomery, Tom Hanks, Keith Loague, Ana Coelho Netto, Suzanne Anderson and Ray Torres are very much appreciated. I would like to thanks, in special, Michele Seidl for all his encouragement and for the great time that we had together as graduate students.

My special thanks to my wife Lenise. You gave up of so many important things in your life to be by my side during the good and bad moments of this journey. I hope that I will be able to justify all this effort. I love you.

Finally, thanks Thales for everything you are and for bringing a special meaning to our lives. You continue to have a lovely smile.

INTRODUCTION

This dissertation consists of two chapters and four appendices dealing with the question of how convex hillslope profiles evolve under the action of diffusive processes, like creep, rainsplash and biogenic activity, and under a specified incision rate at the base of the profile. In Chapter 1, numerical experiments are carried out in order to quantify the time-scale of morphological adjustments of these convex profiles in response to step-changes in the diffusion coefficient or in the baselevel downcutting rate. The relaxation time of these hillslopes for a variety of imposed changes is estimated and the possibility that, under field conditions, an equilibrium condition be attained is discussed.

In Chapter 2, the effects of climatic and tectonic-induced oscillations on convex hillslope profiles evolving by diffusive processes are investigated. A variety of step, sine and ^{18}O-based oscillations in the diffusion coefficient or in the downcutting rate are imposed to equilibrium diffusive hillslope profiles. The effects of these external oscillations on the morphology of the profiles and on the flux of sediments from the hillslopes to the channels are analyzed. The sensitivity of the convex hilltops of soil mantled landscapes to Quaternary oscillations in climate and tectonics is discussed.

Chapter 1

HILLSLOPE EVOLUTION BY DIFFUSIVE PROCESSES: THE TIME SCALE FOR EQUILIBRIUM ADJUSTMENTS

ABSTRACT

Diffusive processes such as creep, rainsplash and biogenic transport, especially in areas where overland flow is unimportant, play a major role in controlling the development of convex hilltops on soil-mantled landscapes. Although many diffusion-based models have been proposed, little attention has been given to the effects of changing transport rates and boundary conditions. In this paper we specifically focus on the time-scale of morphological adjustments of convex hilltops in response to one-step changes in the diffusion coefficient or in the incision rate at the base of the hillslope. If we assume that climatic and/or tectonic shifts will impose corresponding systematic changes in these two parameters, which will consequently lead to adjustments in the hillslope form towards a new equilibrium condition, then the estimation of such relaxation times may allow us to define whether the hilltop convexities that we observe in the field today represent equilibrium or relict forms.

We use numerical and analytical solutions of the one-dimensional diffusion equation to explore whether hilltop convexities can be in equilibrium with contemporary climate and local channel incision rates. An initial equilibrium profile is formed using a diffusive sediment transport and specified lowering rate at the base of the hillslope. A step change in either the diffusion coefficient or in the lowering rate is then imposed and the time for the hillslope to reach equilibrium with the new condition (relaxation time) is determined. Importantly, values of hillslope length, diffusion coefficient and lowering rate are all based on field observations. Two-fold changes in the diffusion coefficient or in

the baselevel downcutting rate result in relaxation times around 70 thousand years and one million years for 25 m and 100 m long hillslopes, respectively.

The new equilibrium condition is first developed at the base of the profile and it then propagates upslope. The time-scale of such morphological adjustments varies substantially depending on whether the hillslope is tending to increase or decrease its convexity from its initial value through time. A dimensionless graph, which may be useful in field studies, is developed which can be used to estimate the relaxation time for any combination of diffusion coefficient, lowering rate and hillslope length. By comparing the relaxation times estimated here with the frequency of the climatic oscillations observed in the last few million years we argue that most of the convex hilltops observed in the field today are likely to represent forms that are far from being truly time-independent morphologies.

INTRODUCTION

Most hilltops in soil mantled landscapes are convex. This form has been attributed to the work of processes such as soil creep, rainsplash and discontinuous surface runoff (see review in Carson and Kirkby, 1972; Summerfield, 1991; Selby, 1993). Mathematical models of hillslope evolution show that the convexity depends on both the hillslope transport process and the rate of incision at the base of the hillslope (e.g., Armstrong, 1980, 1987; Ahnert, 1987a, 1988). Applications of these models to the field raise, however, a number of questions related to the generation and maintenance of hilltop convexities. A

major issue is whether these convex hillslopes actually represent equilibrium forms and if not, whether we can define how far from equilibrium they are. Are the hilltop curvatures observed in the field today associated with specific climatic conditions or do they reflect the integral of the climatic changes and uneven rates of river incision over the last hundreds of thousands or even millions of years? If equilibrium is obtained, does it first occur at the base of the hillslope and propagate towards the divide or does it propagate downslope?

For modeling purposes, hillslope evolution can be thought of as controlled by the competing processes of advective (Lowenherz, 1991) and diffusive transport. Advective transport (sediment movement by water driven processes) tends to be unstable and forms channels and valleys, while diffusive transport (sediment movement due to surface gradient) tends to fill in valleys and is argued to predominate on hillslopes (e.g., Kirkby, 1971; Smith and Bretherton, 1972; Ahnert, 1976; Armstrong, 1976; Loewenherz, 1991; Willgoose et al., 1991; Howard, *in press*).

Since the original theoretical investigations carried out by Culling (1960, 1963, 1965), modeling of landform evolution by a slope-dependent sediment transport law has been widely used at all scales of landscape analysis, from short hillslope profiles to entire mountain ranges. Culling recognized that a slope-dependent transport law, when combined with the conservation of mass equation for landscape erosion, leads to an equation analogous to Fick's Law of Diffusion, hence the reference to this process as diffusion. Subsequently, Kirkby (1971) demonstrated that for certain boundary conditions (i.e., both the divide and the base level fixed horizontally) hillslope profiles develop towards a

"characteristic form" which depends only on the processes' type and rate, and not on the initial morphology. He showed that diffusive sediment transport processes, like creep and rainsplash, smooth the landscape and that a convex hillslope profile would be the characteristic form resulting from their action. Such results supported the qualitative ideas raised much earlier by Davis (1892) and Gilbert (1909), who associated convex hilltops with the geomorphic work of soil creep.

Although the concept argued by Kirkby (1971) and Smith and Bretherton (1972), that specific transport laws generate characteristic forms is useful, inheritance of initial conditions, unsteadiness in boundary conditions and sediment transport processes may lead to misleading interpretations. It has been argued that in these hillslope models the imposed boundary conditions are as important as the operating processes in controlling the resulting hillslope profile (e.g., Armstrong, 1987; Parsons, 1987). Armstrong (1987), for example, showed that even slopes eroding according to one transport law can develop convex, concave or convexo-concave forms depending on the imposed boundary conditions. Furthermore, Dunne (1991) argued that convex hillslope profiles can be generated by sheetwash, a non-diffusive process, when rainstorms are short relative to the time of concentration of runoff.

It is well demonstrated theoretically that certain hillslope profiles when evolving long enough under a constant process and a constant downcutting rate at the base of the slope tend towards an equilibrium form (e.g., Hirano, 1975; Armstrong, 1980,1987; Ahnert, 1987a, 1988). After this stage is achieved, hillslope morphology will be kept approximately constant through time (time-

independent morphology) and such condition will be sustained as long as the downcutting rate and the erosional processes are kept constant. This general notion of equilibrium was implicit in Gilbert's classical laws (1877, p. 115-124) and, specifically for hillslopes, in his law of the slope (Gilbert, 1909, p. 345). Hack (1960, 1975) explicitly elaborated these ideas stating that an equilibrium condition, in which all the elements of the topography are downwasting at the same time, will eventually be attained by landscapes evolving under constant uplift rates and under constant climatic-driven geomorphic processes. Although field evidence supporting the existence of such equilibrium condition is rare, some examples have recently become available in the literature (e.g., Pavich, 1989; Reneau and Dietrich, 1991; Monaghan et al.,1992). Many authors argued, however, that the development of equilibrium landforms is not the norm and that landforms must be considered as palimpsests of forms shaped during different climatic conditions (e.g., Thornbury, 1969; Arnett, 1971; Twidale, 1976; Bloom, 1978; Budel, 1980). Other arguments against the development of such equilibrium morphologies are based on the nonlinear behavior of some geomorphic systems (see review in Phillips and Renwick, 1992).

Under natural field conditions, however, even when it is assumed that the internal and external forces remained approximately constant for a certain period of time, it is also fundamental to take into consideration the relaxation time of the hillslope system, i. e., the time required for a new equilibrium condition to be attained after a perturbation in the system (e.g., Howard, 1965, 1988; Chorley and Kennedy, 1971; Allen, 1974; Thornes and Brunsden, 1977; Brunsden and Thornes, 1979; Brunsden, 1980; Ahnert, 1987a, 1988; Hardisty, 1987). Such time-independent morphology can only be attained when the input parameters to the

hillslope system described above remain approximately constant for a period longer than the hillslope's relaxation time. The recognition of the importance of the system's relaxation time to characterize the dynamic equilibrium stage brings another complicating factor to mathematical models of hillslope evolution, i. e., the necessity to consider evolution in terms of a real temporal scale. However, with the exception of Ahnert (1987a, 1987b, 1988), none of the models discussed above characterized the evolution of hillslope profiles in terms of actual time scales.

The main objective of this paper is to define the relaxation time of equilibrium convex hillslopes to perturbations in the diffusion coefficient or in the lowering rate at its lower boundary. A major issue to be investigated here is the variation of relaxation time with the magnitude and direction of the changes in the diffusion coefficient or in the baselevel downcutting rate. While some authors suggested that the relaxation time might depend on the direction of the change (e.g., Chorley and Kennedy, 1971; Allen, 1974; Renwick, 1985) others argued, at least for the case of changes in the diffusion coefficient, that the relaxation time is not a function of such polarity (e.g., Koons, 1989).

We will examine the relaxation time for one-step changes in the diffusion coefficient and baselevel downcutting rate using a one-dimensional numerical model. In order to make our results relevant to real landscapes we use hillslope lengths, diffusion coefficients and lowering rates based on field data. Furthermore, to make our findings useful in field work, we have developed a dimensionless graph which can be used to determine relaxation times based on estimates of changes in the diffusion coefficient and baselevel lowering rates. We

first review diffusive hillslope evolution theory, then describe our method of numerical modeling and then present the obtained results. The time-scale of morphological adjustments will be used to estimate the relaxation time of convex hillslopes in response to changes in the external parameters.

HILLSLOPE EVOLUTION BY DIFFUSIVE PROCESSES

Although some of the assumptions behind the idea of hillslope evolution by diffusive transport processes were implicitly stated by Gilbert (1877, 1909) and Davis (1892), it was only after the work of Culling (1960) that the underlying mathematical relationships were fully described. Shortly after, analytical solutions for a number of boundary and initial conditions describing simple geomorphological situations became available (Culling,1963,1965; Hirano, 1968).

The diffusion theory when applied to the evolution of hillslope profiles under transport-limited conditions (Gilbert, 1877; Culling, 1963; Kirkby, 1971) assumes a slope-dependent transport law in the form of (1) which states that soil flux (q_S), in terms of mass per unit width of slope [M/LT], is directly proportional to hillslope gradient

$$q_S = K\left(-\frac{\partial z}{\partial x}\right) \tag{1}$$

where z is elevation, x is distance from the divide, and K is a constant of proportionality.

A transport law with a slope dependence in the form expressed by (1) has been widely accepted, both explicitly and implicitly, as accounting for transport processes like creep (e.g., Davison, 1888; Culling, 1963; Schumm, 1967; Kirkby, 1967, 1971, 1985; Gossmann, 1976; Armstrong, 1976, 1980, 1987; Ahnert, 1976, 1987a; Nash, 1980a, 1980b; Band, 1985), rainsplash (e.g., De Ploey and Savat, 1968?; Kirkby, 1971; Dunne, 1980, 1991; Band, 1985), biogenic activity (e.g., Dietrich et al., 1987) and frost heave (e.g., Schumm, 1967). However, field evidence supporting a transport law in the form above is still rare. More recently, field measurements of the concentrations of cosmogenic ^{10}Be along vertical profiles in soil-mantled hillslopes (McKean et al., 1993) provided empirical evidence for such a linear slope dependent transport law for soil creep.

Combining (1) with the continuity equation

$$-\frac{\partial z}{\partial t} = \frac{1}{\rho_b}\frac{\partial q_s}{\partial x}, \tag{2}$$

where ρ_b is the mass density of the soil and t is time, yields

$$-\frac{\partial z}{\partial t} = \frac{1}{\rho_b}\frac{\partial}{\partial x}\left(-K\frac{\partial z}{\partial x}\right). \tag{3}$$

If we assume K to be constant along the hillslope profile we end up with a 1-D homogeneous diffusion-type equation

(4) $$\frac{\partial z}{\partial t} = D\frac{\partial^2 z}{\partial x^2}$$

where D, in fact a diffusion coefficient with units of $[L^2/T]$, is set equal to $K/\rho b$. In words, it states that the change in elevation with time is proportional to the hillslope curvature. Although assuming K as constant along the profile seems to be reasonable for short hillslope (e.g., 20-100 m long) with an "homogeneous" soil mantle, its usage on longer hillslopes with significant variations in bedrock geology, soil properties and vegetative cover along the profile may not be appropriate.

At steady-state, the change in elevation with time $(\partial z/\partial t)$ is constant and can be assumed to be equal to the landscape lowering rate and to the baselevel downcutting rate at the bottom of the hillslope (B_d). Substituting (B_d) in the diffusion-type equation, yields

(5) $$B_d = D\left(\frac{\partial^2 z}{\partial x^2}\right), \text{ or}$$

(6) $$\frac{B_d}{D} = \left(\frac{\partial^2 z}{\partial x^2}\right) = \text{hillslope curvature.}$$

Integrating (6) once with respect to x, yields

(7) $$\frac{\partial z}{\partial x} = \frac{B_d}{D}x + c_1,$$

a linear relationship between hillslope gradient and distance from the divide. For flat divides (c_1=0), the slope of this line, B_d / D, equals the hillslope curvature developed at steady-state. Dietrich et al. (1987) noticed that where the long-term lowering rate of a hillslope can be estimated one can solve equation (7) for the diffusion coefficient. This approach was successfully used (Dietrich et. al., in prep.) to estimate diffusion coefficient values for a number of convex hillslopes in Marin County, near San Francisco-CA (Figure 1).

The diffusion-type equation has been widely used to model the evolution of many different geomorphological systems along a great variety of spatial and temporal scales. Applications included modeling the evolution of hillslope profiles (e.g., Culling, 1960, 1963, 1965; Hirano, 1968, 1975, 1976; Kirkby, 1971; Gossmann, 1976; Trofimov and Moskovkin, 1976, 1983, 1984; Armstrong, 1980, 1987), the evolution of mountain blocks (e.g., Koons, 1989; Anderson and Humphrey, 1989), the morphologic dating of fault scarps and wave-cut sediments (e.g., Nash, 1980a, 1980b, 1984; Colman and Watson, 1983; Mayer, 1984; Hanks et al., 1984; Hanks and Wallace, 1985; Andrews and Hanks, 1985; Hanks and Schwartz, 1987; Hanks and Andrews, 1989), the morphologic dating of late-glacial terrace scarps (e.g., Pierce and Colman, 1986), the evolution of glacial moraines (e.g., Anderson and Humphrey, 1989; Bursik, 1991), the stratigraphic development of nonmarine foreland basins (Jordan and Flemings, 1989); the evolution of longitudinal river profiles (e.g., Culling, 1960; Begin et al., 1981; Begin, 1988; Trofimov and Moskovkin, 1983), and the aggradation of valley bottoms (e.g., Wyrwoll, 1988).

In models like the one discussed here, the erosional constant (D) plays a major role in controlling the general evolution of the initial hillslope profile. Therefore, the assessment of reliable, field-related values for the diffusion coefficient is a major step towards a reasonable simulation of how hillslope profiles evolve, in space and in time, when submitted to diffusive-type processes. Field-oriented methods, based on a variety of techniques, have resulted in a number of estimates of the diffusion coefficient on the hillslope scale (Table I). Most of the available values come from estimates based on the morphologic dating of fault scarps and wave-cut sediments (e.g., Nash, 1980a, 1980b, 1984; Hanks et al., 1984; Rosenbloom and Anderson, *in press*).

METHODS

The evolution of hillslope profiles under diffusive processes was modeled here by solving (4), through both numerical and analytical methods, for a number of field-based initial and boundary conditions. A number of analytical solutions for conditions very similar to the ones simulated here have been presented by Culling (1960, 1963, 1965), Hirano (1968), Carson and Kirkby (1972) and Trofimov and Moskovkin (1983, 1984). They were based on analogies to the transference of heat by conduction (Carslaw and Jaeger, 1959) and on chemical diffusion (Crank, 1975). The analytical solution $z(x,t)$ for the situation described in Figure 1 takes the form of

$$z(x,t) = \sum_{n=0}^{\infty} \cos\left[\frac{\pi x}{L}\left(n+\frac{1}{2}\right)\right]\left[c_n e^{c\,t} + \left[\alpha_n\left(\frac{-1}{c}\right)\left[\beta\, t + \left(1-e^{c\,t}\right)\left(1+\frac{\beta}{c}\right)\right]\right]\right] - \tag{8}$$

$$- B_d\, t \cos\frac{\pi x}{L}$$

where

$$c_n = \frac{2}{L}\int_0^L f(x)\cos\frac{(2n+1)\pi x}{2L}\,dx\ , \tag{9}$$

$$\beta = D\left(\frac{\pi}{L}\right)^2, \tag{10}$$

$$\alpha_n = \frac{(-1)^{n+1}}{\pi} B_d \left[\frac{1}{n-\frac{1}{2}} + \frac{1}{n+\frac{3}{2}}\right], \text{ and} \tag{11}$$

$$c = -D\left[\frac{\pi}{L}\left(n+\frac{1}{2}\right)\right]^2. \tag{12}$$

The step-by-step development of this solution, including the definition of all the parameters above, is presented in Appendix 1.

Although the analytical solutions are helpful to the understanding of the general behavior of the system to be modeled, numerical solutions were used here in most of the simulations because of their greater flexibility in handling more complex field-oriented initial and boundary conditions. Details about the finite-differences scheme used to obtain the numerical solution and the program used to implement it are in Appendices 2 and 3, respectively.

We have concentrated our experiments on the one-dimensional evolution of hillslopes under transport-limited conditions (Gilbert, 1877; Culling, 1963; Kirkby, 1971), i.e., at any time there will be soil available to be transported by the erosional process (see Figure 2). As argued by many authors (e.g., Howard, 1988; Koons 1989) although the one-dimensional analysis is clearly not sufficient to model the evolution of large areas, such as, entire drainage basins, it can be very helpful in defining the relative importance of the physical parameters involved in the problem. The assumption of transport-limited conditions clearly limits the applicability of the obtained results to hillslopes developed on unconsolidated sediments, on deep weathering profiles, or on soil-mantled areas where the surface lowering rate and the bedrock lowering rate are approximately the same.

Diffusion coefficient values estimated by the methods previously described (see Table I) varied from 4×10^{-4} m^2/yr to about 400×10^{-4} m^2/yr. In trying to stay close to the values estimated in the field but also assuming that higher values can probably exist, we have used in the simulations diffusion coefficient values varying from 4 to 4000 ($\times 10^{-4}$ m^2/yr). The diffusion coefficient is maintained constant during the simulations.

Hack (1960) suggested that under constant geomorphic processes, a dynamic equilibrium morphology would develop in areas undergoing constant uplift rates. For modeling purposes we approximated such condition by imposing a constant rate of baselevel downcutting (B_d) at the bottom of the hillslope (boundary condition at the base of the hillslope). Although Figure 2 suggests that the lower boundary condition is a channel, this is not required.

Hilltop convexities are commonly bordered downslope by straight, landslide-dominated profiles. In our model the lower boundary condition is just an incision rate by what ever process occurs there. Landsliding, episodic upslope migration of knickpoints (e.g., Seidl and Dietrich, 1992) and periodic debris flows in channels will cause this incision to be unsteady at smaller time intervals, hence by holding the lower boundary condition constant (or by changing it an then holding it constant) we are modeling the time-averaged effect of these episodic erosional events.

Compilations obtained for a variety of climatic conditions, relief characteristics, and bedrock geology, suggest that denudation rates may vary between 10^{-6} m/yr and 10^{-3} m/yr (e.g., Saunders and Young, 1983; Milliman and Meade, 1983; Young and Saunders, 1986). More recently estimates based on the accumulation rate of colluvium inside hollows (Reneau, 1988; Reneau et al., 1989) and on bedrock-to-soil conversion rates obtained from the accumulation of cosmogenic isotopes in the soil (Pavich, 1989; Monagham et al., 1992) resulted in values also inside this range. Based on these values we imposed in our simulations baselevel downcutting rates (B_d) varying from -10^{-5} m/yr to -10^{-2} m/yr (the negative sign denotes incision) which represent one order of magnitude above both the minimum and maximum field-estimated values.

The simulations to be presented here used as initial condition convex hillslopes 25 m and 100 m long. These lengths were selected because we believe that models like the one used here are more appropriate to the study of hilltop convexities and short hillslopes. Longer hillslopes, when evolving towards an increase in final hillslope curvature, may develop gradients far above the limiting

stability angle (Carson, 1971) of the material and will require, as done by other authors (e.g., Anderson and Humphrey, 1989; Anderson, *in press*), the incorporation of a landslide term in the transport law described by (1). Hillslope lengths were kept constant during the entire simulation andfor most of the experiments we started with a constant hillslope curvature (B_d/D) of -0.025 m^{-1} which is a typical value for convex hilltops in Marin County, California (see Figure 1). Such initial morphology is assumed to be a reasonable approximation of certain hillslopes in the field that have already developed a constant curvature $\left[\left(\partial^2 z/\partial x^2\right) = \text{constant}\right]$ at some previous equilibrium condition, and are then experiencing a new climatic and/or tectonic regime. New external conditions are represented in the model by changes in D or B_d which will, if the model is allowed to run to equilibrium, lead to a new constant hillslope curvature value (B_d/D). The computed time to equilibrium then defines the relaxation time.

RESULTS

Evolution Towards Equilibrium

Figure 3 shows a 25 m long convex hillslope evolving under diffusive processes for 100 Ka (thousand of years). The initial profile has a constant curvature of 0.025 m^{-1} and it is assumed to represent some previous equilibrium morphology obtained, for example, under the combination of a baselevel downcutting rate of -10^{-4} m/yr (B_{d1}) and a diffusion coefficient of 40×10^{-4} m^2/yr. Figure 3A presents the morphological response (plotted for each 10 Ka interval) associated with a 2-fold increase in the baselevel downcutting rate.

Clearly, the hillslope profiles evolve towards an equilibrium condition which is shown here by the development of a time-independent morphology by around 90 Ka. For each simulation like this one we computed the spatial and temporal variations in slope (Figure 3B), curvature (Figure 3C) and erosion rate (Figure 3D). By integrating with respect to distance each one of the time lines in Figure 3D we obtained a plot of the variation of the sediment flux (Q_t), for the entire hillslope, with time (Figure 3E).

As expected from the theoretical analysis presented before (see Equation 7), the hillslopes in this experiment become steeper with time, driven by a greater absolute ratio B_d/D, in other words, by a greater imposed final hillslope curvature. Consequently, both hillslope curvature and erosion rate increase with time towards constant values along the entire profile. The total sediment flux increases asymptotically to its new equilibrium value (Q_{tss}), such that

(13) $$Q_{tss} = - B_d \times L$$

where Q_{tss} is in m^2/yr, B_d is in m/yr and L, the hillslope length, is in meters.

This brings our discussion to the question of how we defined equilibrium in our experiments. We followed a criterion similar to the one used by Ahnert (1987a, 1987b, 1988) which was to assume that the temporal variation in the erosion rate is a good approximation of the degree of approach to equilibrium. Because of the asymptotic behavior of Q_t we have approximated the equilibrium condition by the moment in which the total sediment flux (Q_t) attains 90% of its value at the steady state condition (Q_{tss}), which is defined by (8). For the

conditions simulated in Figure 3, 90% of the sediment flux at steady state was obtained at 90 Ka (Figure 3E). This amount of time can be thought of as an estimate of the relaxation time (R_t) of the hillslope system in response, in this case, to a 2-fold increment in the absolute baselevel downcutting rate (B_d).

Figure 4 shows a similar experiment where, instead, we imposed a 2-fold increase in the diffusion coefficient on an equilibrium hillslope. In this case, the response was a general tendency to flatten the profiles (Figures 4A and 4B), driven by a smaller final hillslope curvature. As expected, both hillslope curvature and erosion rate (Figures 4C and 4D) decrease with time towards new equilibrium values which are approximately constant along the entire hillslope. The total sediment flux (Figure 4E) decreased asymptotically with time towards steady state and 90% of its value was obtained after 70 Ka, defining the relaxation time of the hillslope system associated with a 2-fold increment in the diffusion coefficient.

The Relaxation Time of Hillslope Profiles

In order to estimate the relaxation time of diffusional hillslopes over a wide range of diffusion coefficients and baselevel downcutting rates, we set up a series of numerical experiments in which we started with convex hillslopes already in equilibrium and we then introduced one-step changes (up or down) in D or B_d. Each change was maintained until the new equilibrium condition was attained. In these experiments there is no reaction time (Chorley and Kennedy, 1971; Allen, 1974), i. e., the hillslopes immediately start to respond to the imposed

changes of input. In this paper, the terms step-up and step-down changes in D or B_d will refer to the absolute values of this parameters.

Figure 5 shows the response of the total sediment flux (Q_t) associated with one-step up (Figure 5A) and with one-step down changes (Figure 5B) in the diffusion coefficient, while the baselevel downcutting rate was kept constant. For each one of these two situations we imposed 2-fold and 10-fold changes in D and the results were plotted until the moment when the new equilibrium condition was attained. Thus the end of each one of the Q_t lines in Figure 5 represents an estimate of the relaxation time of the hillslope profile associated with each one of the imposed changes. For step-up changes (Figure 5A), in which we increased the magnitude of the imposed change, from 2-fold to 10-fold, relaxation time decreased from about 70 Ka to 30 Ka. For step-down changes (Figure 5B), in which we increased the magnitude of the change, the associated relaxation time increased from 165 Ka to 1275 Ka, approximately.

The results associated with one-step changes in baselevel downcutting rate (Figure 6) showed that, for both step-up (Figure 6A) and step-down changes (Figure 6B), the relaxation time increased when we increased the magnitude of the change. As in the case of changes in D, the relaxation time was longer for step-down changes in B_d than for step-up changes. While changes in D resulted in a peak in the sediment flux immediately after the change, the response associated with changes in B_d was more subtle.

Figure 7 summarizes the results obtained for one-step increases (right side) and one-step decreases (left side) in the diffusion coefficient for 25 m and

100 m long hillslopes over a wide range of imposed changes. The initial condition was the same one used in the experiments presented in Figures 5 and 6, i.e., a convex hillslope developed at equilibrium by the combination of a baselevel downcutting rate of - 10^{-4} m/yr and a diffusion coefficient of 4×10^{-3} m^2/yr. These figures show that the longer the hillslope, the longer the relaxation time associated with any specific change. A 2-fold change in the diffusion coefficient gives relaxation times around 70 Ka for 25 m long hillslopes and around 1.0 Ma (million of years) for 100 m long hillslopes. For one-step increases greater than a 2-fold, the relaxation time decreases when we increase the magnitude of the change. For step-down changes, the relaxation time increases when we increase the magnitude of change.

A similar analysis was carried out to estimate the relaxation times associated with one-step changes in the baselevel downcutting rate (Figure 8). The initial condition was the same as before. The results show that there is a great dependency of the relaxation time on the baselevel downcutting rate for changes smaller than a 2-fold. For greater changes (both increases and decreases), the relaxation time is much less sensitive to changes in the baselevel downcutting than it is for changes in the diffusion coefficient. Two-fold changes in the baselevel downcutting rate for 25 m and 100 m long hillslopes give relaxation times around 100 Ka and 1.5 Ma, respectively.

Relaxation Time and Final Relief

In this section we analyze how the relaxation time of hillslope profiles is related to the magnitude of the final relief (F_r), i.e., the relief obtained at the equilibrium condition. Here, relief means the difference in elevation between the hilltop and the base of the hillslope and the results refer to profiles 25 m long. It is common in diffusive problems to specify the time by the dimensionless quantity $(D\,t) / L^2$, which is known as the Fourier number (e.g., Carslaw and Jaeger, 1959). Based on this, Anderson (*in press*) argued that the time scale for the approach to steady state in a problem similar to the one simulated here would be well approximated by the ratio

(14) $$L^2 / D .$$

In the same way, some authors have shown that the steady-state relief for the convex profiles simulated here is expressed by

(15) $$F_r = (|B_d| / 2D)\ L^2$$

(e.g., Carson and Kirkby, 1972, p. 299; Anderson, *in press*).

Figure 9 and Figure 10 compare some of our results for the relaxation time and final relief, obtained by solving the time-dependent problem given by (4), with the values obtained if one uses the respective steady-state equations described above. The plots in these two figures show the amount of time required to attain equilibrium and the amount of relief developed at such

condition for each imposed change. Figure 9 shows such relationships when the direction of the change is towards an increase in hillslope curvature (in absolute values), i.e., resulting from an increase in the absolute value of B_d (plots 9A and 9B) or from a decrease in D (plots 9C and 9D) while Figure 10 shows the same relationships for changes towards a decrease in hillslope curvature. The results presented in these two figures suggest that while the relief at equilibrium estimated by (15) is similar to the numerical solution (the 10% difference is related to the criteria we used in the definition of equilibrium here), the use of (14) as an approximation for the relaxation time of convex hillslope profiles is not valid, especially for changes smaller than a 2-fold. Such result was expected because there is not a B_d term in (14), resulting in a constant relaxation time along the entire range of changes in B_d.

The influence of final relief on relaxation time helps explain the differences between Figures 7 and 8 and the dependency of relaxation time on whether diffusivity and lowering rate are increasing or decreasing. Increases in B_d or decreases in D will cause the mean slope to increase for a given fixed hillslope length, hence the final equilibrium relief must increase. Development of relief takes time, therefore increasing relief is associated with increasing relaxation time. Because of the increasing transport caused by increasing B_d, however, the rate of increase of relaxation time with increasing B_d declines with increasing B_d changes. Large decreases in diffusivity, initially slow the erosion down and it is not until the mean slope is sufficiently steepened that equilibrium is reached, so large decreases in diffusivity mean large increases in relaxation time.

On the other hand, a decrease in B_d or increase in D will decrease the mean slope and hence the final relief, but the relaxation time response is not the same. The larger the decrease in lowering rate, the more transport rate diminishes and the longer it takes to reach equilibrium. So even though the final relief is smaller for larger decreases in B_d, the relaxation time is larger. In contrast, increasing diffusivity above a factor of 2, while causing the final relief to diminish, also causes the sediment transport rate to be initially higher (until the slope declines) hence the relaxation time is shorter.

In sum, then, the larger the change in B_d the longer the relaxation time, although the magnitude of increase differs depending on whether the lowering rate is increasing or decreasing. If diffusivity decreases, the relaxation time increases, but if it increases, the relaxation time first increases until diffusivity is about 2 times the initial value and then it progressively decreases with increasing diffusivity.

Propagation of the Equilibrium Condition

To investigate how equilibrium develops along a profile, we have plotted the relaxation time as a function of distance from the divide on a 100 m long hillside for a variety of changes in B_d and in D (Figure 11). The initial condition, a convex profile with a curvature of -0.025 m^{-1}, was kept constant in all the simulations presented here. Figure 11A shows the results obtained when we varied the baselevel downcutting rate and maintained the diffusion coefficient constant while Figure 11B shows the opposite situation. A new criterion was

used to define approximate equilibrium because the total sediment flux approach, used until now, would not allow us to define which parts of the hillslope profile had already attained equilibrium. In these experiments, the equilibrium condition was arbitrarily defined by the stage in which the hilltop develops a convexity that is 90% of the local hillslope curvature at steady-state which is known from the new imposed ratio B_d/D.

The results show that for the cases presented in both Figure 11A and Figure 11B, the relaxation time gets longer the closer to the divide, i. e., showing that the equilibrium propagates upslope. This upslope migration starts slowly at the base of the profile and then accelerates as the equilibrium gets closer and closer to the hilltop. When we compute the lag-time between the achievement of the equilibrium at the bottom and at the top of the profile we observe that while this amount of time is very similar for the imposed changes in B_d (Figure 11A) it may vary significantly for changes in D (Figure 11B).

Dimensional Analysis

In order to clarify the nature of the physical processes being modeled a dimensional analysis was carried out by the classical Buckingham's Pi Theorem (see for ex., Dym and Ivey, 1980). The basic idea was to make our findings more useful in field work by obtaining a dimensionless graph in which the relaxation time could be determined based on estimates of changes in diffusivity and downcutting rate. One set of three dimensionless parameters $[\Pi_1, \Pi_2, \Pi_3]$ obtained from such analysis is:

(16) $$\Pi_1 = W_i L ,$$

(17) $$\Pi_2 = \frac{D R_t}{L^2} ,$$

(18) $$\Pi_3 = \frac{B_d}{D} L = W_f L ,$$

where W_i and W_f are the initial and final hillslope curvatures, respectively. This graph allows us to determine the relaxation time based on the hillslope length and on estimates of the initial and final values of the diffusivity and incision rates. The development of such analysis is fully described in Appendix 4, and a non-dimensional graph associated with our problem is presented in Figure 12.

DISCUSSION

Estimates of the relaxation time of hillslopes in the geomorphological literature are still rare, and comparisons are difficult because of the different objectives and criteria used to define this time. The relaxation times estimated here for hillslope profiles evolving under diffusive processes ranged from tens of thousands of years to a few millions of years. The specific values were controlled by the length of the hillslope as well as by the type, magnitude and direction of the imposed changes in the inputs. Although the simulations carried out here were only associated with the one dimensional evolution under transport-limited conditions their results proved to be very helpful in defining the relative

importance of the parameters controlling the time-scale of morphological adjustments of convex hillslopes.

The fact that the relaxation time increased with the square of the hillslope length was expected from the solution of a pure linear diffusive evolution and such behavior has been shown by other authors (e.g., Carson and Kirkby, 1972, Koons, 1989; Anderson, *in press*). A different relationship was obtained by Ahnert (1987a) who observed that, for hillslopes evolving under slow mass movements, the relaxation time increased linearly with increments in the length of the profile.

Both changes in the diffusion coefficient and in the baselevel downcutting rate play important roles in controlling the magnitude of the relaxation time on hillslope profiles. For increments smaller than a 2-fold change, the relaxation time was shown to be positively correlated with the increasing diffusion coefficient. For increments greater than this value it was shown to be negatively correlated, and this resulted from the fact that the final relief decreased when we increased the magnitude of the change. A similar relationship was observed by Ahnert (1987a) for hillslopes shaped by suspended-load wash denudation. He showed that the relaxation time was negatively correlated with the intensity of denudational process, which in his case was the precipitation. Our results also show a positive correlation between the relaxation time and the absolute value of the baselevel downcutting rate for increments smaller than a 10-fold. For greater increments, the relaxation time was shown to be much less sensitive to changes in the baselevel downcutting. Ahnert (1987a) also approached this question and although his hillslopes were eroded by different processes he also observed a

positive correlation between the relaxation time and the rate of baselevel lowering (in absolute terms).

The results summarized in Figures 7 and 8 show that the time-scale of morphological adjustments following changes in the diffusion coefficient or in the baselevel downcutting rate will vary substantially depending on whether the absolute value of the hillslope curvature is increasing or decreasing. Although such behavior was previously suggested for other geomorphological systems by some authors (e.g., Chorley and Kennedy, 1971; Allen, 1974; Renwick, 1985), it has not yet been demonstrated for hillslopes.

Equilibrium condition, for all the simulated cases, first developed at the base of the hillslope and then propagated upslope. The upslope migration of equilibrium starts slowly and then accelerates. In his model Ahnert (1987a) also observed that near the base of the hillslope the equilibrium is established faster. However, he showed that when it moves upslope its progress gets more and more retarded. He attributed this change to the decrease in the contributing area and, consequently, in the overland flow discharge.

These results support the idea that hilltop convexities are the segments of hillslopes with the longest relaxation time. If we assume that climatic shifts will impose corresponding systematic changes in the diffusion coefficient, which will consequently lead to morphological adjustments in the hillslope system then the hilltop convexities observed in the field today may represent morphologies that are far from being equilibrium forms. In addition, the magnitude and direction of the climatic and/or tectonic change, i.e., towards and increase or decrease in D or

B_d values, is shown to play an important role in controlling the amount of time required for a new equilibrium condition to be attained. In order to expand these results to include the response associated with climatic and/or tectonic oscillations Fernandes and Dietrich (Chapter 2) have set up a series of experiments to investigate the time-scale of morphological adjustments of hillslope profiles in response to cyclic oscillations in the diffusion coefficient or in the baselevel downcutting rate.

Another interesting point is the difference in the form of the total sediment flux curve associated with changes in D and B_d observed in Figures 5 and 6, respectively. Although our simulations dealt with very simple conditions in terms of transport processes, the fact that step-increases in D result in a peak in the sediment flux immediately after the increase suggests that some drainage basins may develop extensive aggradation cycles concentrated immediately after a climatic-induced increase in the diffusion coefficient. Although step-increases in B_d (in absolute terms) result in sediment fluxes greater than the ones generated by the same amount of changes in D, the associated response is much more subtle. This subtlety may allow the channels to transport the sediments delivered from the hillslopes, thereby preventing the accumulation of thick deposits in the drainage basin.

An important question that needs to be further addressed is the use of a diffusion-based approach to model larger areas, e.g., entire mountain ranges, in which major variations in topography, climate, vegetation and bedrock geology might occur. As was argued by some authors (e.g., Anderson and Humphrey, 1989; Koons, 1989; Anderson, *in press*) there are some important issues that need

to be taken into consideration when scaling-up the related parameters which result, for example, in defining an effective diffusivity which is much larger than the one estimated at the hillslope scale. Another major issue is the use of a precipitation gradient for estimate a diffusion coefficient gradient (e.g., Koons, 1989). Although it may seem very attractive when modeling large-scale features, there is still no field evidence supporting the straight application of such relationships. As was shown by McKean et al. (1993), spatial variations in bedrock geology (e.g., from sandstone to shale) may play the most important role in controlling the magnitude of the diffusion coefficient value and seem to explain the one order of magnitude increase in D from Marin County to Concord (both in California) while annual precipitation is reduced by one half.

CONCLUSIONS

For field-constrained values in the diffusion coefficient and in the baselevel downcutting rate, 2-fold changes give relaxation times around 70 Ka and 1 Ma, for hillslopes 25 m and 100 m long, respectively. The time required for such morphological adjustments to be attained following one-step changes in the diffusion coefficient or in the baselevel downcutting rate differs depending on whether the initial hillslope is tending to increase or decrease its convexity through time.

Step-increases in the diffusion coefficient result in a peak in the sediment flux delivered from the hillslopes immediately after the change. This suggests that under field conditions some drainage basins may develop aggradation

cycles concentrated immediately after a climatic-induced increase in the diffusion coefficient.

Because the relaxation times estimated here are much longer than the frequency of the climatic oscillations observed in the last few million years, it seems likely that most of the convex hillslopes that we see today in the field are not true time-independent morphologies despite having well developed smooth convexities. This will be especially true for the convex hilltops because they have the longest response times of the hillslope system.

REFERENCES

Ahnert, F., Brief description of a comprehensive three-dimensional process-response model of landform development. *Z. Geomorphol. Suppl. Band*, 25, 29-49, 1976.

Ahnert, F., Approaches to dynamic equilibrium in theoretical simulations of slope development. *Earth Surf. Proc. Landf.*, 12, 3-15, 1987a.

Ahnert, F., Process-response models of denudation at different spatial scales. In F. Ahnert (Ed.), *Geomorphological Models* , Catena Supplement, 31-50, 1987b.

Ahnert, F., Modelling landform change. In M. G. Anderson (Ed.), *Modelling Geomorphological Systems* , John Wiley, New York, 375-400, 1988.

Allen, J. R. L., Reaction, relaxation and lag in natural sedimentary systems: general principles, examples and lessons. *Earth-Sci. Reviews*, 10, 263-342, 1974.

Anderson, R., Evolution of the Santa Cruz Mountains, California, through tectonic growth and geomorphic decay. *J. Geophys. Res.*, (in press).

Anderson, R. S., and Humphrey, N. F., Interaction of weathering and transport processes in the evolution of arid landscapes. In T. A. Cross (Ed.), *Quantitative Dynamic Stratigraphy*, Prentice Hall, 349-361, 1989.

Andrews, D. J., and Hanks, T. C., Scarp degradation by linear diffusion: inverse solution for age. *J. Geoph. Res*, 90, 10,193-10,208, 1985.

Armstrong, A. C., A three-dimensional simulation of slope forms. *Z. Geomorphol. Suppl. Band*, 25, 20-28, 1976.

Armstrong, A. C., Simulated slope development sequences in a three-dimensional context. *Earth Surf. Proc.*, 5, 265-270, 1980.

Armstrong, A. C., Slopes, boundary conditions, and the development of convexo-concave forms - some numerical experiments. *Earth Surf. Proc. Landf.*, 12, 17-30, 1987.

Arnett, R. R., Slope form and geomorphological processes: an Australian example. *Inst. of Brit. Geogr., Spec. Publ.*, 3, 81-92, 1971.

Band, L. E., Simulation of slope development and the magnitude and frequency of overland flow erosion in an abandoned hydraulic gold mine. In M. J. Woldenberg (Ed.), *Models in Geomorphology*, Allen & Unwin, Boston, 191-211, 1985.

Begin, Z. B., Application of a diffusion-erosion model to alluvial channels which degrade due to base-level lowering. *Earth Surf. Proc. Landf.*, 13, 487-500, 1988.

Begin, Z. B., Meyer, D. F., and Schumm, S. A., Development of longitudinal profiles of alluvial channels in response to base-level lowering. *Earth Surf. Proc. Landf.*, 6, 49-68, 1981.

Black, T. A. and Montgomery, D. R., Sediment transport by burrowing mammals, Marin County, California. *Earth Surf. Proc. Landf.*, 16, 163-172, 1991.

Bloom, A. L., *Geomorphology - A Systematic Analysis of Late Cenozoic Landforms*. Prentice-Hall, New Jersey, 1978.

Brunsden, D., Applicable models of long term landform evolution. *Z. Geomorphol. Suppl. Band*, 36, 16-26, 1980.

Brunsden, D., and Thornes, J. B., Landscape sensitivity and change. *Trans. Inst. Brit. Geogr.*, 4(4), 1979.

Budel, J., Climatic and Climatomorphic Geomorphology. *Z. Geomorph. N. F. Suppl. Bd.*, 36, 1-8, 1980.

Bursik, M., Relative dating of moraines based on landform degradation, Lee Vining Canyon, California. *Quat. Res.*, 35, 451-455, 1991.

Carslaw, H. S., and Jaeger, J. C., *Conduction of heat in solids*. Oxford University Press, Oxford, 2nd ed., 1959.

Carson, M. A., An application of the concept of threshold slopes to the Laramie Mountains, Wyoming. *Institute of British Geographers, Special Publication*, 3, 31-47, 1971.

Carson, M. A., and Kirkby, M. J., *Hillslope form and process*. Cambridge University Press, 1972.

Chorley, R. J., and Kennedy, B. A., *Physical Geography: A Systems Approach*. . Prentice-Hall International, London, 1971.

Colman, S. M., and Watson, K., Ages estimated from a diffusion equation model for scarp degradation. *Science*, 221, 263-265, 1983.

Crank, J., *Mathematics of Diffusion*. Oxford University Press, Oxford, 2nd ed., 1975.

Culling, W. E. H., Analytical theory of erosion. *J. Geol.*, 68, 336-344, 1960.

Culling, W. E. H., Soil creep and the development of hillside slopes. *J. Geol.*, 71, 127-161, 1963.

Culling, W. E. H., Theory of erosion on soil-covered slopes. *J. Geol.*, 73, 230-254, 1965.

Davis, W. M., The convex profile of badland divides. *Science*, 20, 245, 1892.

Davison, C., Note on the movement of scree-material. *Quarter. J. Geol. Soc. London*, 44, 232-238, 1888.

De Ploey, J., and Savat, J., Contribution à l'étude de l'érosion par le splash. *Z. Geomorphol.*, 12, 174-193, 1968.

Dietrich, W. E., Reneau, S. L., and Wilson, C. J., Overview: 'zero-order basins' and problems of drainage density, sediment transport and hillslope morphology. *IAHS Publ.*, 165, 27-37, 1987.

Dunne, T., Formation and controls of channel networks. *Prog. Phys. Geogr.*, 4, 211-239, 1980.

Dunne, T., Stochastic aspects of the relations between climate, hydrology and landform evolution. *Trans. Japanese Geomorphological Union*, 12, 1-24, 1991.

Fernandes, N. F. and Dietrich, W. E., The effects of climatic and tectonic-induced oscillations on hillslopes evolving by diffusive processes : some numerical experiment (Chapter 2 of this Dissertation).

Gilbert, G. K., *Report on the Geology of the Henry Mountains (Utah)*. U. S. Geographical and Geological Survey of the Rocky Mountains Region, Washington, D.C., 1877.

Gilbert, G. K., The convexity of hilltops. *J. Geol.*, XVII(4), 344-350, 1909.

Gossmann, H., Slope Modelling with Changing Boundary Conditions - Effects of Climate and Lithology. *Zeitsch. fur Geomorph. N. F., Suppl. Bd.*, 25, 72-88, 1976.

Hack, J. T., Interpretation of Erosional Topography in Humid Temperate Regions. *Am. J. Sci.*, 258A, 80-97, 1960.

Hack, J. T., Dynamic Equilibrium and Landscape Evolution. In W. N. Melhorn and R. C. Flemal (Eds.), *Theories of Landform Development*. State University of New York, New York, 87-102, 1975.

Hanks, T. C., and Andrews, D. J., Effect of far-field slope on morphologic dating of scarplike landforms. *J. Geophys. Res.*, 94, 565-573, 1989.

Hanks, T. C., Bucknam, R. C., Lajoie, K. R., and Wallace, R. E., Modification of Wave-Cut and Faulting-Controlled Landforms. *J. Geophys. Res.*, 89, 5771-5790, 1984.

Hanks, T. C., and Schwartz, D. P., Morphologic dating of the pre-1983 fault scarp on the Lost River Fault at Doublespring Pass Road, Cluster County, Idaho. *Bull. Seismol. Soc. Am.*, 77, 837-846, 1987.

Hanks, T. C., and Wallace, R. E., Morphological Analysis of the Lake Lahontan Shoreline and Beachfront Fault Scarps, Pershing County, Nevada.*Bull. Seismol. Soc. Am.*, 75, 835-846, 1985.

Hardisty, J., The transport response function and relaxation time in geomorphic modelling. *Catena Supplement*, 10, 171-179, 1987.

Hirano, M., A mathematical model of slope development - an approach to the analytical theory of erosional topography. *J. Geosc., Osaka City University*, 11, 13-52, 1968.

Hirano, M., Simulation of developmental process of interfluvial slopes with reference to graded form. *J. Geol.*, 83, 113-123, 1975.

Hirano, M., Mathematical model and the concept of equilibrium in connection with slope shear ratio. *Z. Geomorphol. Suppl. Band*, 25, 50-71, 1976.

Howard, A. D., Geomorphological systems - equilibrium and dynamics. *Am. J. Sci.*, 263, 302-312, 1965.

Howard, A. D., Equilibrium models in geomorphology. In M. G. Anderson (Ed.), Modelling Geomorphological Systems, John Wiley, New York, 49-72, 1988.

Howard, A. D., A detachment-limited model of drainage basin evolution. *Water Res. Res.*, (in press).

Jordan, T. E., and Flemings, P. B., From Geodynamic Models to Basin Fill - A Stratigraphic Perspective. In T. A. Cross (Ed.), *Quantitative Dynamic Stratigraphy*, Prentice Hall, Englewood Cliffs, 149-163, 1989.

Kirkby, M. J., Measurement and theory of soil creep. *J. Geol.*, 75, 359-378, 1967.

Kirkby, M. J., Hillslope process-response models based on the continuity equation. *Inst. British Geographers, Spec. Publ.*, 3, 15-30, 1971.

Kirkby, M. J., A model for the evolution of regolith-mantled slopes. In M. J. Woldenberg (Ed.), *Models in Geomorphology*, Allen and Unwin, Boston, 213-237, 1985.

Koons, P. O., The topographic evolution of collisional mountain belts: a numerical look at the Southern Alps, New Zealand. *Am. J. Sci.*, 289, 1041-1069, 1989.

Loewenherz, D. S., Stability and the initiation of channelized surface drainage: a reassessment of the short wavelength limit. *J. Geophys. Res.*, 96, 8453-8464, 1991.

Mayer, L., Dating quaternary fault scarps formed in alluvium using morphologic parameters. *Quat. Res.*, 22, 300-313, 1984.

McKean, J. A., W. E. Dietrich, R. C. Finkel, J. R. Southon, and Caffee, M. W., Quantification of soil production and downslope creep rates from cosmogenic ^{10}Be accumulations on a hillslope profile. *Geology*, 21, 343-346, 1993.

Milliman, J. D., and Meade, R. H., World-wide delivery of river sediment to the oceans. *J. Geol.*, 91, 1-21, 1983.

Monaghan, M. C., J. A. McKean, W. E. Dietrich, and Klein, J., ^{10}Be chronometry of bedrock-to-soil conversion rates. *Earth and Planet. Sci. Letters*, 111, 483-492, 1992.

Nash, D., Forms of bluffs degraded for different lengths of time in Emmet County, Michigan, U.S.A. *Earth Surf. Proc.*, 5, 331-345, 1980a.

Nash, D., Morphologic dating of degraded normal fault scarps. *J. Geol.*, 88, 353-360, 1980b.

Nash, D. B., Morphological dating of fluvial terrace scarps and fault scarps near West Yellowstone, Montana. *Geol. Soc. Am. Bull.*, 95, 1413-1424, 1984.

Parsons, A. J., Process, form and boundary conditions along valley-side slopes. In V. Gardiner (Ed.), *International Geomorphology 1986*, John Wiley, New York, 89-104, 1987.

Pavich, M. J., Regolith residence time and the concept of surface age of the piedmont "peneplain". *Geomorphology*, 2, 181-196, 1989.

Phillips, J. D., and Renwick, W. H. (Eds.), *Geomorphic systems*. Elsevier, Amsterdam, 1992.

Pierce, K. L., and Colman, S. M., Effect of height and orientation (microclimate) on geomorphic degradation rates and processes, late-glacial terrace scarps in Central Idaho. *Geol. Soc. Am. Bull.*, 97, 869-885, 1986.

Reneau, S. L., *Depositional and erosional history of hollows: application to landslide location and frequency, long-term erosion rates, and the effects of climatic change.* Ph.D, University of California at Berkeley, 1988.

Reneau, S. L., Dietrich, W. E., Wilson, C. J. and Roger, J. D., Colluvial deposits and associated landslide in the northern San Francisco Bay Area, California, USA. *IV International Symp. on Landslides, Toronto*, 425-430, 1984.

Reneau, S. L., and Dietrich, W. E., Erosion rates in the Southern Oregon Coast Range - evidence for an equilibrium between hillslope erosion and sediment yield. *Earth Surf. Proc. Landf.*, 16, 307-322, 1991.

Reneau, S. L., W. E. Dietrich, M. Rubin, & Donahue, D. J., Analysis of hillslope erosion rates using dated colluvial deposits. *J. Geol.*, 97, 45-63, 1989.

Renwick, W. H., A synthesis of equilibrium and historical models of landform development. *J. Geogr.*, 84, 205-210, 1985.

Rosenbloom, N. A., and Anderson, R. . Hillslope and channel evolution in a marine terraced landscape, Santa Cruz, California. *J. Geophys. Res.*, (in press).

Saunders, I., and Young, A., Rates of surface processes on slopes, slope retreat and denudation. *Earth Surf. Proc. Landf.*, 8, 473-501, 1983.

Schumm, S. A., Rates of surficial rock creep on hillslopes in Western Colorado. *Science*, 155, 560-561, 1967.

Seidl, M. A., and Dietrich, W. E., The problem of channel erosion into bedrock. In K. H. Schmidt & J. d. Ploey (Eds.), *Functional Geomorphology*, Catena Verlag, Cremlinger, 101-124, 1992.

Selby, M. J., *Hillslope Materials & Processes*, Oxford University Press, New York, 2nd. ed., 1993.

Smith, T. R., and Bretherton, F. P., Stability and the Conservation of Mass in Drainage Basin Evolution. *Water Res. Res.*, 8(6), 1506-1529, 1972.

Summerfield, M. A., *Global Geomorphology: An Introduction to the Study of Landforms*. Longman, 1991.

Thornbury, W. D., *Principles of Geomorphology*, John Wiley, New York, 2nd ed., 1969.

Thornes, J. B., and Brunsden, D., *Geomorphology and Time*, Methuen, London, 1977.

Trofimov, A. M., and Moskovkin, V. M., On the problem of stable profiles of deluvial slopes. *Z. Geomorphol. Suppl. Band*, 25, 110-113, 1976.

Trofimov, A. M., and Moskovkin, V. M., Mathematical simulation of stable and equilibrium river bed profiles and slopes. *Earth Surf. Proc. Landf.*, 8, 383-390, 1983.

Trofimov, A. M., and Moskovkin, V. M., Diffusion models of slope development. *Earth Surf. Proc. Landf.*, 9, 435-453, 1984.

Twidale, C. R., On the survival of palaeoforms. *Am. J. Sci.*, 276, 77-95, 1976.

Willgoose, G., Bras, R. L., and Rodriguez-Iturbe, I., Results from a new model of river basin evolution. *Earth Surf. Proc. Landf.*, 16, 237-254, 1991.

Wyrwoll, K. H., Determining the causes of pleistocene stream-aggradation in the central coastal areas of Western Australia. *Catena*, 15, 39-51, 1988.

Young, A., and Saunders, I., Rates of surface processes and denudation. In A. D. Abrahams (Ed.), *Hillslope Processes*, Allen & Unwin, Boston, 3-27, 1986.

TABLE I - Estimates of the diffusion coefficient (D).

D ($\times 10^{-4}$ m^2/yr)	Method (*)	Material	Climate	Source
4.4	A	alluvium	semi-arid	Nash (1980b)
10	A	cohesionless	semi-arid	Hanks et al. (1984)
20	A	sands & gravels		Nash (1984)
40 - 60	B	coarse soils	Mediterranean	Dietrich et al. (in prep.)
50	C	coarse soils		Reneau (1988; cited by McKean et al., 1993)
100	A		Mediterranean	Rosenbloom & Anderson (in press)
110	A		temperate	Hanks et al. (1984)
120	A	wave-cut bluffs; sandy	humid-temperate	Nash (1980a)
360	D	clay-rich soils		McKean et al. (1993)

* A = morphological dating; B = hillslope curvature; C = colluvial transport rates; D = accumulation of ^{10}Be in soils.

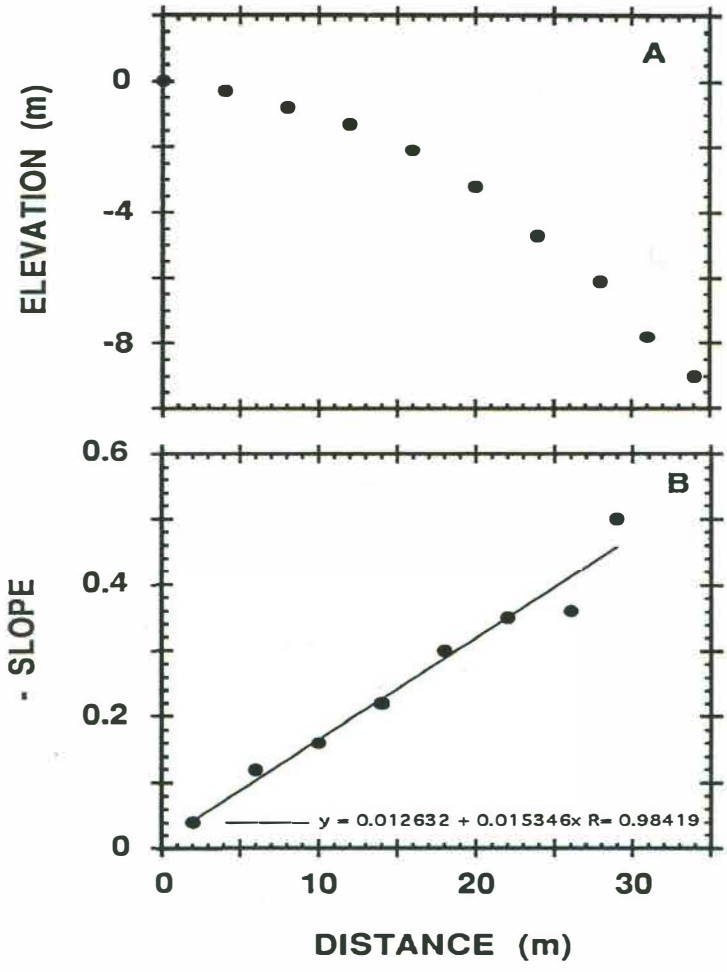

Figure 1 - Estimation of the diffusion coefficient from hillslope convexity at Marin County, California. Plot (A) shows the survey of the hillslope curvature while plot (B) presents the change in slope with distance from the divide for the same hillslope. The site is extensively described elsewhere (e.g., Reneau et al., 1984; Black and Montgomery, 1991). Assuming the baselevel downcutting rate (B_d) as approximately equal to the lowering rate, then the slope of this line is equal to B_d/D, where D is the diffusion coefficient. Substituting the measured value for B_d in this site (Reneau, 1988), a diffusion coefficient of approximately 50 $x10^{-4}$ m^2/yr is obtained. [modified from Dietrich et al. , in prep; data collected by David Montgomery].

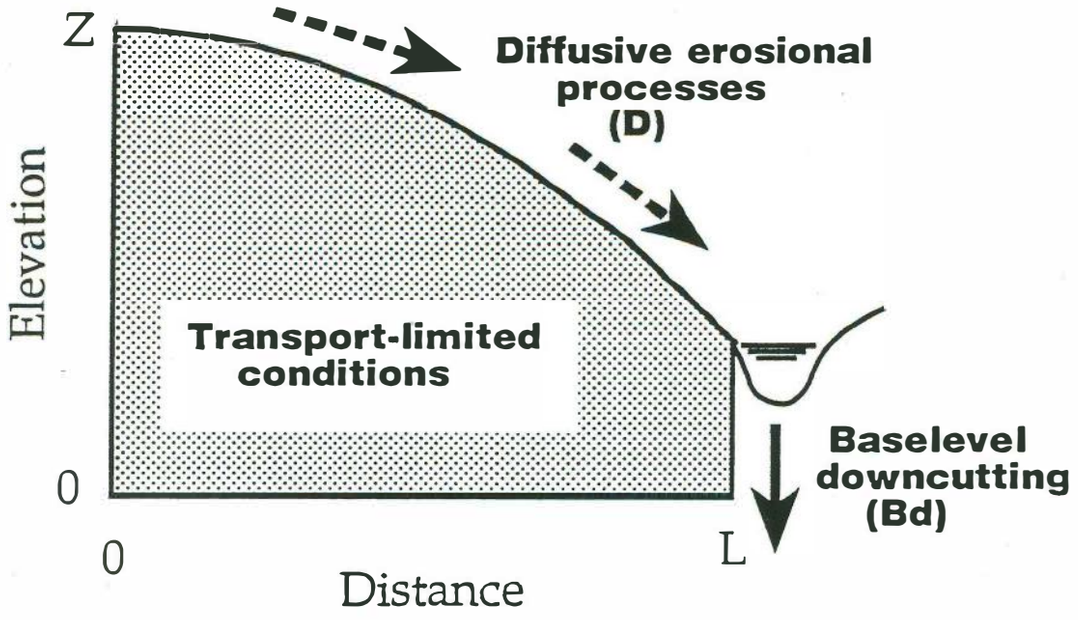

Boundary Conditions

$$\left.\frac{\partial z}{\partial x}\right|_{(0,t)} = 0 \quad \text{(flat divide)}$$

$$z(L,t) = B_d\, t$$

Initial Condition

$$\frac{\partial^2 z}{\partial x^2} = \text{constant}$$

Figure 2 - Sketch diagram of the diffusion-based model used in this paper. The initial profile is always a hillslope with constant curvature and transport-limited conditions prevail during the entire evolution. The evolving profile is submitted to a constant diffusive erosional processe and to a constant incision rate at the bottom of the hillslope, while the divide remais flat.

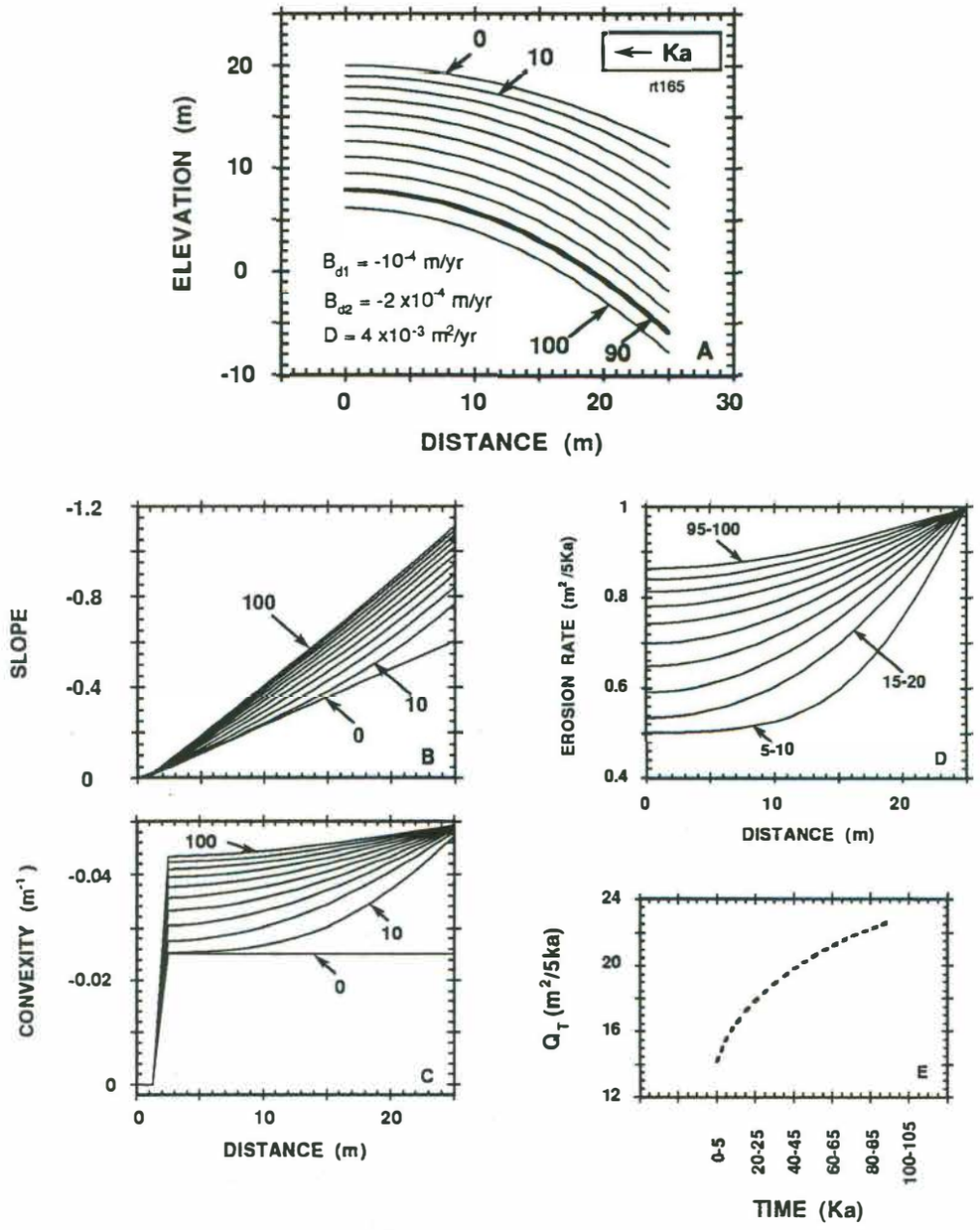

Figure 3 - Morphological response of an initially convex profile when sumitted to a 2-fold increase in the baselevel downcutting rate (from B_{d1} to B_{d2}). The initial hillslope curvature and the diffusion coefficient (kept constant during the entire simulation) are 0.025 m^{-1} and 40 x 10^{-4} m^2/yr, respectively. Figure 3A plots elevation against distance from the divide during 100 Ka (thousand of years), with each line representing a 10 Ka interval. Figures 3B, 3C and 3D show the temporal variation of slope, convexity and erosion rate against distance from the divide. Figure 3E shows the variation of the total sediment flux (Q_T)with time until 90% of its value at the steady-state condition is obtained.

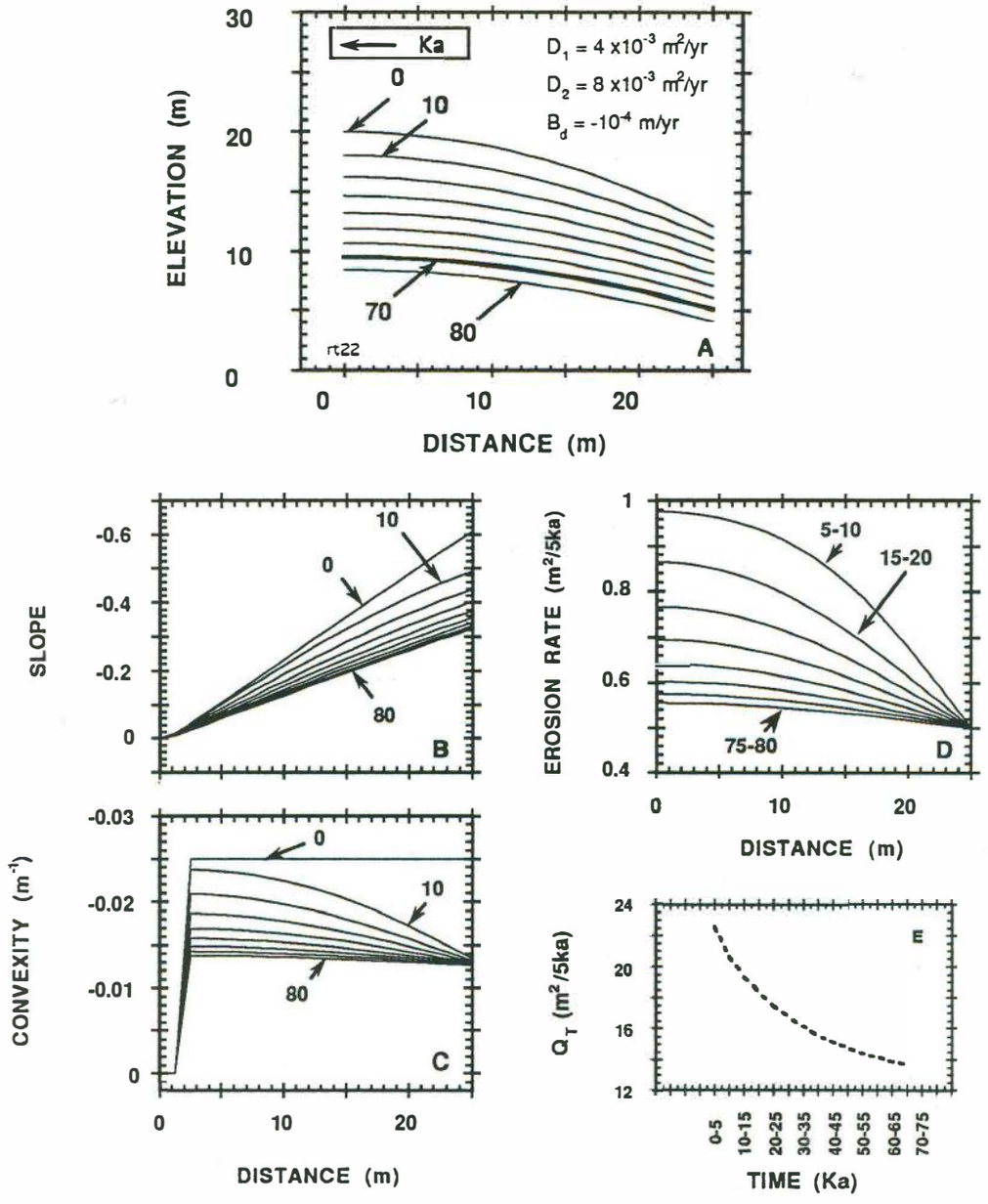

Figure 4 - Morphological response of an initially convex profile when sumitted to a 2-fold increase in the diffusion coefficient (from D_1 to D_2). The initial hillslope curvature and the baselevel downcutting rate (kept constant during the entire simulation) are 0.025 m^{-1} and -10^{-4} m/yr, respectively. Figure 4A plots elevation against distance from the divide during 80 ka, with each line representing a 10 ka interval. Figures 4B, 4c and 4d show the temporal variation of slope, convexity and erosion rate against distance from the divide. Figure 4e shows the variation of the total sediment flux (Q_T) with time until 90% of its value at the steady-state condition is obtained.

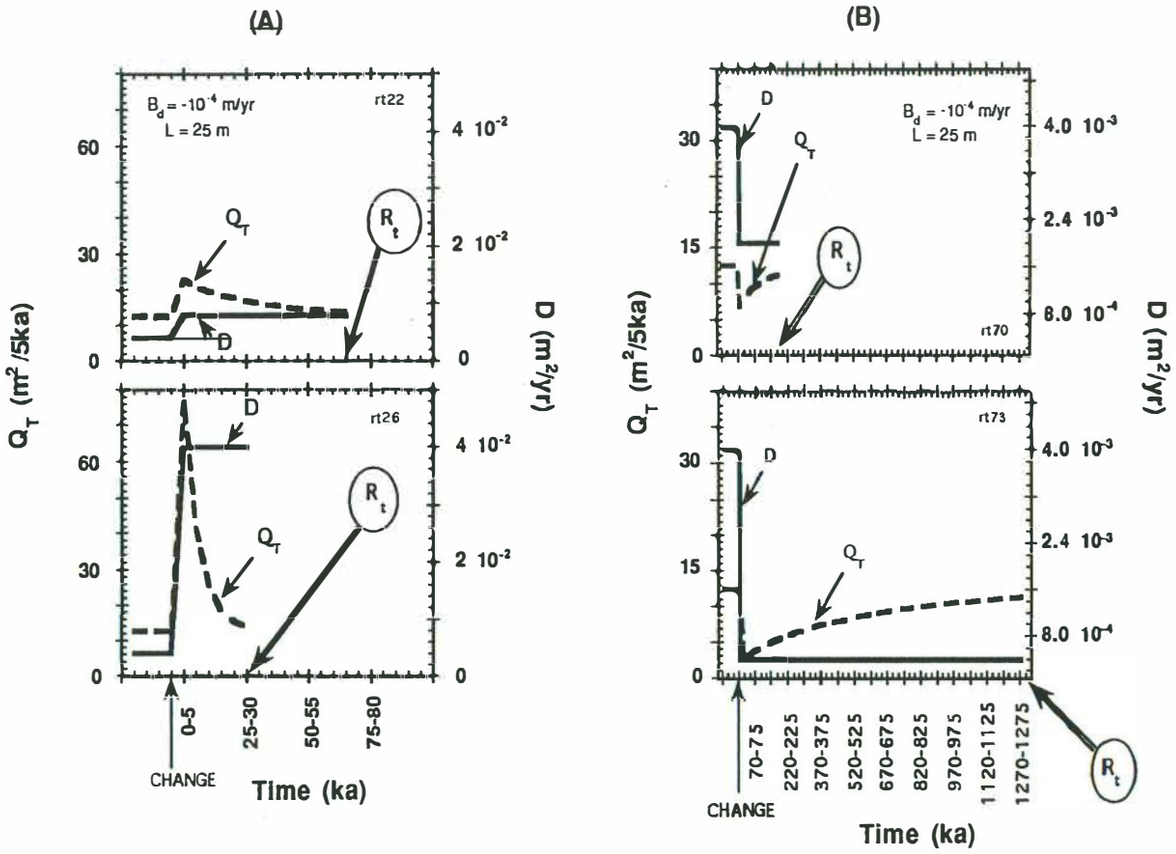

Figure 5 - Variation of the total sediment flux (Q_T) with time when one-step changes in the diffusion coefficient are imposed on an initially convex hillslope. Figure 5A shows the results associated with step-up changes (2-fold - top; 10-fold - bottom) while Figure 5B shows the ones for step-down changes (2-fold - top; 10-fold - bottom). The baselevel downcutting rate is the same for all the simulation (-10^{-4} m/yr) and the hillslopes are 25 meters long. The relaxation time (R_t) estimated in each experiment is shown by the arrow.

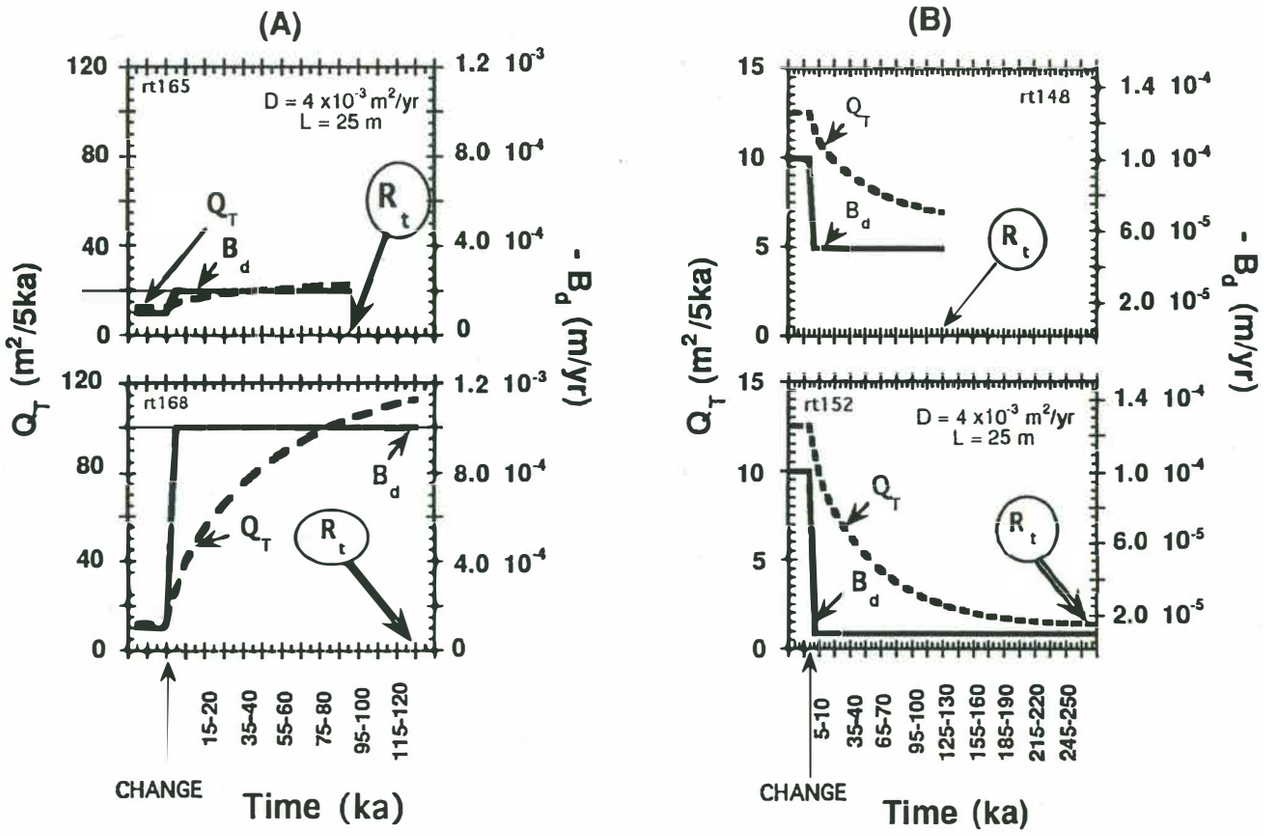

Figure 6 - Experiments similar to the ones presented in Figure 5 but now the diffusion coefficient is kept constant and we imposed one-step changes up (Figure 6A) and down (Figure 6B) in the baselevel downcutting rate. The relaxation time (R_t) estimated in each experiment is shown by the arrow.

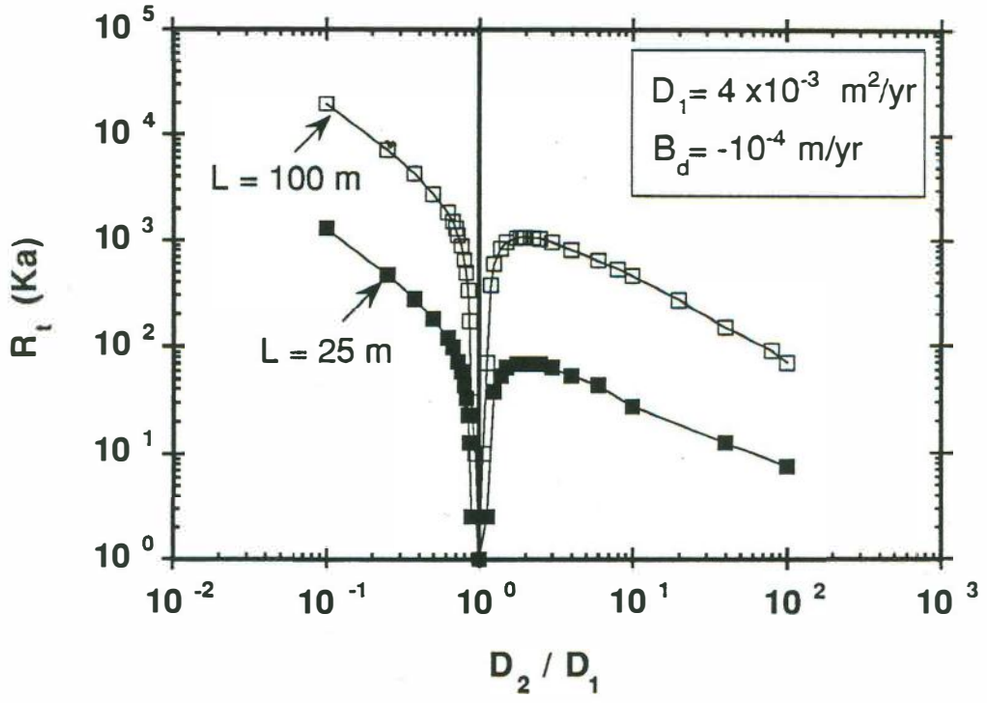

Figure 7 - Relaxation time (R_t) associated with one-step changes in the diffusion coefficient for hillslope profiles 100 m and 25 m long. The right side shows the results for step-up changes ($D_2>D_1$) and the left side shows the results for step-down changes ($D_2<D_1$). The baselevel downcutting is the same in all the simulations presented in this plot.

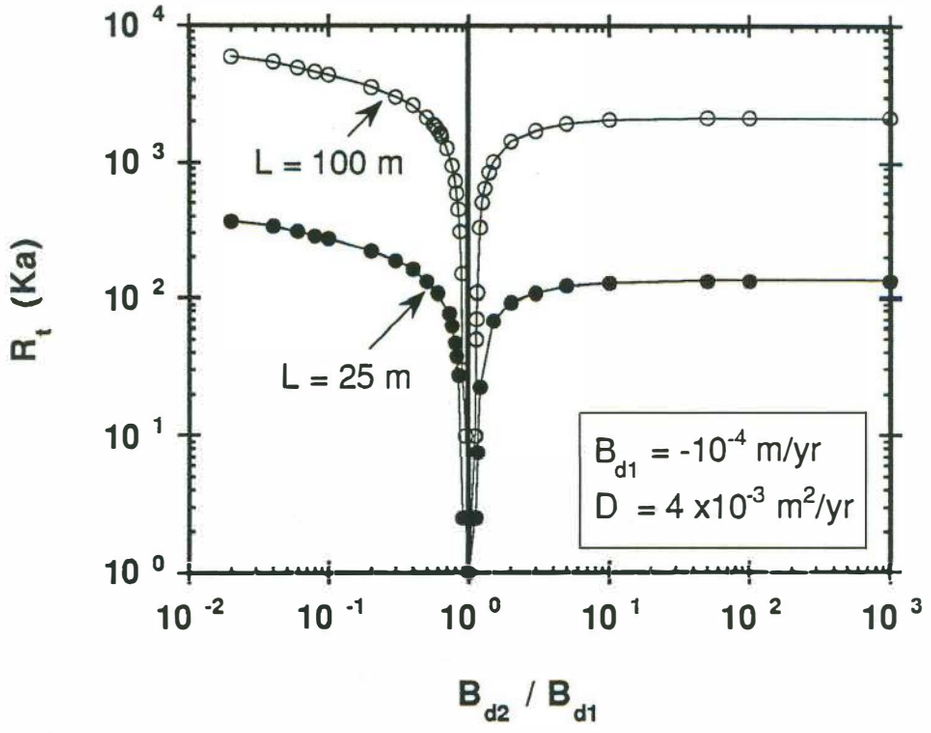

Figure 8 - Relaxation time (R_t) associated with one-step changes in the baselevel downcutting rate for hillslope profiles 100 m and 25 m long. The right side shows the results for step-up changes ($B_{d2}>B_{d1}$) and the left side shows the results for step-down changes ($B_{d2}<B_{d1}$). The diffusion coefficient is the same in all the simulations presented in this plot.

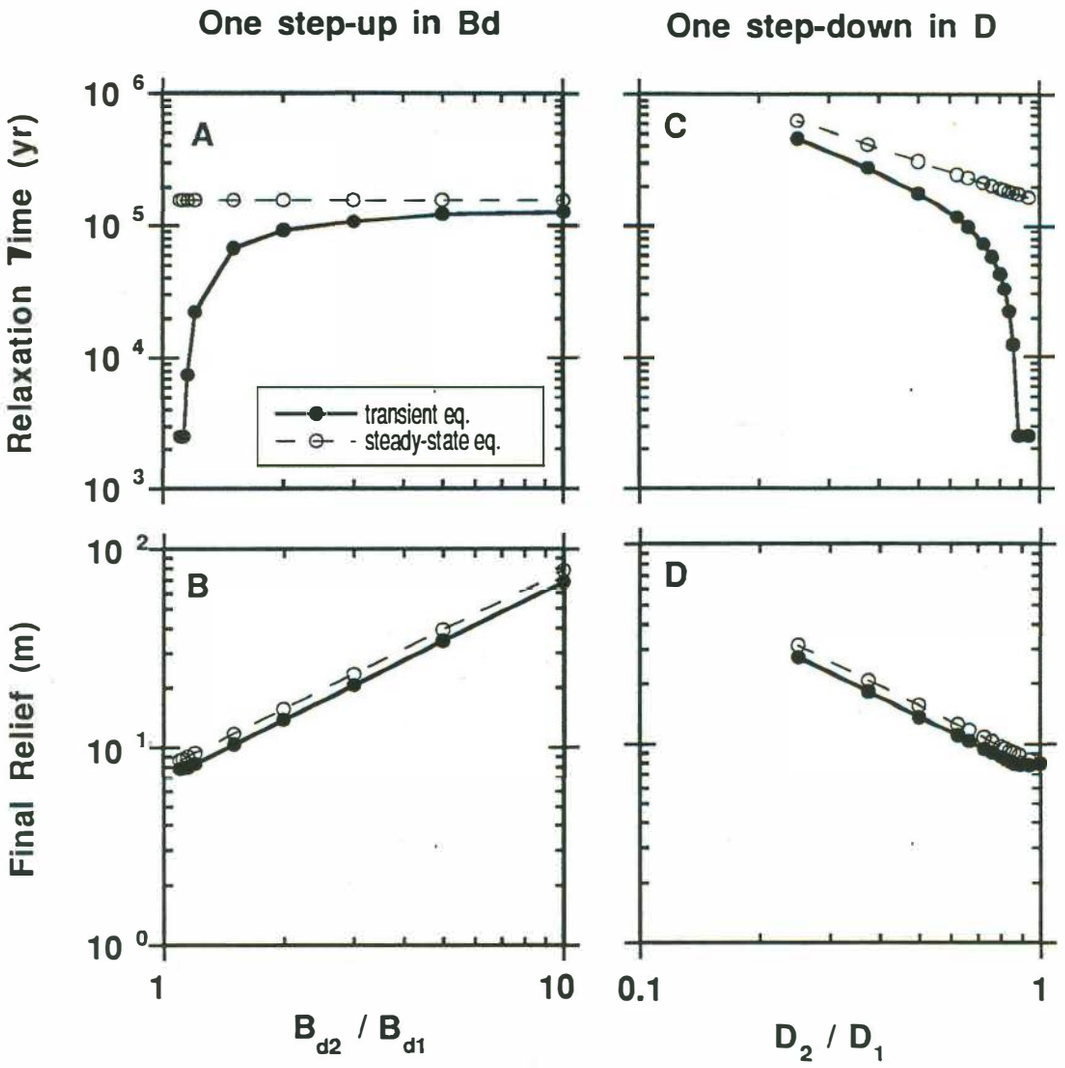

Figure 9 - Relaxation time and final relief when the imposed changes in B_d or D are in the direction of an increase in the final hillslope convexity. Plots 9A and 9B show the relaxation time and the associated final relief for one step-up changes in baselevel downcuttind rate, while plots 9C and 9D show the same analysis for one step-down changes in the diffusion coefficient. B_{d1} is 10^{-4} m/yr and D_1 is 40 x10^{-4} m^2/yr.

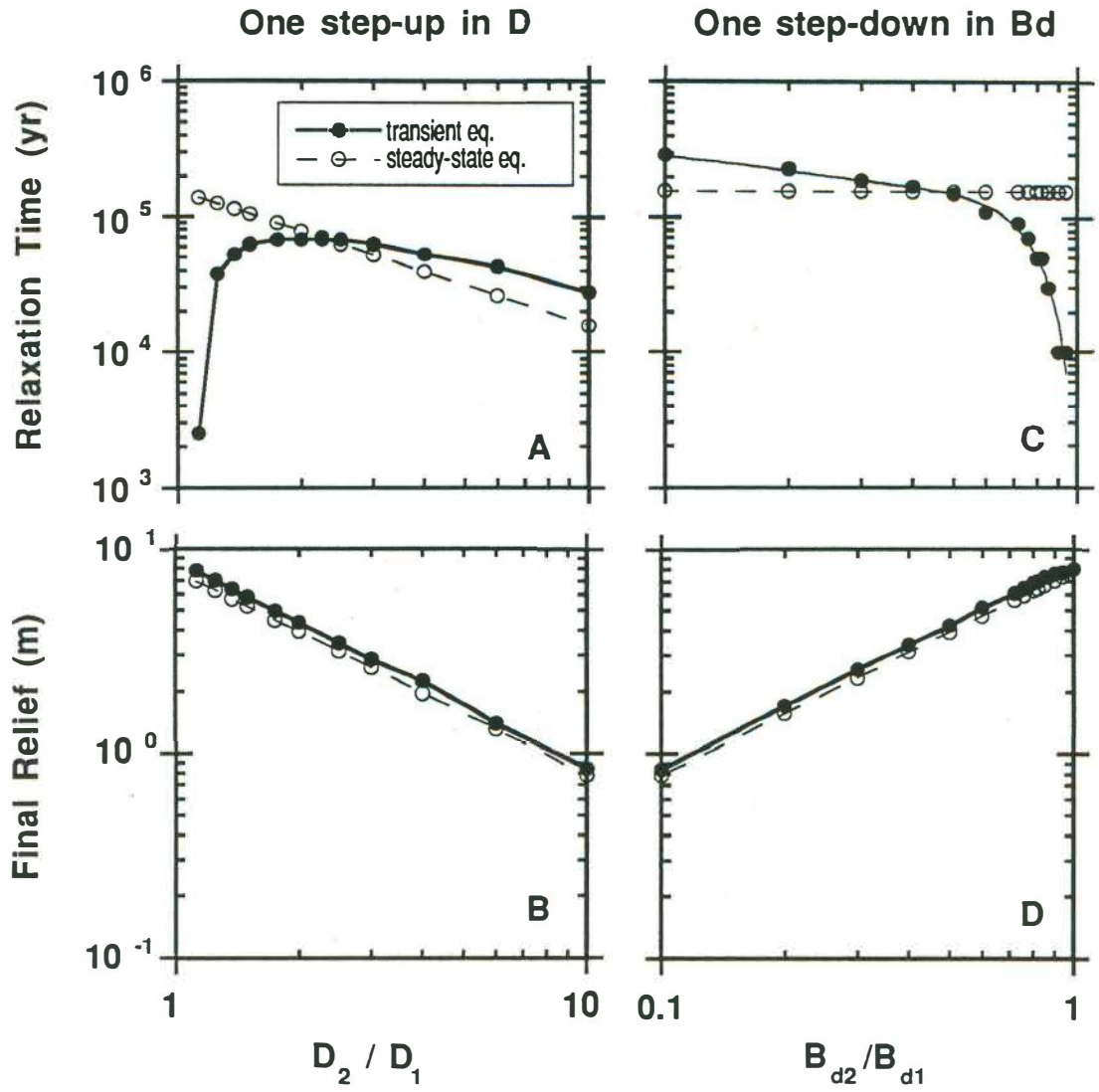

Figure 10 - Analysis similar to the one presented in Figure 9, but now for changes in B_d or D leading to a decrease in the final hillslope convexity. Plots 10A and 10B show the relaxation time and the associated final relief for one step-up changes in the diffusion coefficient, while plots 10C and 10D show the same analysis for one step-down changes in the baselevel downcutting rate. The initial value for the diffusion coefficient (D_1) and for the baselevel downcutting rate (B_{d1}) are the same as in Figure 9.

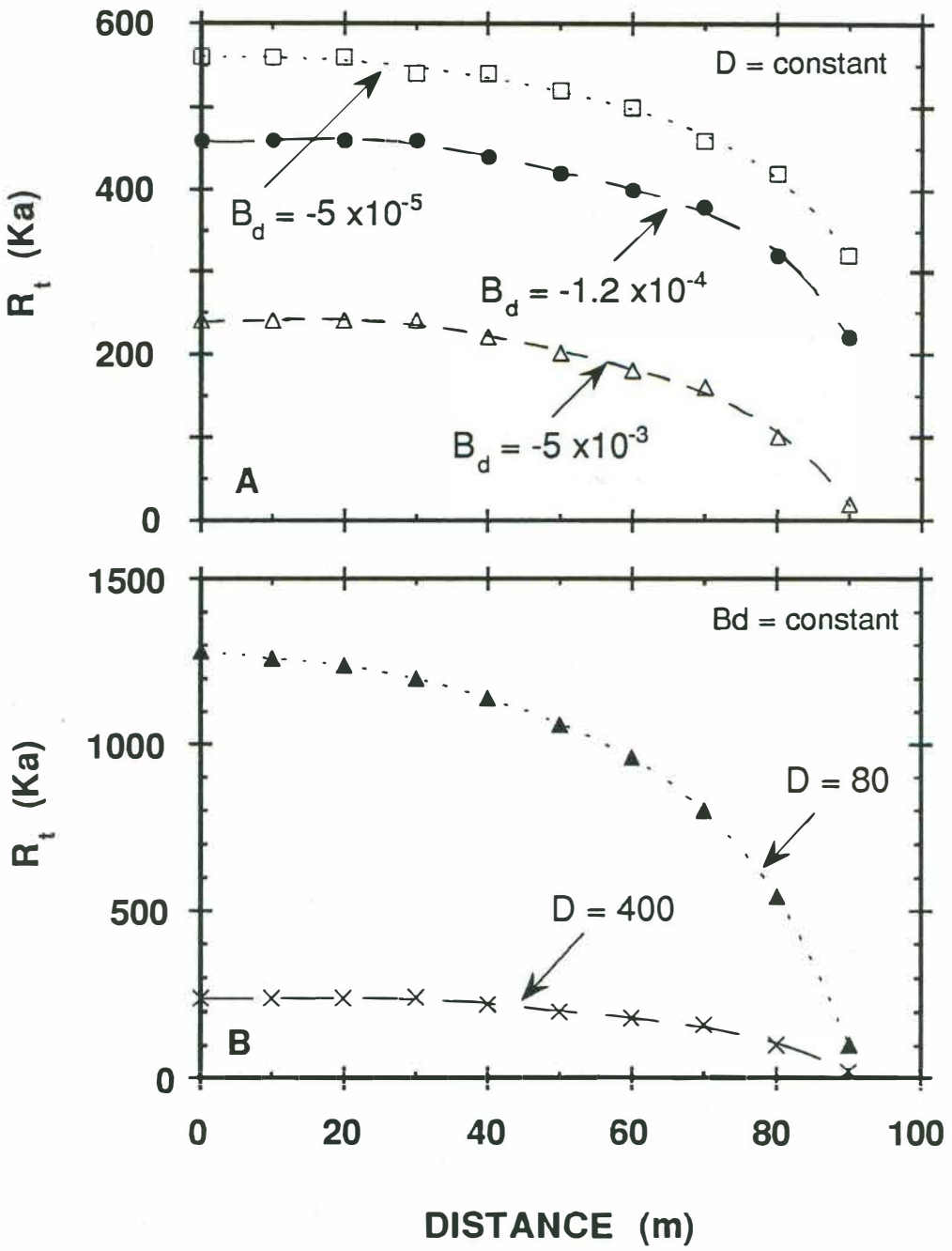

Figure 11 - Relaxation time (R_t) as a function of distance from the divide for hillslopes 100 m long. This figure shows how the equilibrium condition propagates along the hillslope when one-step changes are imposed in the baselevel downcutting rate (Plot 11A) and in the diffusion coefficient (Plot 11B). The initial condition, a convex profile with a curvature of -0.025 m^{-1}, is the same for all simulations. B_d values are in m/yr while D values are in x10^{-4} m^2/yr.

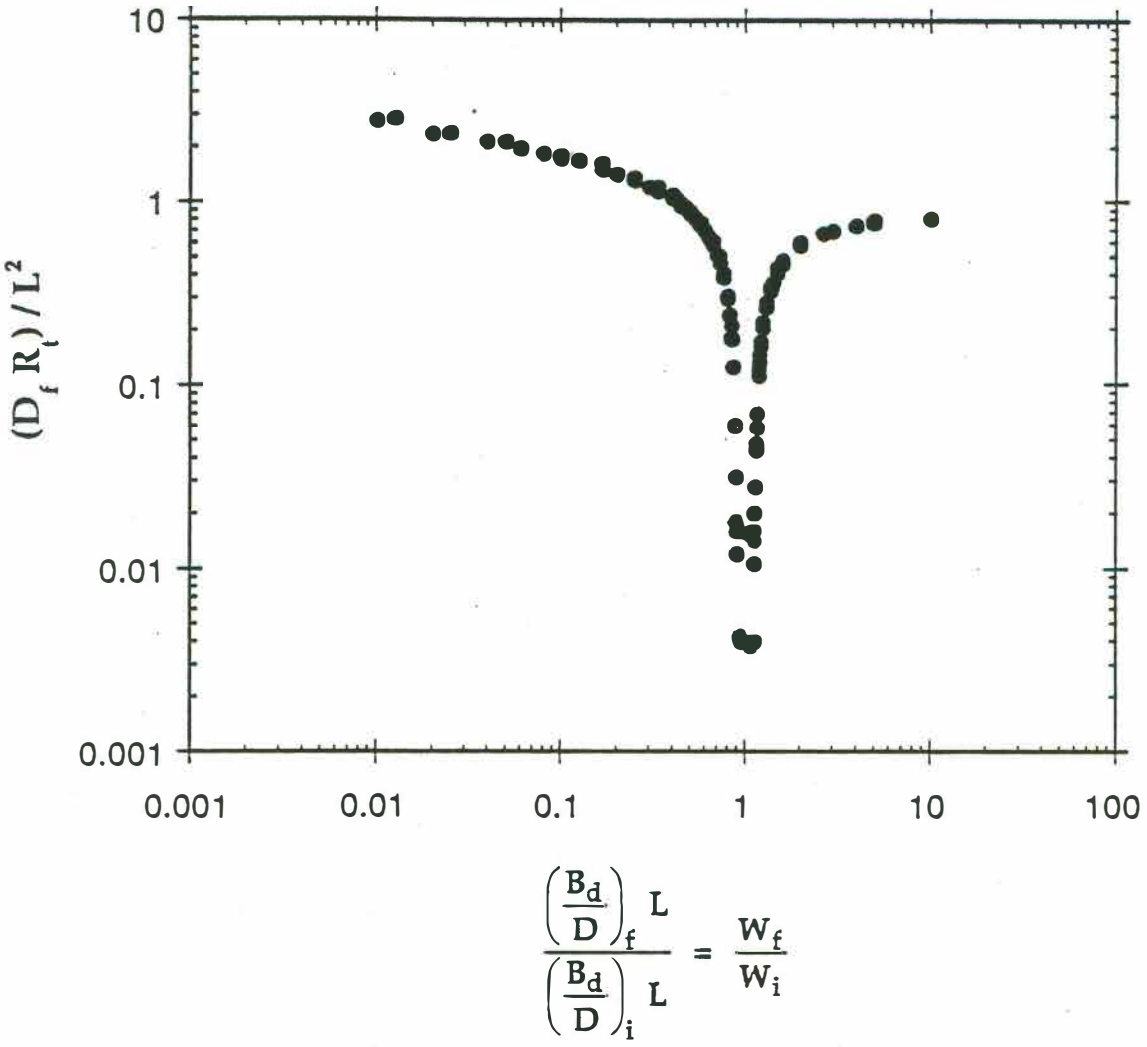

Figure 12 - Relationship between the three dimensionless parameters that describe our problem. In the y-axis we plot the parameter defined by (17), while in the x-axis we are plot a new dimensionless parameter characterized by the ratio between the other two parameters defined in (18) and (16). Notice that this new parameter, defined by the ratio between the final and the initial hillslope curvature, can be interpreted as the ratio of the change imposed on the diffusion coefficient or in the baselevel downcutting rate.

Chapter 2

THE EFFECTS OF CLIMATIC AND TECTONIC-INDUCED OSCILLATIONS ON HILLSLOPES EVOLVING BY DIFFUSIVE PROCESSES : SOME NUMERICAL EXPERIMENTS

ABSTRACT

Convex hilltops are common features on most soil-mantled landscapes. Although it is widely recognized that diffusive (slope-dependent) processes are generally responsible for the convexity little is known about the influence of climatic oscillations and variable boundary incision rates (tectonics) on the shape. In addition, considerable effort has been spent deciphering river and hillslope deposits for their climatic and tectonic signature, yet the delayed response of hillslopes may tend to decouple the sediment flux rates from changes in external forcing. In this paper we model the effects of climatic and tectonic oscillations that took place in the last 500 thousands of years on convex hillslopes evolving by diffusive processes. We specifically focus on how equilibrium convex hillslopes respond, both in terms of form and sediment flux, to step, sine and ^{18}O-constrained oscillations in the diffusion coefficient or in the downcutting rate at the bottom of the profile.

The hillslope profiles are shown to respond very differently depending on whether the imposed oscillations take place in the diffusion coefficient or in the incision rate. Step and sine oscillations in the diffusion coefficient cause the total sediment flux to eventually oscillate around the initial equilibrium value and the shorter the profile, the closer to the equilibrium it will be by the end of each cycle. Step and sine changes in the downcutting rate cause the sediment flux to oscillate around an equilibrium value located half the way between the lower and upper equilibrium values, which are associated with the minimum and maximum imposed values of the incision rates, respectively. Although the sediment flux is in phase with the ^{18}O-based oscillations in the diffusion coefficient, ^{18}O-based

oscillations in the downcutting rate cause cumulative effects on the response of the sediment flux. The results suggest that the convex hilltops of soil mantled landscapes, once formed, are forms difficult to be perturbed with modest variations in the diffusion coefficient or in the downcutting rate and may, at least for the case of long convex hillslopes, represent paleoforms that have been formed much before the climatic and tectonic oscillations that took place during the Quaternary.

INTRODUCTION

Landscapes evolve through diverse geologic materials under the influence of varying climate and tectonics. The evolving river system records, although often rather obscurely, the influence of varying climate and tectonics through such features as strath and fill terraces and in the shape of the longitudinal profile. Hillslopes, on the other hand, are harder to read. Colluvial deposits, landslide features and fault scarps have been used to explain the influence of varying climate and tectonics (see review in Bull, 1991). While these features can be rather unambiguous, there remains considerable debate about whether the overall morphology of hillslopes, and, specifically, the longitudinal profile is controlled by current tectonic and climatic regimes or instead records either a dominant period in the past or the integral effect of both climatic and tectonic variations (see review in Bloom, 1978; Carson and Kirkby, 1972).

Many authors have shown that an equilibrium form will eventually be developed by hillslope profiles evolving long enough under a constant process and

a constant incision rate at the base of the slope (e.g., Hirano, 1975; Armstrong, 1980, 1987; Ahnert, 1987, 1988; Fernandes and Dietrich, Chapter 1). Such results support the general idea of equilibrium that was implicitly stated by Gilbert (1877, 1909) and that was later refined by Hack (1960, 1975). While over some long time scale a "dynamic equilibrium" may be achieved at the large landscape scale, it seems unlikely that any particular hillslope in the landscape will experience a constant rate of incision at its base or evolve under a steady climate condition.

Applying these models to the hillslopes in the field raise, however, a number of questions regarding the development and maintenance of hilltop convexities. A major problem underlying all of them, is the difficulty in estimating the relaxation time of hillslopes in response to changes in the external factors. As pointed out by Wolman and Gerson (1978), the effectiveness of a geomorphological event can only be fully assessed when one takes into consideration not only the return period of such events, but also the relaxation time associated with them. Although the return periods of climatic changes during the past 3 million years can be estimated from the oxygen isotopic record of deep-sea sediments (e.g., Shackleton et al., 1988; Ruddiman and Raymo, 1988; Pirazzoli, 1993), the same is still not true for the relaxation time of hillslopes. Because the relaxation time of hillslopes is hard to determine empirically, model-based studies become essential.

Some models have been proposed to explore the effects of varying climate and basal incision on hillslope morphology. The complex spatial and temporal record of variations in the external factors has been usually approximated by one-step changes and/or by long-term step oscillations in the parameters of the models

that are assumed to be directly dependent on the climatic and/or tectonic regimes. The effects of climatic changes on hillslopes, for example, have been usually modeled by imposing periodic step changes on the type of the predominant denudation process (e.g., Ahnert, 1988) or by imposing one-step changes in the magnitude of the erosional process (see Chapter 1). Similarly, the effects of tectonic changes have been approximated by imposing periodic step changes (Ahnert, 1988) and one-step changes (see Chapter 1) in the rate of downcutting at the base of the hillslope.

In Chapter 1 we addressed this question by carrying out a number of numerical experiments in which one-step changes in the diffusion coefficient or in the downcutting rate were imposed on diffusive hillslopes already in equilibrium. Because the obtained relaxation times were much longer than the frequency of the climatic oscillations observed in the last few million years they suggested that most of the convex hillslopes that we see in the field today are unlikely to be truly time-independent morphologies. In this paper, we will build upon that study and focus on modeling the morphological effects of climatic and tectonic oscillations on convex hillslopes evolving under diffusive processes.

Although tectonic changes might happen in the form of pulses, climatic changes, at least during the last few million years, have shown to behave in an oscillatory way (e.g., Shackleton et al., 1988; Ruddiman and Raymo, 1988; Pirazzoli, 1993). For diffusive models, such changes can be assumed to induce direct and indirect modifications in the magnitude of the diffusion coefficient and/or the downcutting rate. In fact, we can expect that the combination of sea level and tectonic oscillations will cause the baselevel of hillslope profiles to

oscillate. We can also expect that even without sea level oscillation, uplift relative to baselevel may be transmitted up network via knickpoint propagation (e.g., Siedl and Dietrich, 1992), generating pulses of incision in the hillslopes. Therefore, it is important to characterize the time-scale of morphological adjustments of hillslopes responding to an oscillatory behavior in such external factors.

Here we explore whether hillslopes evolving by diffusive processes under oscillatory climate and baselevel lowering may attain a new average equilibrium form reflecting the period and amplitude of oscillation or whether such hillslopes are always changing shape in a delayed response to changes in the external forcing. We examine the influence of hillslope length on this problem and distinguish the response due to variations in diffusivity from the response due to the changes in baselevel lowering rate. Most of the simulations are started with an initially equilibrium hillslope which is then perturbed by changing the diffusivity or boundary lowering rate. By plotting the ratio of sediment flux from the hillslope to the equilibrium value at the initial condition we can estimate the time-scale of morphological adjustments of diffusional hillslopes in response to oscillations in climate and tectonics.

NUMERICAL EXPERIMENTS

A series of numerical experiments were carried out in order to characterize the time-scale of morphological adjustments of one dimensional hillslopes evolving under diffusive processes and exposed to oscillations in the external factors. The numerical experiments concentrate on the evolution of hillslopes

profiles under transport-limited conditions (Gilbert, 1877; Culling, 1963; Kirkby, 1971), i.e., the model assumes that at any time there will be soil available to be transported by the erosive processes.

Modeling the evolution of hillslopes by a diffusion-type equation has been widely used in geomorphology during the last few decades (e.g., Culling, 1960, 1963, 1965; Hirano, 1968, 1975, 1976; Kirkby, 1971; Gossmann, 1976; Trofimov and Moskovkin, 1976, 1983, 1984; Nash, 1980a, 1980b, 1984; Armstrong, 1980, 1987; Colman and Watson, 1983; Mayer, 1984; Hanks et al., 1984; Hanks and Wallace, 1985; Andrews and Hanks, 1985; Anderson and Humphrey, 1989; Koons, 1989; Bursik, 1991).

Diffusive hillslope models assume that soil flux (q_S), in terms of mass per unit width of slope [M/LT], for profiles evolving under transport-limited conditions (Gilbert 1877; Culling, 1963; Kirkby, 1971), is directly proportional to hillslope gradient

$$q_S = K\left(-\frac{\partial z}{\partial x}\right), \qquad (1)$$

in which z is elevation, x is distance from the divide, and K is a constant of proportionality. A transport law in this form has been widely accepted as accounting for transport processes like creep, rainsplash, biogenic activity, and frost heave (see review in Chapter 1). By combining (1) with the continuity equation one ends up with a diffusion-type equation

$$\frac{\partial z}{\partial t} = D\frac{\partial^2 z}{\partial x^2} \qquad (2)$$

stating that the change in elevation with time is proportional to the hillslope curvature, and in such case, the constant D is a diffusion coefficient with units of $[L^2/T]$.

We used a finite differences scheme to obtain numerical solutions of Equation 2 when oscillations in the diffusion coefficient or in the downcutting rate are imposed to equilibrium initial profiles. The numerical scheme, as well as, the computer program used to implement it, are presented in Appendices 2 and 3, respectively. In Chapter 1 we compiled field-derived estimates of the diffusion coefficient available in the geomorphological literature. It is shown that, for the hillslope scale, the diffusion coefficient may vary, at least, two orders of magnitude (from 4 to 400 $x10^{-4}$ m^2/yr). A variety of boundary conditions can be imposed on hillslope profiles evolving under diffusive processes. In the numerical simulations to be presented here, the hillslope profiles will always have flat divides and a baselevel downcutting rate (B_d) will be imposed at their bottom (see Figure 1). For modeling purposes, this downcutting rate can be approximated by the landscape lowering rate, which can be estimated from a variety of methods (see review in Chapter 1),

A variety of initial conditions were considered. We chose to use an equilibrium convex profile which has constant curvature. The imposed oscillations can then be seen as causing a perturbation about some equilibrium profile and the

effect of relaxation time on morphology and sediment discharge can be clearly observed. This initial condition would represent a hillslope that had reached approximate equilibrium under relatively stable climatic and tectonic conditions but then enters into a period of oscillatory conditions. This may be an appropriate model for any large scale hilltop convexity (longer than 100 m) in which the landscape was well developed before the Quaternary, such as in the "half-oranges" of southeastern Brazil (e.g., Meis and Moura, 1984; Clapperton, 1993). This model could also apply to shorter hillslopes (shorter than 25 m) in which even during the full glacial or interglacial, these shorter hillslopes could adjust fully to prevailing conditions. In order to characterize the effects of hillslope length on the time-scale of morphological adjustments the simulations were carried out on profiles 25 and 100 meters long.

In most of the numerical experiments to be presented here, the initial profile has a curvature of 0.025 m^{-1} which represents the curvature of the convex hilltops observed today in Marin County, California. As discussed in Chapter 1, such curvature would eventually be developed, for example, on diffusive profiles evolving long enough under a diffusion coefficient of 40 $x10^{-4}$ m^2/yr and a downcutting rate of 10^{-4} m/yr.

The analysis of how diffusive hillslopes respond to imposed oscillations will be approached by characterizing the temporal variation of the sediment flux from the entire hillslope profile. As argued by Howard (1988), such a criterion seems to be a good index to characterize the approach to equilibrium. As discussed in Chapter 1, the total sediment flux for equilibrium diffusional hillslopes can be easily determined, and such criterion was used by them in order to characterize

the relaxation time of hillslopes evolving by diffusive processes. For each simulation, we will plot the total sediment flux (Q_t), usually in m^2/5ka, against time, and such response will be then compared to the imposed oscillations in the diffusion coefficient or in the downcutting rate. For some simulations, we will also plot the hillslope profiles obtained at specific time intervals after the beginning of the experiments.

Three sets of numerical experiments were done, in which, for each case, either the diffusion coefficient or the downcutting rate was varied. In the first group of simulations we imposed step oscillations, in the second sine oscillations, while in the third we imposed oscillations that follow the ^{18}O isotopic record of deep-sea sediments.

1) Step Oscillations

In this group of simulations we imposed step changes in the diffusion coefficient from 40 (initial condition) to 80 $\times 10^{-4}$ m^2/yr or in the downcutting rate from 10^{-4} (initial condition) to 2 $\times 10^{-4}$ m/yr. Between twenty and thirty changes (up and down) were imposed to the initial equilibrium profile and each change was maintained for 40 ka (thousand of years).

2) Sine Oscillations

We imposed sine oscillations in the diffusion coefficient or in the downcutting rate in which the oscillations had a 40 ka and a 80 ka periodicity. These values were chosen because they approximate the periods of the oscillations

observed in the ^{18}O record of deep sea sediments for the last 2.5 Ma B.P. (e.g., Ruddiman and Raymo, 1988). The amplitudes of the imposed oscillations for the diffusion coefficient case were 40 $x10^{-4}$ m^2/yr and 80 $x10^{-4}$ m^2/yr, representing 2-fold and 3-fold changes with respect to the initial condition value. For the downcutting rate, we imposed sine oscillations with amplitudes of 10^{-4} m/yr and 2 $x10^{-4}$ m/yr representing, again, 2-fold and 3-fold changes with respect to the initial value. Each simulation lasts for about 500 ka.

3) Oscillations Based on the ^{18}O Record of Deep Sea Sediments

In this group of experiments we imposed oscillations in the diffusion coefficient or in the downcutting rate similar to the pattern of oscillations observed in the ^{18}O record of deep sea sediments. The ^{18}O isotopic curve compiled in Summerfield (1991; fig. 17.3) was digitized for the last 500 ka with a 5 ka interval (see Figure 2) and then interpolated for every 50 years, which was the time for each iteration in the main program. Two sub-groups of experiments were carried out depending on whether the climatic changes were assumed to imply changes in the diffusion coefficient or in the downcutting rate.

3.1) ^{18}O Changes Interpreted as Changes in the Diffusion Coefficient

Run 3.A - This simulation sets the diffusion coefficient for today to be greater than it was 20 ka ago. The amplitude of the changes observed in the ^{18}O record during the last 500 ka (Figure 2) is assumed to represent changes in the diffusion coefficient of the order of 20 $x10^{-4}$ m^2/yr (Figure 3a). The diffusion coefficient at

the beginning of the simulation (500 Ka ago) is arbitrarily set to be 40 $x10^{-4}$ m^2/yr. This value, combined with the imposed constant incision rate of 10^{-4} m/yr, allows us to have an equilibrium initial condition represented by a convex hillslope with a curvature of 0.025 m^{-1}. We carry this simulation for 100 m long hillslopes **(Run 3.A1)** and 25 m long hillslopes **(Run 3.A2)**.

Run 3.B - As in run 3.A, it assumes that the diffusion coefficient today is greater than it was 20 ka ago. However, it now assumes that the range of the changes observed in the ^{18}O record during the last 500 ka (Figure 2) is of the order of 40 $x10^{-4}$ m^2/yr (Figure 3b). The initial condition is the same as in Run 3.A. We carry this simulation for 100 m long hillslopes **(Run 3.B1)** and 25 m long hillslopes **(Run 3.B2)**.

Run 3.C - This run sets the diffusion coefficient for today to be smaller that it was 20 ka ago. The range of the changes in ^{18}O record is assumed to represent changes in the diffusion coefficient of the order of 40 $x10^{-4}$ m^2/yr (Figure 3c). The initial condition is the same as in the two previous runs. We carry this simulation for 100 m long hillslopes **(Run 3.C1)** and 25 m long hillslopes **(Run 3.C2)**.

3.2) ^{18}O Changes Interpreted as Changes in the Downcutting Rate

Run 3.D - The downcutting rate was set to be greater during glacial periods (e.g., 20 ka B.P.) than it is today. The amplitude of the changes observed in the ^{18}O record during the last 500 ka (Figure 2) is assumed to represent changes in the downcutting rate of the order of 10^{-4} m/yr (Figure 4a). The downcutting rate at the

beginning of the simulation (500 Ka ago) is arbitrarily set to be 10^{-4} m/yr. This value, combined with the imposed diffusion coefficient of 40 $x10^{-4}$ m^2/yr, allows us to have an equilibrium initial condition represented by a convex hillslope with a curvature of 0.025 m^{-1}. We carry this simulation for 100 m long hillslopes **(Run 3.D1)** and 25 m long hillslopes **(Run 3.D2)**.

Run 3.E - The same as run 3.D, with the only difference that the range of the changes in the ^{18}O record is assumed to represent changes in the downcutting rate of the order of $2x10^{-4}$ m/yr (see Figure 4b). We carry this simulation for 100 m long hillslopes **(Run 3.E1)** and 25 m long hillslopes **(Run 3.E2)**.

These two runs (3.D and 3.E) may be considered as good analogies for diffusive hillslopes evolving in drainage basins close to coasts. In such areas, higher incision rates are expected to be associated with periods of low sea-levels; and vice-versa.

RESULTS

Step Oscillations

Figures 5 and 6 show the temporal response of the total sediment flux (Q_t) to step-wise changes in the diffusion coefficient (between 40 and 80 $x10^{-4}$ m^2/yr) for hillslopes 100 m and 25 m long, respectively. In both cases, the initial condition is a convex profile with a curvature of 0.025 m^{-1} and the equilibrium value for the total sediment flux is plotted in these figures as an horizontal dashed line. The

baselevel downcutting rate (B_d) was kept constant during the entire experiment (10^{-4} m/yr) and each change in the diffusion coefficient was maintained for 40 ka. As expected, Q_t increases with increases in the diffusion and decreases with decreases in the diffusion coefficient. The equilibrium value, in terms of sediment flux, does not vary with the diffusion coefficient. In fact, although the flux increases or decreases immediately in response to changes in diffusivity, the sediment flux tends, with time, to go back to its equilibrium value.

For 100 m long hillslopes (Figure 5), we plot two curves for the sediment flux response. Q_t-1 plots the response if we had just imposed the first one-step change in the diffusion coefficient and had maintained it for the entire simulation. This is similar to the results for one-step changes presented before (Fernandes and Dietrich, Chapter 1). Q_t-2 shows the response associated with the oscillations in the diffusion coefficient. This curve oscillates about the general equilibrium value but it does not come close to it because, as shown in Chapter 1, the relaxation time (R_t) of this long hillslope, is much longer than the frequency of the oscillations in the diffusion coefficient imposed in these experiments. For the 25 m long case (Figure 6), because the relaxation time is very similar to the frequency of the step oscillations, Q_t nearly reaches the equilibrium values between step changes. Hence, for hillslopes 25 m long, by the end of each change the sediment flux attains values very close to (about 85%) the equilibrium value.

The response of Q_t to step-wise changes in the downcutting rate for hillslope profiles 100 m long is presented in Figure 7. The diffusion coefficient was kept constant during the entire experiment and, again, each step lasted for 40 ka. Notice that by imposing oscillations in the downcutting rate we are also changing

the equilibrium value for the total sediment flux. Lines A and B in Figure 7 represent such equilibrium values for the lower (initial) and upper values, respectively, of the imposed downcutting rate.

The general response for step-oscillation in the incision rate, in terms of sediment flux, is very different from the one observed for step-oscillations in the diffusion coefficient. Spikes on the sediment flux happen at the beginning of each new cycle and result from the fact that the hillslope curvature, at that point in the evolution, is not in equilibrium with the new imposed conditions. After the spike, the sediment flux slowly tends to an equilibrium condition until a new imposed cycle happens. The results show that Q_t tends to oscillate around an intermediate equilibrium value in terms of sediment flux, which is located half the way between the equilibrium values for the upper and lower imposed downcutting rates.

Sine Oscillations

Figures 8 through 15 show a series of numerical experiments in which we imposed sine oscillations in the diffusion coefficient. The effects of the hillslope length, the period, and the amplitude of these oscillations on the sediment flux were analyzed. Figure 8 shows the response of hillslope profiles 100 m long to sine oscillations in the diffusion coefficient. Such oscillations had a periodicity of 40 ka and an amplitude of 40 $x10^{-4}$ m^2/yr, resulting from changes in the diffusion coefficient from 40 $x10^{-4}$ m^2/yr to 80 $x10^{-4}$ m^2/yr. The sediment flux curve follows very closely the changes in the diffusion coefficient and a lag time can not be observed. Similar to what we observed for step changes in the diffusion coefficient

on 100 m long hillslopes (Figures 5), the oscillation sediment flux slowly approaches the equilibrium value (dashed line). The same general trend is observed when we double the period of the oscillations while keeping the rest the same (Figure 9). The response of the sediment flux when such step oscillations have an amplitude of 80 $x10^{-4}$ m^2/yr, resulting from changes in the diffusion coefficient from 40 $x10^{-4}$ m^2/yr to 120 $x10^{-4}$ m^2/yr, are presented in Figures 10 and 11. As one might have expected, although the amplitude of the response in the sediment flux increases, the general behavior displayed before is not affected by the increment in the amplitude of the oscillations.

Figures 12 through 15 show experiments similar to the ones described above but now for hillslope profiles 25 m long. In general, these curves show the same trends that were observed for 100 m long profiles. The main difference, as was also observed for step changes in the diffusion coefficient, is that the sediment flux curve approaches the equilibrium value faster than it did on 100 m long profiles. In addition, the time required for the sediment flux curve to attain the stage of constant oscillatory movement around the equilibrium value seems to be not affected by changes in the amplitude of the oscillation (compare Figure 12 to 14, and Figure 13 to 15) but it decreases when we increase the periodicity of the oscillations (compare Figure 12 to 13, and Figure 14 to 15).

Figures 16 through 19 show the response of hillslopes when sine oscillations in the downcutting rate are imposed to them. We carried out these simulations for similar conditions, in terms of periods, amplitudes and hillslope lengths, to the ones previously discussed for sine oscillations in the diffusion coefficient. With the exception of the spikes immediately after the change, the sediment flux, in general,

shows a behavior similar to the one observed for step changes in the downcutting rate. As expected, the spikes disappear when the changes are imposed slowly. Again, the sediment flux tends to oscillate around a new equilibrium value, which is located half the way between the lower and upper equilibrium values for the imposed downcutting rates. As expected, such new stage of "oscillatory equilibrium" is attained much faster on shorter profiles. A major difference is the fact that a lag time between the imposed change and the response in terms of sediment flux now exists. In addition, when we increase the period of the oscillations in the downcutting rate both this lag time and the amplitude of the oscillations in the sediment flux increase.

Oscillations Based on the ^{18}O Record

As we described before, in this set of experiments we impose oscillations in the diffusion coefficient or in the downcutting rate that are based on the ^{18}O isotopic record of deep sea sediments. Figure 2 shows the original ^{18}O curve and Figure 3 presents the three different interpretations of this record as climatically-driven changes in the diffusion coefficient. In the same way, Figure 4 shows how such oscillations were transformed into changes in the downcutting rate.

Figures 20 through 29 show the results obtained when diffusive hillslope profiles, 100 m and 25 m long, evolve under the oscillations in the diffusion coefficient and in the downcutting rate. For each case we plot the imposed oscillation in the diffusion coefficient or in the downcutting rate (a); in the middle,

the evolution of the associated hillslope profile with time (b); and at the bottom, the resulting changes in the total sediment flux (c).

Figures 20 and 23 show the response of hillslope profiles 100 m and 25 m long, respectively, when evolving under relatively small oscillatory conditions in the diffusion coefficient (as given in Figure 3a). Figures 20b and 23b show that the changes in the diffusion coefficient of the order of the ones assumed by Scenario A do not generate significant changes in equilibrium hillslope profiles during the simulated time. In addition, the total sediment flux (Figures 20c and 23c) behaves in phase with the imposed oscillations during the entire experiments.

Figures 21 and 24 present the results for profiles 100 m and 25 m long, respectively, when the changes in the diffusion coefficient are larger (see Figure 3b). Because the range of the imposed changes in the diffusion coefficient is twice as big as the previous Runs, the effects of such oscillations on the hillslope profiles are clearly observed (see Figures 21b and 24b). Most of the visible changes happen along the mid and upper parts of the profile. At the bottom of the hillslopes, the imposed oscillations in the diffusion coefficient are not felt because of the dominance of the boundary condition in setting the local erosion rate, and the profiles evolve very close to a dynamic equilibrium stage, basically controlled by a constant rate of downcutting.

The plots presented in Figures 22 and 25 show the results for Runs 3.C1 and 3.C2, for hillslopes 100 m and 25 m long, respectively. The effects of the oscillations in the diffusion coefficient on the hillslope profiles (Figures 22b and 25b) can be observed farther downslope than the ones related to Scenario B. The final

morphology, both in terms of hillslope curvature and amount of soil removed, is very different from the one obtained at the end of the simulation under Run 3.B. In addition, a lag time exists between the imposed change and the response of the sediment flux.

Figures 26 through 29 present the experiments in which oscillations in the downcutting rate, described by Runs 3.D and 3.E, are imposed to equilibrium diffusive hillslopes. The resulting profiles associated with Run 3.D (see Figures 26b and 28b) show that the changes in the downcutting rate affect only the bottom of the hillslope, where they are imposed. Such changes are quickly smoothed by the diffusive processes and are not observed in the upper segments, where the profiles evolve in a condition very close to dynamic equilibrium. Another interesting result is presented by the response of the total sediment flux (see Figures 26c and 28c). The resulting curves are much smoother than the imposed changes and cumulative effects are clearly observed. A similar trend is observed when the oscillations in the incision rate follow Run 3.E (see Figures 27 and 29). In none of the cases does the total sediment flux attains a value smaller than its initial one. The changes towards smaller values of the downcutting rate are less effective in generating a decrease in the total sediment flux resulting, for both hillslopes 100 m and 25 m long, in a cumulative increment in the total sediment flux with time.

DISCUSSION

The response of diffusive hillslope profiles evolving under cyclic changes varies significantly according to the type and magnitude of the imposed

oscillations, and to whether such oscillations affect the diffusion coefficient or the downcutting rate. As suggested by many authors (e.g., Hirano, 1975; Brunsden, 1980; Renwick, 1985; Ahnert, 1988; Howard, 1988), an equilibrium condition will not be attained when cyclic changes, in which the duration of the cycles is smaller than the relaxation time of the profile, are imposed to hillslopes. The shorter the hillslope profile is, the closer to such equilibrium value the sediment flux will be by the end of each oscillation.

When step oscillations are imposed to the incision rate, the sediment flux eventually oscillates around an intermediate equilibrium value which is located half the way between the upper and lower equilibrium values. Ahnert (1987, 1988), although using a more complex model and a different criterion to define the approach to the equilibrium condition (he used relief instead of sediment flux), obtained similar results. These results support the idea that when hillslopes evolve under long term step or sine fluctuations, in which the duration of the cycles is smaller than the relaxation time of the profiles, the morphology will eventually oscillate around an equilibrium form

The amount of time required for the sediment flux curve to attain the stage of constant oscillatory movement around the equilibrium value on hillslopes evolving under step and sine oscillations in the diffusion coefficient increases with the length of the hillslope. This was already shown, although for one-step changes, by the dimensionless analysis carried out by Fernandes and Dietrich (Chapter 1). The time to attain this stage of constant oscillatory movement, specifically for the case of sine oscillations, seems to be insensitive to changes in the amplitude of the imposed changes, but it decreases when we increase the period of the oscillations.

Sine oscillations in the incision rate lead to results similar to the ones described above for the case of changes in the diffusion coefficient. The main difference is the absence of the spikes in the sediment flux immediately after the change. In addition, there is a lag time between the imposed oscillations in the downcutting rate and the associated response in the sediment flux. Moreover, both this lag time and the amplitude of the oscillations in the sediment flux curve increase when we increase with the period of the imposed oscillations.

The sediment flux response to oscillations in the diffusion coefficient that are driven by the ^{18}O record is in phase with the diffusivity variations, and does not vary with the hillslope length. The resulting morphological effects associated with such oscillations are only observed in the upper and mid parts of the hillslope profile. The slope near the channel is governed by the incision rate.

The response to ^{18}O-based oscillations in the downcutting rate differs from that for diffusivity. Although the sediment flux tends, in general, to oscillate in response to the changes in the incision rate, the response is smoother and has a smaller amplitude than it had for changes in the diffusion coefficient. In addition, it never attains a value smaller than the initial (equilibrium) one, generating a cumulative increment in the sediment flux with time. In relative terms, the shorter the hillslope, the greater such cumulative effects will be. The morphological effects of such changes in the incision rate are only observed at the bottom of the hillslope profiles. The hilltops seem to be not affected by such oscillations in the incision rate, and evolve, as argued by Ahnert (1987, 1988), in a condition very close to a typical dynamic equilibrium (Hack, 1960, 1975).

CONCLUSIONS

Modeling of profile and sediment flux response of an initially equilibrium convex profile to modest (but probably realistic) variations in diffusivity and boundary incision rates about the equilibrium values reveals that the hillslope form may undergo small changes even though the sediment flux from the hillslope may vary substantially. Sediment flux lags the variation in incision but closely follows that due to diffusivity variation. Periodic changes in diffusivity act across the entire hillslope but have the largest effect close to the divide, whereas such changes of incision rate at the base of the hillslope affect most strongly the hillslope adjacent to the channel but have small influence near the divide. These results do depend, however, on the assumption that all sediment arriving at the base of the slope is removed.

Because the sediment flux from convex hillslopes responds distinctly between oscillations in the diffusion coefficient and in the downcutting rate, it may offer better constraints to our ability in reading the sediment record of thick alluvial fills in the field, helping to sort out the effects that Quaternary climatic and tectonic oscillations left in the landscape. Climatic changes may be expected to affect, at the same time, both the diffusion coefficient and the incision rate. Consequently, more field studies are urged to focus on the question of how the diffusion coefficient and the downcutting rates are affected when climatic changes take place.

The results suggest that the convex hilltops of soil mantled landscapes, once formed, represent morphological features difficult to be perturbed with modest variations in the diffusion coefficient or in the downcutting rate. Although short (<~25 m) convex hillslopes may have been formed by diffusive processes since the late Pleistocene, longer convex profiles (>~ 100m) may represent paleoforms that have been formed much before the climatic and tectonic oscillations that took place during the Quaternary.

REFERENCES

Ahnert, F., Approaches to dynamic equilibrium in theoretical simulations of slope development. *Earth Surf. Proc. Landf.*, 12, 3-15, 1987.

Ahnert, F., Modelling landform change. In M. G. Anderson (Ed.), *Modelling Geomorphological Systems* , John Wiley, New York, 375-400, 1988.

Anderson, R. S., and Humphrey, N. F., Interaction of weathering and transport processes in the evolution of arid landscapes. In T. A. Cross (Ed.), *Quantitative Dynamic Stratigraphy*, Prentice Hall, 349-361, 1989.

Andrews, D. J., and Hanks, T. C., Scarp degradation by linear diffusion: inverse solution for age. *J. Geoph. Res*, 90, 10193-10208, 1985.

Armstrong, A. C., Simulated slope development sequences in a three-dimensional context. *Earth Surf. Proc.*, 5, 265-270, 1980.

Armstrong, A. C., Slopes, boundary conditions, and the development of convexo-concave forms - some numerical experiments. *Earth Surf. Proc. Landf.*, 12, 17-30, 1987.

Bloom, A. L., *Geomorphology - A Systematic Analysis of Late Cenozoic Landforms.* Prentice-Hall, New Jersey, 510p., 1978.

Brunsden, D., Applicable models of long term landform evolution. *Z. Geomorphol. Suppl. Band*, 36, 16-26, 1980.

Bull, W., *Geomorphic response to climatic change* . Oxford University Press, 326p., 1991.

Bursik, M., Relative dating of moraines based on landform degradation, Lee Vining Canyon, California. *Quaternary Research*, 35, 451-455, 1991.

Carson, M. A., and Kirkby, M. J., *Hillslope form and process.* Cambridge University Press, 1972.

Clapperton, C., *Quaternary Geology and Geomorphology of South America.* Elsevier, Amsterdam, 779p., 1993.

Colman, S. M., and Watson, K., Ages estimated from a diffusion equation model for scarp degradation. *Science*, 221, 263-265, 1983.

Culling, W. E. H., Analytical theory of erosion. *J. Geol.*, 68, 336-344, 1960.

Culling, W. E. H., Soil creep and the development of hillside slopes. *J. Geol.*, 71, 127-161, 1963.

Culling, W. E. H., Theory of erosion on soil-covered slopes. *J. Geol.*, 73, 230-254, 1965.

Gilbert, G. K., *Report on the Geology of the Henry Mountains (Utah).* U. S. Geographical and Geological Survey of the Rocky Mountains Region, Washington, D.C., 1877.

Gilbert, G. K., The convexity of hilltops. *J. Geol.*, XVII(4), 344-350, 1909.

Gossmann, H., Slope Modelling with Changing Boundary Conditions - Effects of Climate and Lithology. *Zeitsch. fur Geomorph. N. F., Suppl. Bd.*, 25, 72-88, 1976.

Hack, J. T., Interpretation of Erosional Topography in Humid Temperate Regions. *Am. J. Sci.*, 258A, 80-97, 1960.

Hack, J. T., Dynamic Equilibrium and Landscape Evolution. In W. N. Melhorn and R. C. Flemal (Eds.), *Theories of Landform Development*. State University of New York, New York, 87-102, 1975.

Hanks, T. C., Bucknam, R. C., Lajoie, K. R., and Wallace, R. E., Modification of Wave-Cut and Faulting-Controlled Landforms. *J. Geophys. Res.*, 89, 5771-5790, 1984.

Hanks, T. C., and Wallace, R. E., Morphological Analysis of the Lake Lahontan Shoreline and Beachfront Fault Scarps, Pershing County, Nevada.*Bull. Seismol. Soc. Am.*, 75, 835-846, 1985.

Hirano, M., A mathematical model of slope development - an approach to the analytical theory of erosional topography. *J. Geosc., Osaka City University*, 11, 13-52, 1968.

Hirano, M., Simulation of developmental process of interfluvial slopes with reference to graded form. *J. Geol.*, 83, 113-123, 1975.

Hirano, M., Mathematical model and the concept of equilibrium in connection with slope shear ratio. *Z. Geomorphol. Suppl. Band*, 25, 50-71, 1976.

Howard, A. D., Equilibrium models in geomorphology. In M. G. Anderson (Ed.), Modelling Geomorphological Systems, John Wiley, New York, 49-72, 1988.

Kirkby, M. J., Hillslope process-response models based on the continuity equation. *Inst. British Geographers, Spec. Publ.*, 3, 15-30, 1971.

Koons, P. O., The topographic evolution of collisional mountain belts: a numerical look at the Southern Alps, New Zealand. *Am. J. Sci.*, 289, 1041-1069, 1989.

Mayer, L., Dating quaternary fault scarps formed in alluvium using morphologic parameters. *Quat. Res.*, 22, 300-313, 1984.

Meis, M. R. M. and Moura, J. R. S., Upper Quaternary sedimentation and hillslope evolution: southeastern Brazilian plateau. *Am. J. Sci.*, 284,241-254.

Nash, D., Forms of bluffs degraded for different lengths of time in Emmet County, Michigan, U.S.A. *Earth Surf. Proc.*, 5, 331-345, 1980a.

Nash, D., Morphologic dating of degraded normal fault scarps. *J. Geol.*, 88, 353-360, 1980b.

Nash, D. B., Morphological dating of fluvial terrace scarps and fault scarps near West Yellowstone, Montana. *Geol. Soc. Am. Bull.*, 95, 1413-1424, 1984.

Pirazzolli, P. A., Global sea-level changes and their measurement. *Global and Planetary Change*, 8, 135-148, 1993.

Renwick, W. H., A synthesis of equilibrium and historical models of landform development. *J. Geogr.*, 84, 205-210, 1985.

Ruddiman, W. F., and Raymo, M. E., Northern Hemisphere climate régimes during the past 3 Ma: possible tectonic conections. *Phil. Trans. R. Soc. Lond.*, B-318, 411-430, 1988.

Seidl, M. A., and Dietrich, W. E., The problem of channel erosion into bedrock. In K. H. Schmidt & J. d. Ploey (Eds.), *Functional Geomorphology*, Catena Verlag, Cremlinger, 101-124, 1992.

Shackleton, N. J., Imbrie, F. R. S. J., and Pisias, N. G., The evolution of oceanic oxygen-isotope variability in the North Atlantic over the past three million years. *Phil. Trans. R. Soc. Lond.*, B-318, 679-688, 1988.

Summerfield, M. A., *Global Geomorphology: An Introduction to the Study of Landforms*. Longman, 1991.

Trofimov, A. M., and Moskovkin, V. M., On the problem of stable profiles of deluvial slopes. *Z. Geomorphol. Suppl. Band*, 25, 110-113, 1976.

Trofimov, A. M., and Moskovkin, V. M., Mathematical simulation of stable and equilibrium river bed profiles and slopes. *Earth Surf. Proc. Landf.*, 8, 383-390, 1983.

Trofimov, A. M., and Moskovkin, V. M., Diffusion models of slope development. *Earth Surf. Proc. Landf.*, 9, 435-453, 1984.

Wolman, G., and Gerson, R., Relative Scales of time and effectiveness of climate in watershed geomorphology. *Earth Surf. Proc.*, 3, 189-208, 1978.

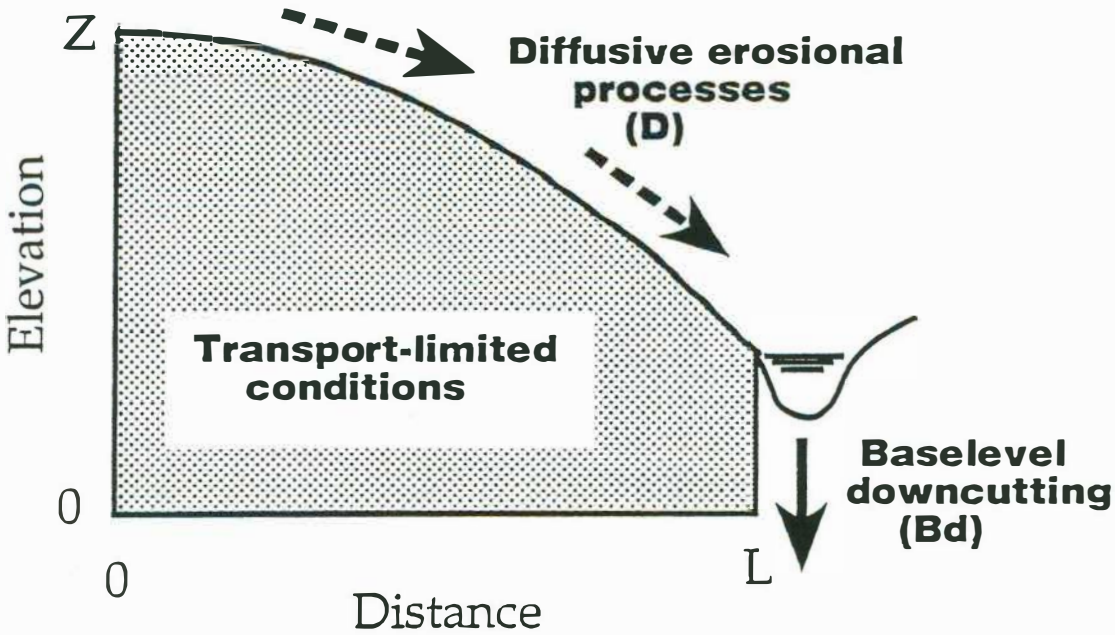

Boundary Conditions

$$\left.\frac{\partial z}{\partial x}\right|_{(0,t)} = 0 \quad \text{(flat divide)}$$

$$z(L,t) = B_d\, t$$

Initial Condition

$$\frac{\partial^2 z}{\partial x^2} = \text{constant}$$

Figure 1 - Sketch diagram of the diffusion-based model used here. The initial morphology is always a convex-up profile with constant curvature and transport-limited conditions are assumed during the entire evolution. The profile evolves under a constant diffusion coefficient (D) and a constant incision rate (B_d) at the bottom of the hillslope, while the divide is kept flat (slope zero). Although such incision rate is shown here as river incision, other processes like landsliding can play a similar role (from Chapter 1).

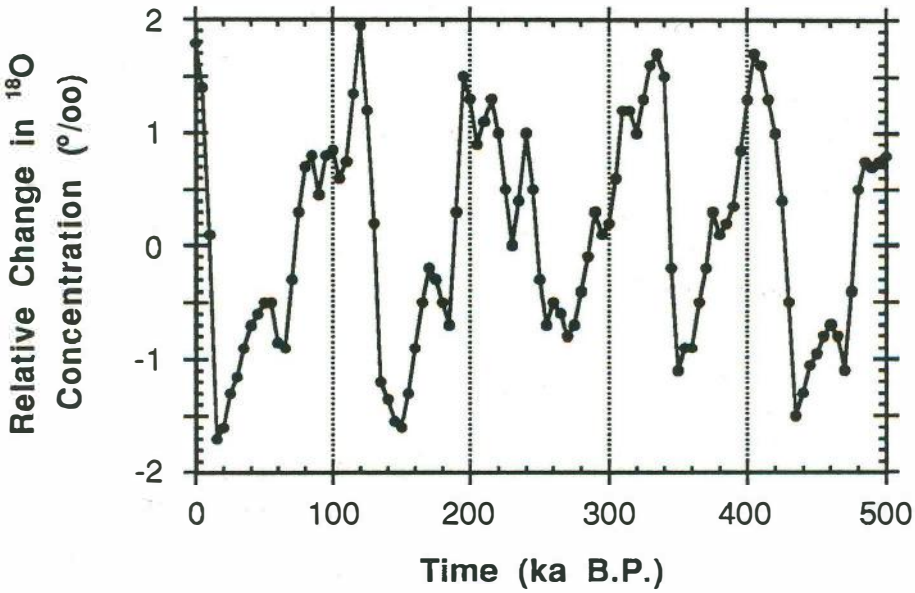

Figure 2 - ^{18}O isotopic record of deep sea sediments for the last 500 ka, and digitized for every 5ka (modified from Summerfield, 1991, figure 17.3).

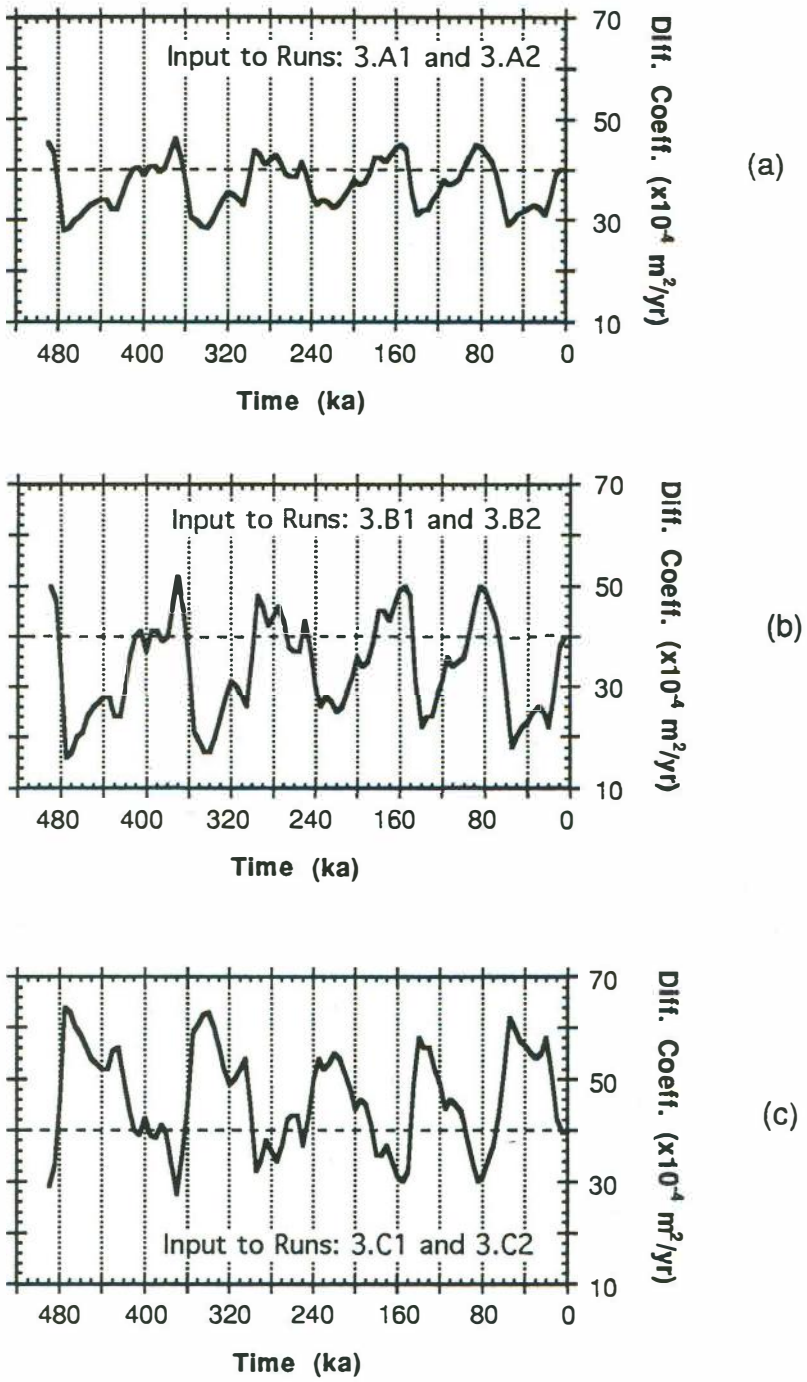

Figure 3 - Three interpretations of the ^{18}O oscillations (see Figure 2) as changes in the diffusion coefficient: Run 3.A (a), Run 3.B (b), and Run 3.C (c). In all the graphs we plot the changes in the diffusion coefficient with time from the beginning of the experiment. See text for the explanation of how these 3 curves were derived from Figure 2.

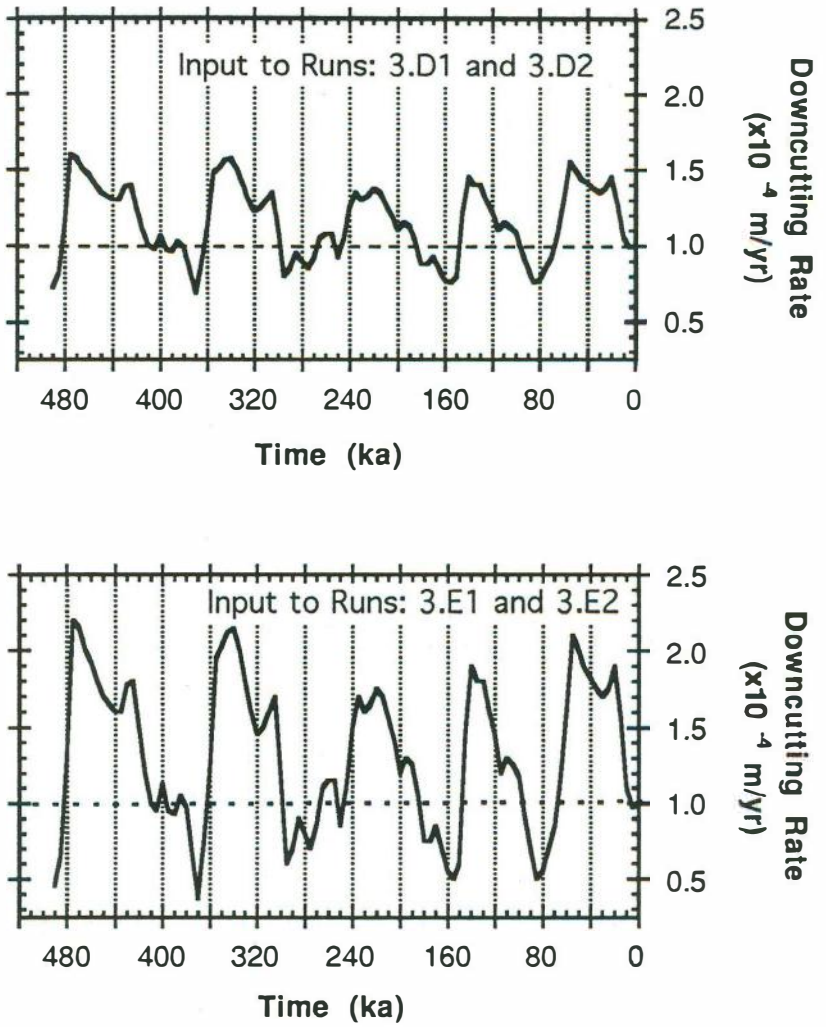

Figure 4 - Two interpretations of the ^{18}O oscillations (see Figure 2) as changes in the downcutting rate: Run 3.D (a), and Run 3.E (b). In all the graphs we plot the changes in the diffusion coefficient with time from the beginning of the experiment. See text for the explanation of how these 3 curves were derived from Figure 2.

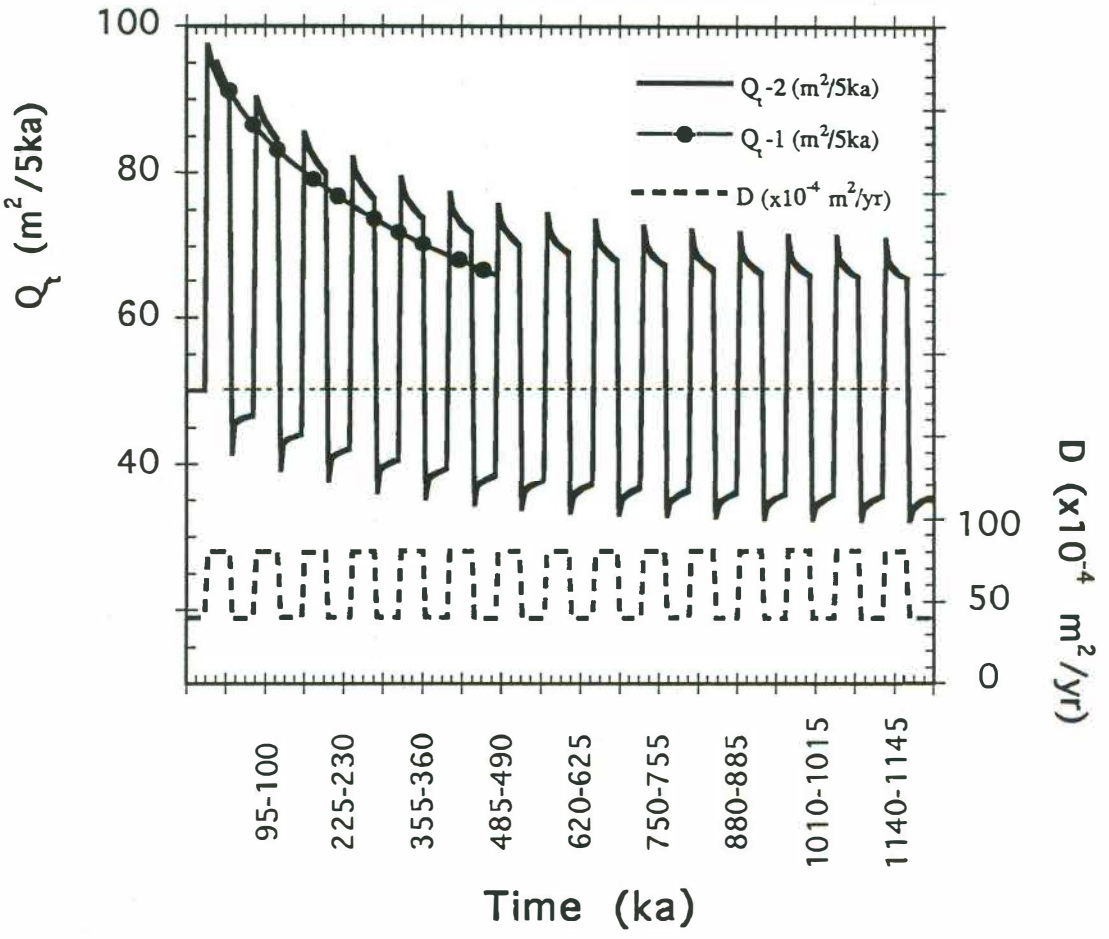

Figure 5 - Temporal response of the total sediment flux (Q_t) to step-wise oscillations in the diffusion coefficient (D). The hillslope profile is 100 m long and the diffusion coefficient changes from 40 to 80 ($x10^{-4}$ m^2/yr), and vice-versa. Q_t -2 shows the response of the sediment flux to the oscillations while Q_t -1 shows the response of the sediment flux if we had imposed just the first step-change (and had sustained it for the entire simulation). The downcutting rate is kept constant (10^{-4} m/yr), and the horizontal dashed line in the middle of the plot is the equilibrium value for the total sediment flux.

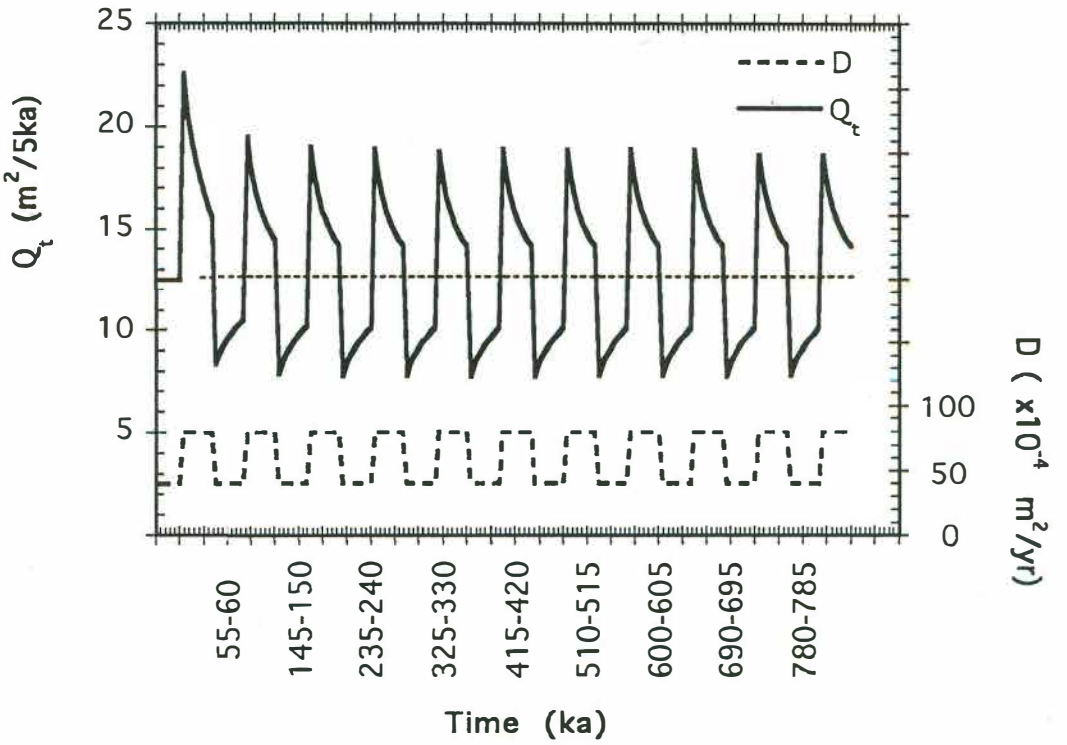

Figure 6 - Temporal response of the total sediment flux (Q_t) to step-wise oscillations in the diffusion coefficient (D). The hillslope profile is 25 m long and the diffusion coefficient changes from 40 to 80 (x10^{-4} m^2/yr), and vice-versa. The downcutting rate is kept constant (10^{-4} m/yr), and the horizontal dashed line in the middle of the plot is the equilibrium value for the total sediment flux.

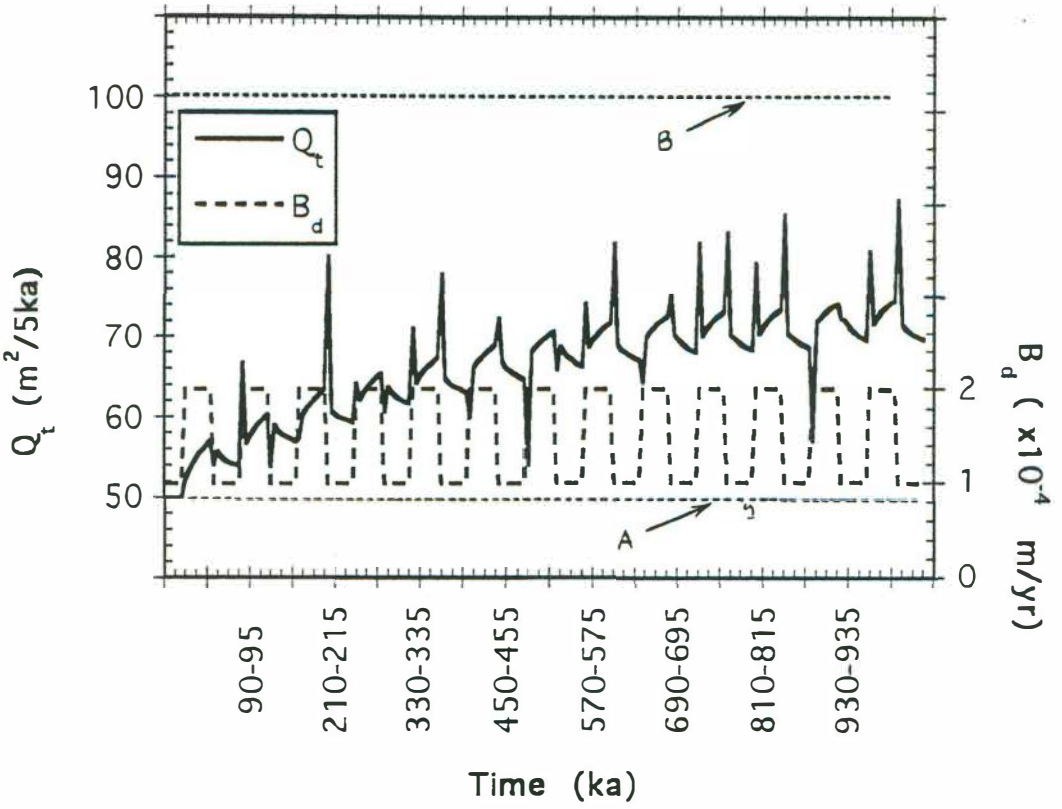

Figure 7 - Temporal response of the total sediment flux (Q_t) to step-wise oscillations in the downcutting rate (B_d). The hillslope profile is 100 m long and the downcutting rate changes from 1.0 to 2.0 ($x10^{-4}$ m/yr), and vice-versa. The diffusion coefficient is kept constant (40 $x10^{-4}$ m^2/yr) during the entire simulation. Lines A and B represent the equilibrium values for the sediment flux, associated with the lower (initial) and upper values of the downcutting rate, respectively.

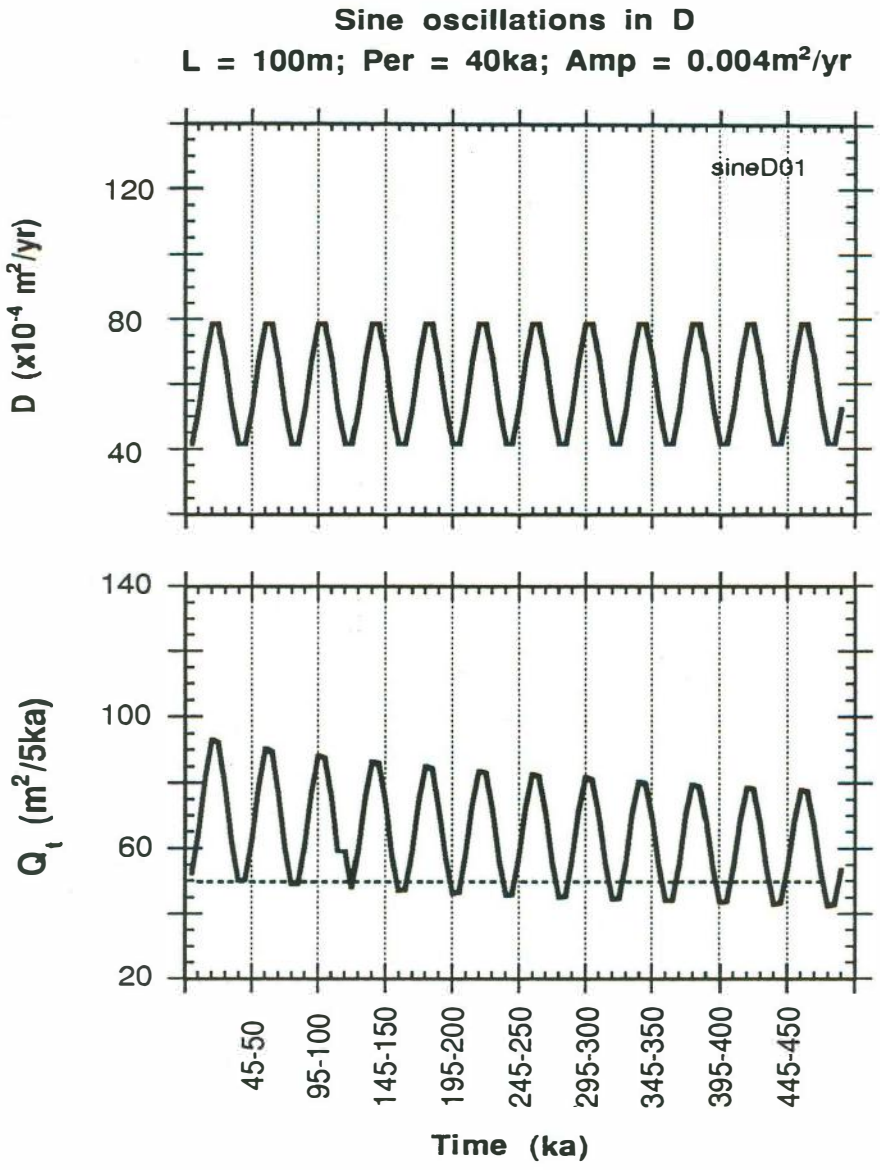

Figure 8 - Temporal response of the total sediment flux (Q_t) to sine oscillations in the diffusion coefficient (D). The hillslope profile is 100 m long and the diffusion coefficient oscillates between 40 and 80 ($x10^{-4}$ m^2/yr). The imposed oscillations have a periodicity of 40 ka and an amplitude of 40 $x10^{-4}$ m^2/yr. The downcutting rate is kept constant (10^{-4} m/yr), and the horizontal dashed line in the bottom plot is the equilibrium (initial) value for the total sediment flux.

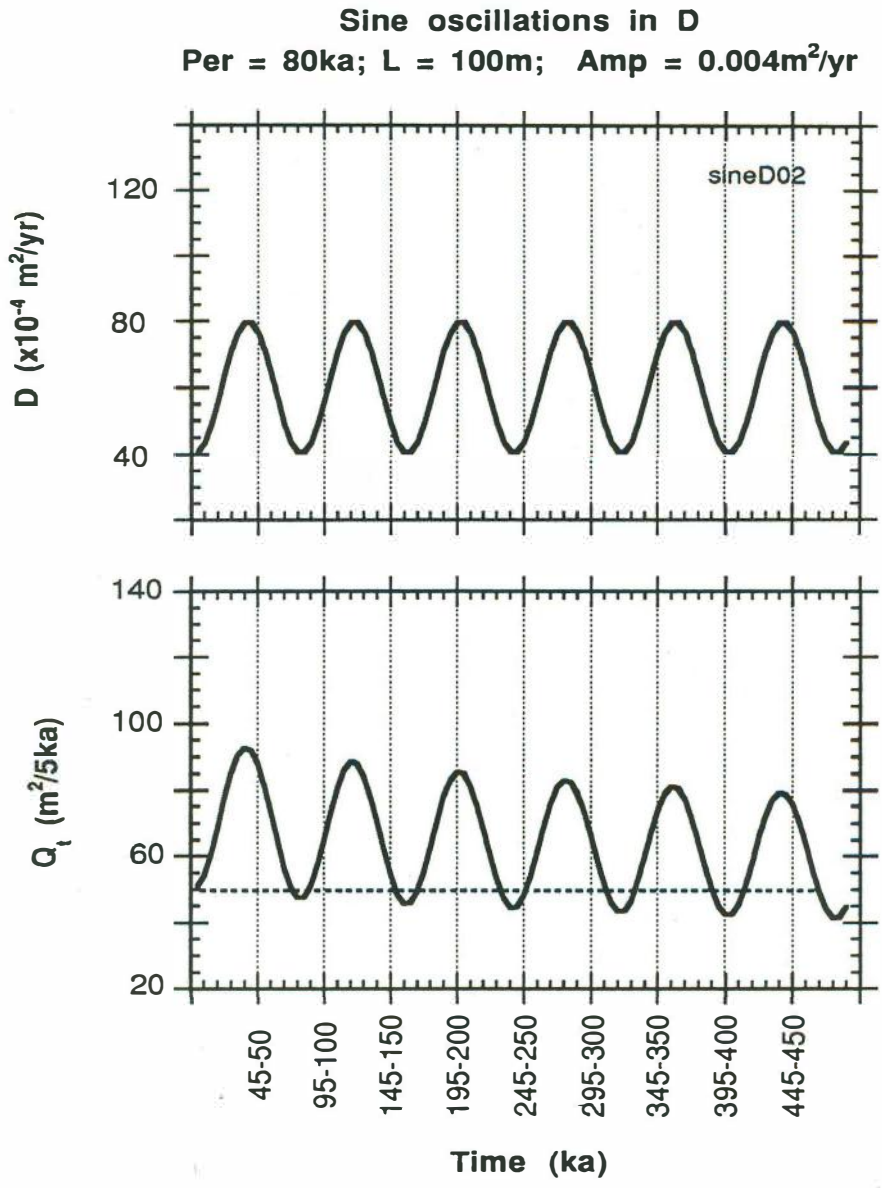

Figure 9 - Temporal response of the total sediment flux (Q_t) to sine oscillations in the diffusion coefficient (D). The hillslope profile is 100 m long and the diffusion coefficient oscillates between 40 and 80 ($x10^{-4}$ m^2/yr). The imposed oscillations have a periodicity of 80 ka and an amplitude of 40 $x10^{-4}$ m^2/yr. The downcutting rate is kept constant (10^{-4} m/yr), and the horizontal dashed line in the bottom plot is the equilibrium (initial) value for the total sediment flux.

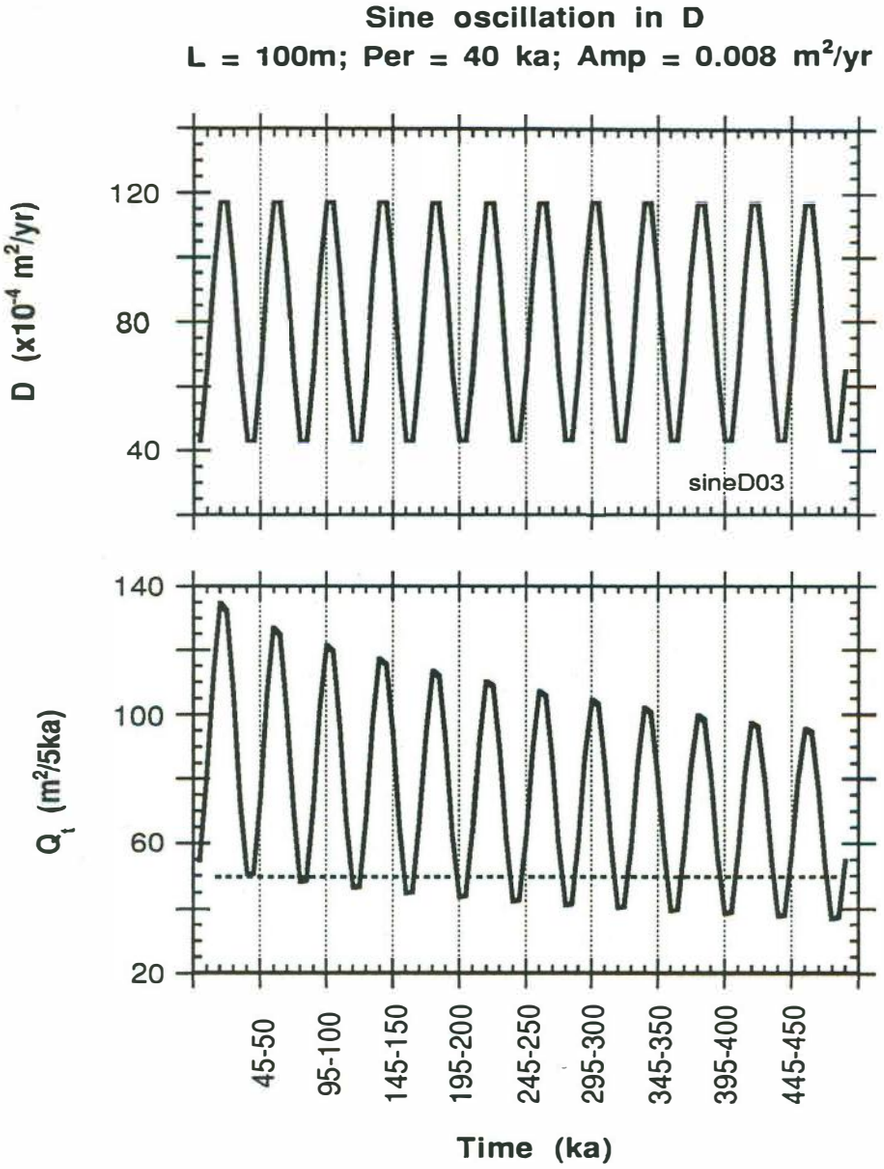

Figure 10 - Temporal response of the total sediment flux (Q_t) to sine oscillations in the diffusion coefficient (D). The hillslope profile is 100 m long and the diffusion coefficient oscillates between 40 and 120 ($x10^{-4}$ m^2/yr). The imposed oscillations have a periodicity of 40 ka and an amplitude of 80 $x10^{-4}$ m^2/yr. The downcutting rate is kept constant (10^{-4} m/yr), and the horizontal dashed line in the bottom plot is the equilibrium (initial) value for the total sediment flux.

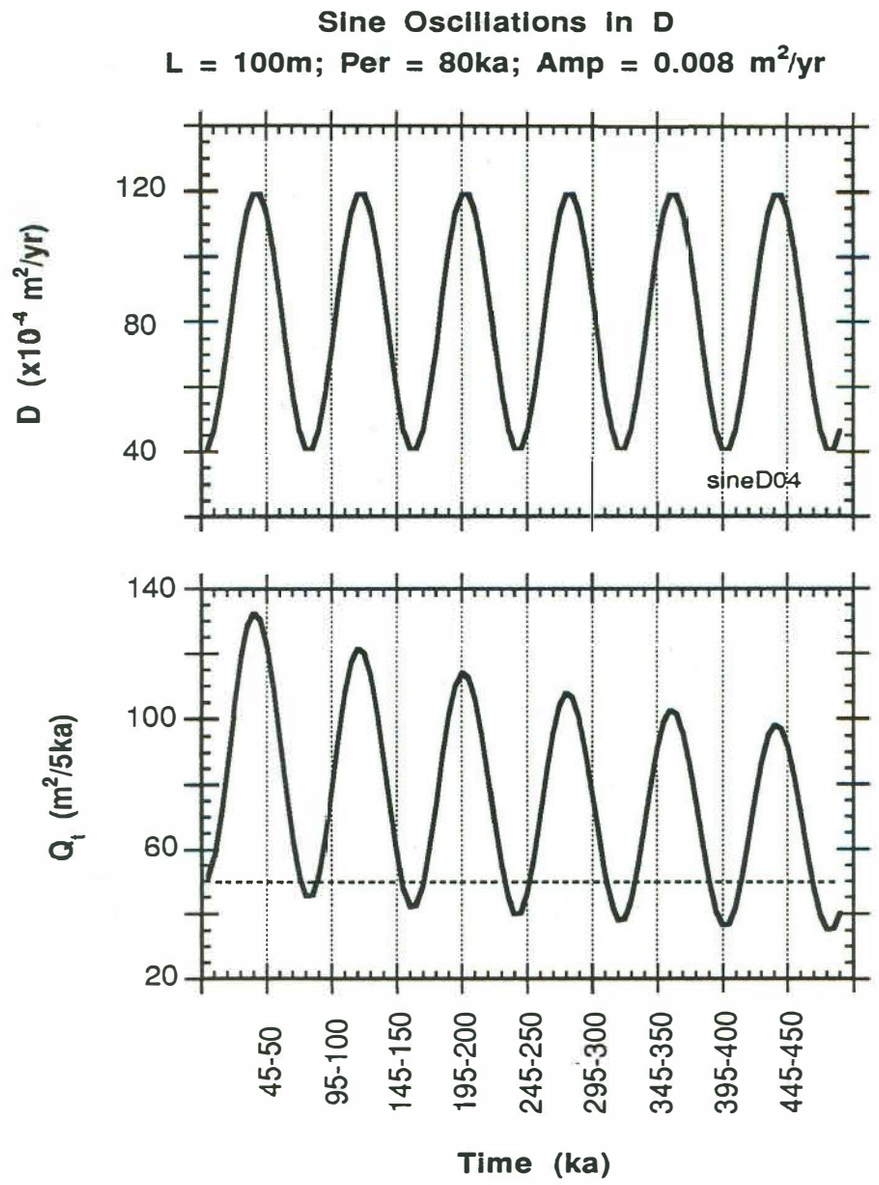

Figure 11 - Temporal response of the total sediment flux (Q_t) to sine oscillations in the diffusion coefficient (D). The hillslope profile is 100 m long and the diffusion coefficient oscillates between 40 and 120 ($x10^{-4}$ m^2/yr). The imposed oscillations have a periodicity of 80 ka and an amplitude of 80 $x10^{-4}$ m^2/yr. The downcutting rate is kept constant (10^{-4} m/yr), and the horizontal dashed line in the bottom plot is the equilibrium (initial) value for the total sediment flux.

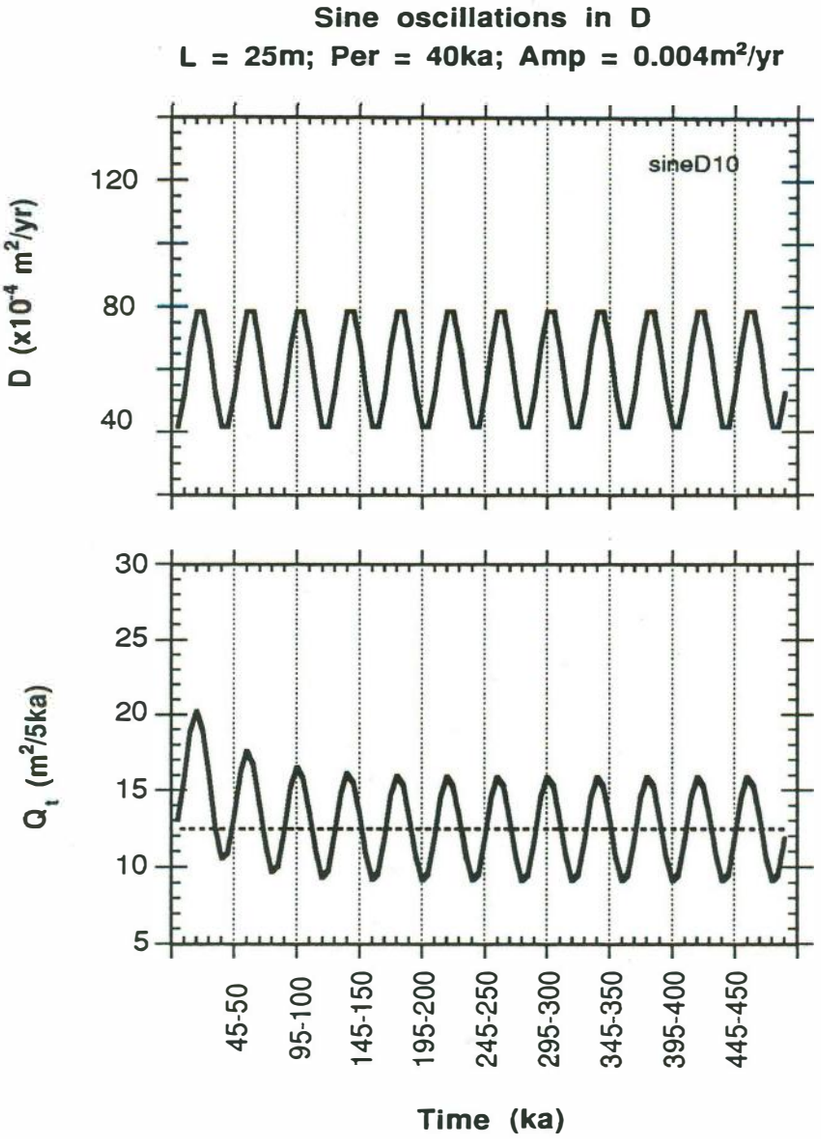

Figure 12 - Temporal response of the total sediment flux (Q_t) to sine oscillations in the diffusion coefficient (D). The hillslope profile is 25 m long and the diffusion coefficient oscillates between 40 and 80 ($x10^{-4}$ m^2/yr). The imposed oscillations have a periodicity of 40 ka and an amplitude of 40 $x10^{-4}$ m^2/yr. The downcutting rate is kept constant (10^{-4} m^2/yr), and the horizontal dashed line in the bottom plot is the equilibrium (initial) value for the total sediment flux.

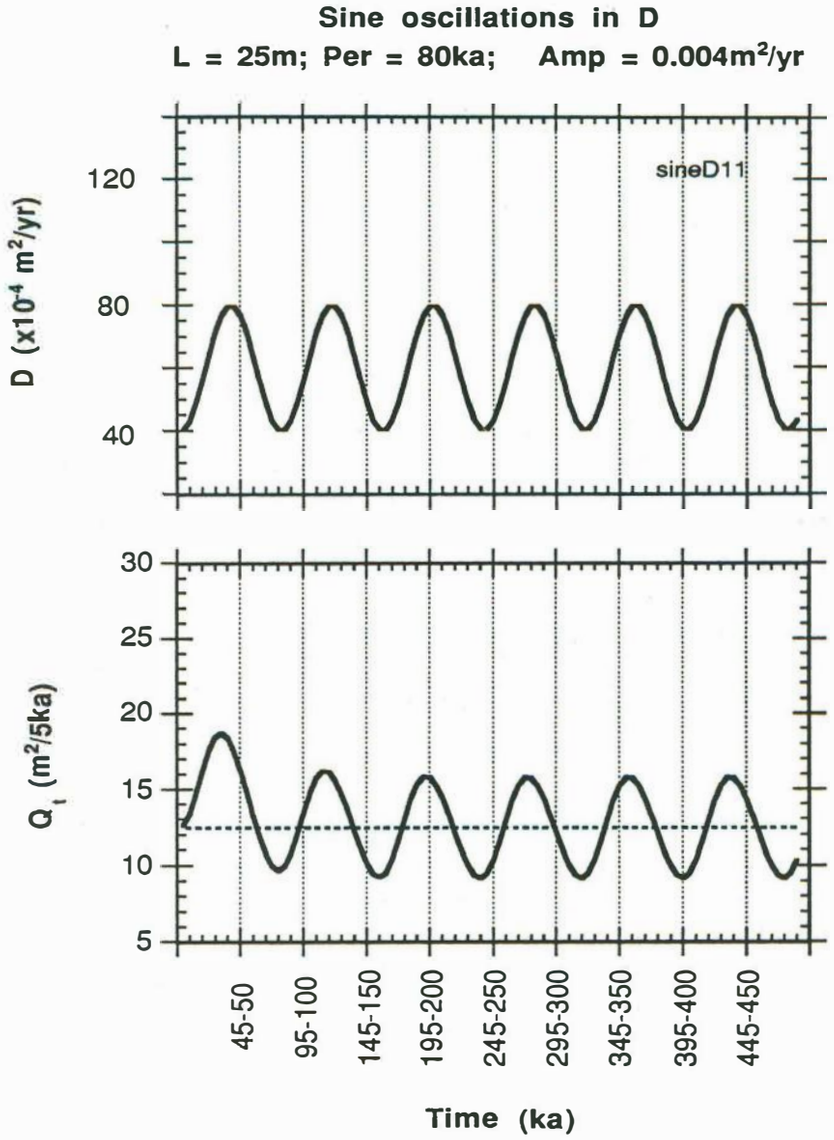

Figure 13 - Temporal response of the total sediment flux (Q_t) to sine oscillations in the diffusion coefficient (D). The hillslope profile is 25 m long and the diffusion coefficient oscillates between 40 and 80 ($x10^{-4}$ m^2/yr). The imposed oscillations have a periodicity of 80 ka and an amplitude of 40 $x10^{-4}$ m^2/yr. The downcutting rate is kept constant (10^{-4} m/yr), and the horizontal dashed line in the bottom plot is the equilibrium (initial) value for the total sediment flux.

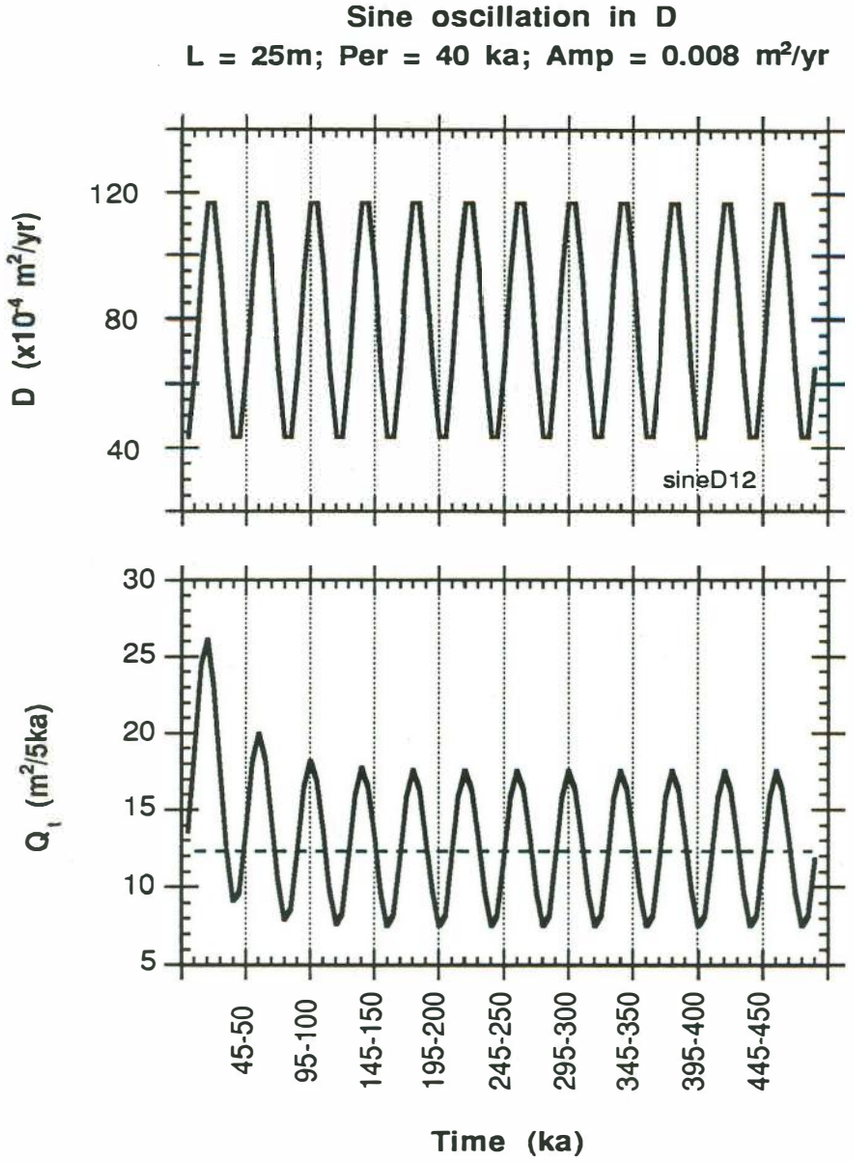

Figure 14 - Temporal response of the total sediment flux (Q_t) to sine oscillations in the diffusion coefficient (D). The hillslope profile is 25 m long and the diffusion coefficient oscillates between 40 and 120 ($x10^{-4}$ m^2/yr). The imposed oscillations have a periodicity of 40 ka and an amplitude of 80 $x10^{-4}$ m^2/yr. The downcutting rate is kept constant (10^{-4} m/yr), and the horizontal dashed line in the bottom plot is the equilibrium (initial) value for the total sediment flux.

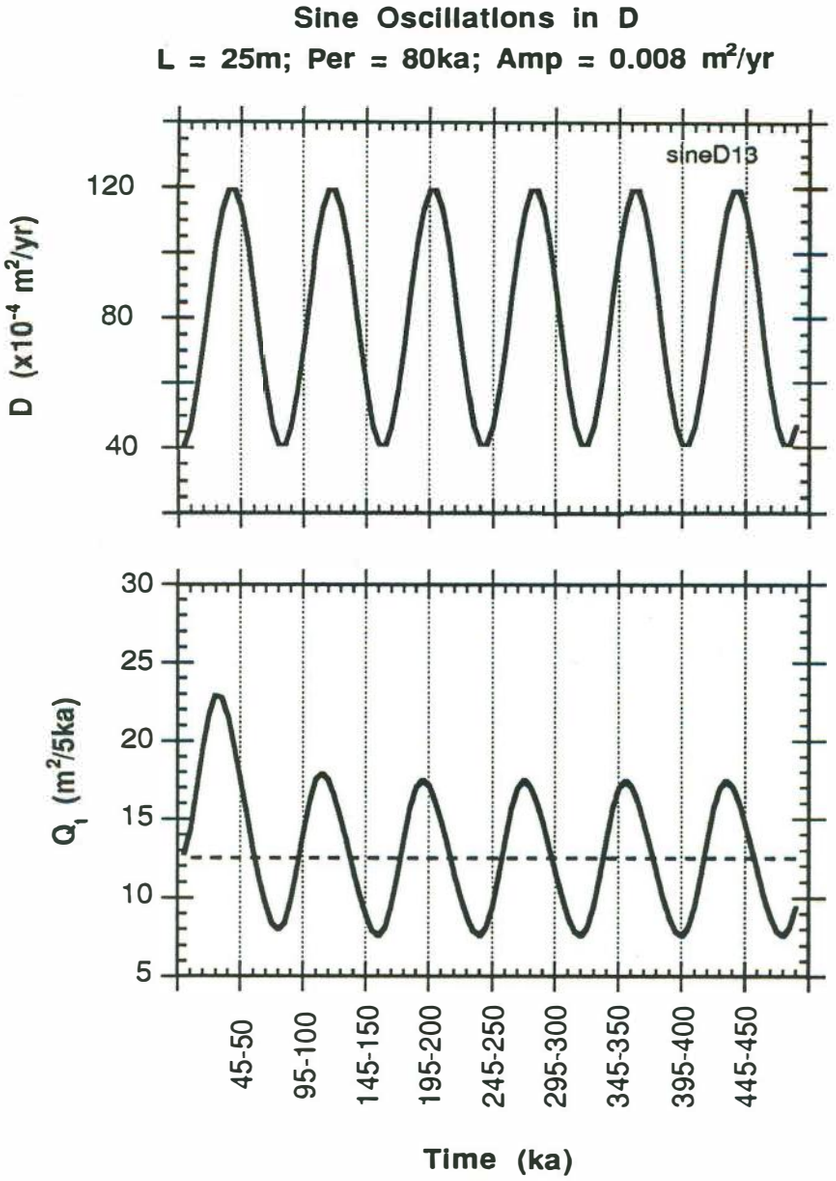

Figure 15 - Temporal response of the total sediment flux (Q_t) to sine oscillations in the diffusion coefficient (D). The hillslope profile is 25 m long and the diffusion coefficient oscillates between 40 and 120 ($x10^{-4}$ m^2/yr). The imposed oscillations have a periodicity of 80 ka and an amplitude of 80 $x10^{-4}$ m^2/yr. The downcutting rate is kept constant (10^{-4} m/yr), and the horizontal dashed line in the bottom plot is the equilibrium (initial) value for the total sediment flux.

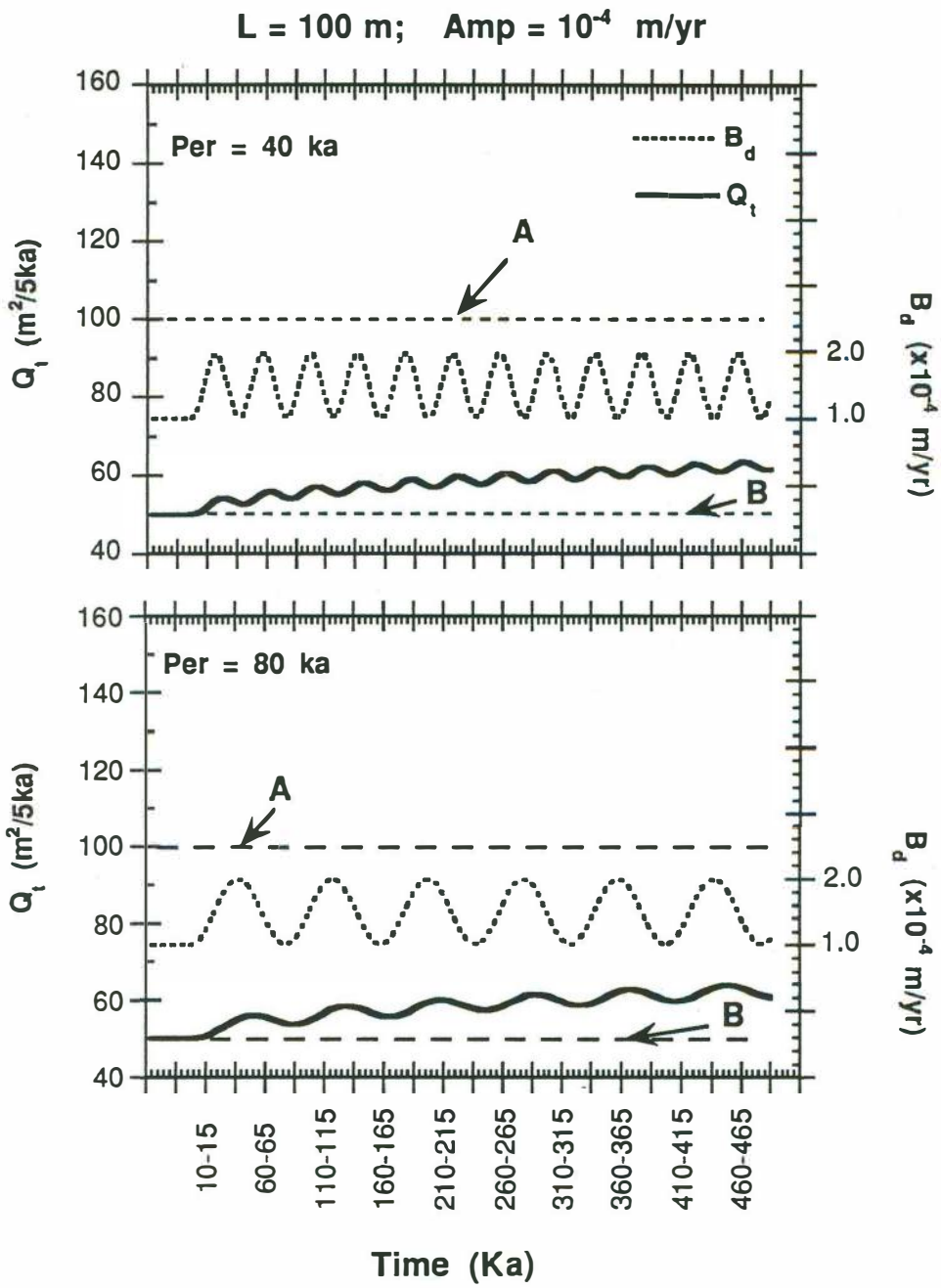

Figure 16 - Temporal response of the total sediment flux (Q_t) to sine oscillations in the downcutting rate (B_d). The hillslope profile is 100 m long and the downcutting rate oscillates between 1.0 and 2.0 ($x10^{-4}$ m/yr), resulting in an amplitude of 10^{-4} m/yr. The imposed oscillations have a periodicity of 40 ka (top) and 80 ka (bottom). The diffusion coefficient is kept constant (40 $x10^{-4}$ m^2/yr), and the horizontal lines in both plots represent the equilibrium values for the sediment flux associated with the lower (B) and upper (A) downcutting rates.

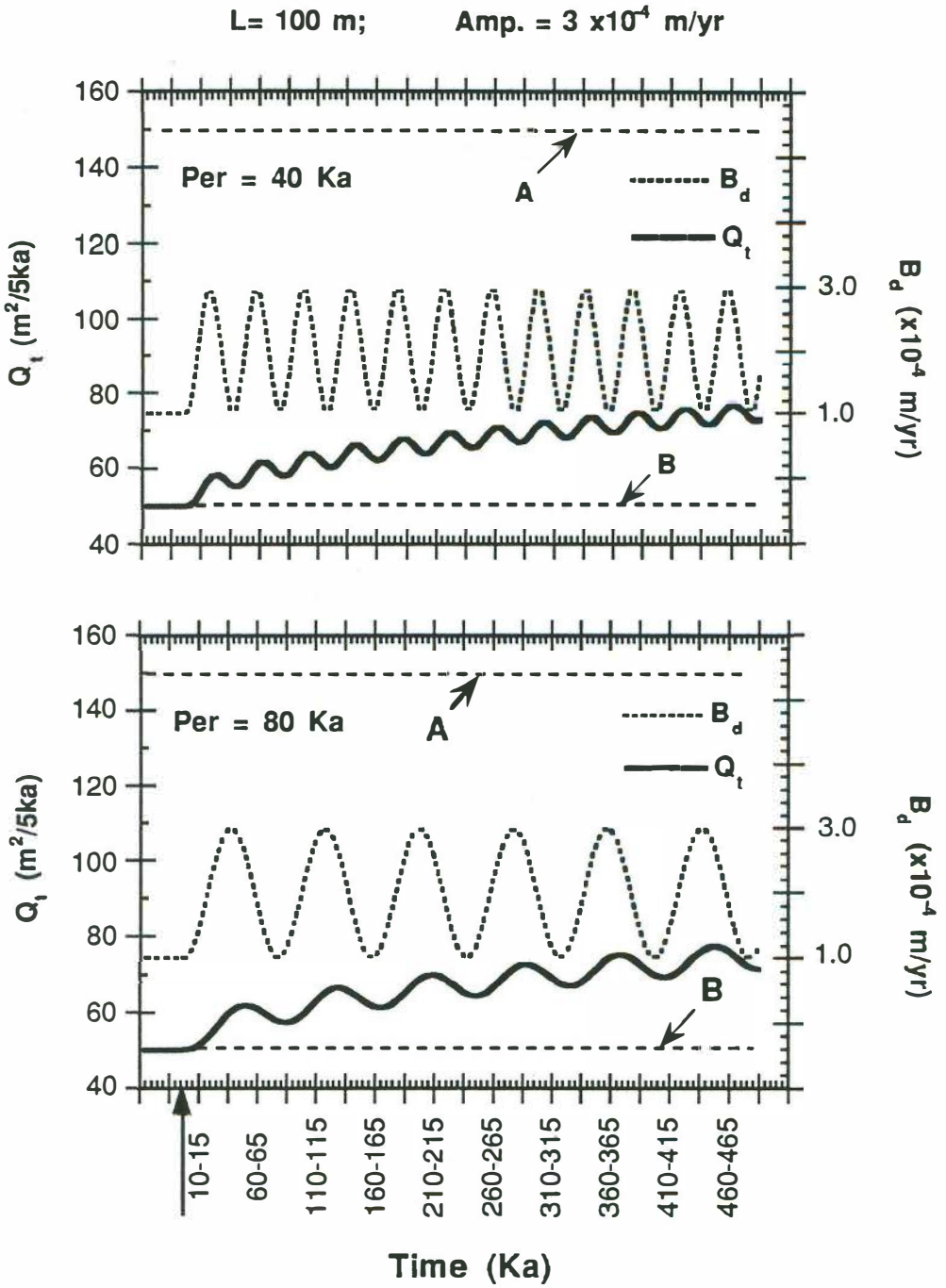

Figure 17 - Temporal response of the total sediment flux (Q_t) to sine oscillations in the downcutting rate (B_d). The hillslope profile is 100 m long and the downcutting rate oscillates between 1.0 and 3.0 ($x10^{-4}$ m/yr), resulting in an amplitude of 2.0 $x10^{-4}$ m/yr. The imposed oscillations have a periodicity of 40 ka (top) and 80 ka (bottom). The diffusion coefficient is kept constant (40 $x10^{-4}$ m^2/yr), and the horizontal lines in both plots represent the equilibrium values for the sediment flux associated with the lower (B) and upper (A) downcutting rates.

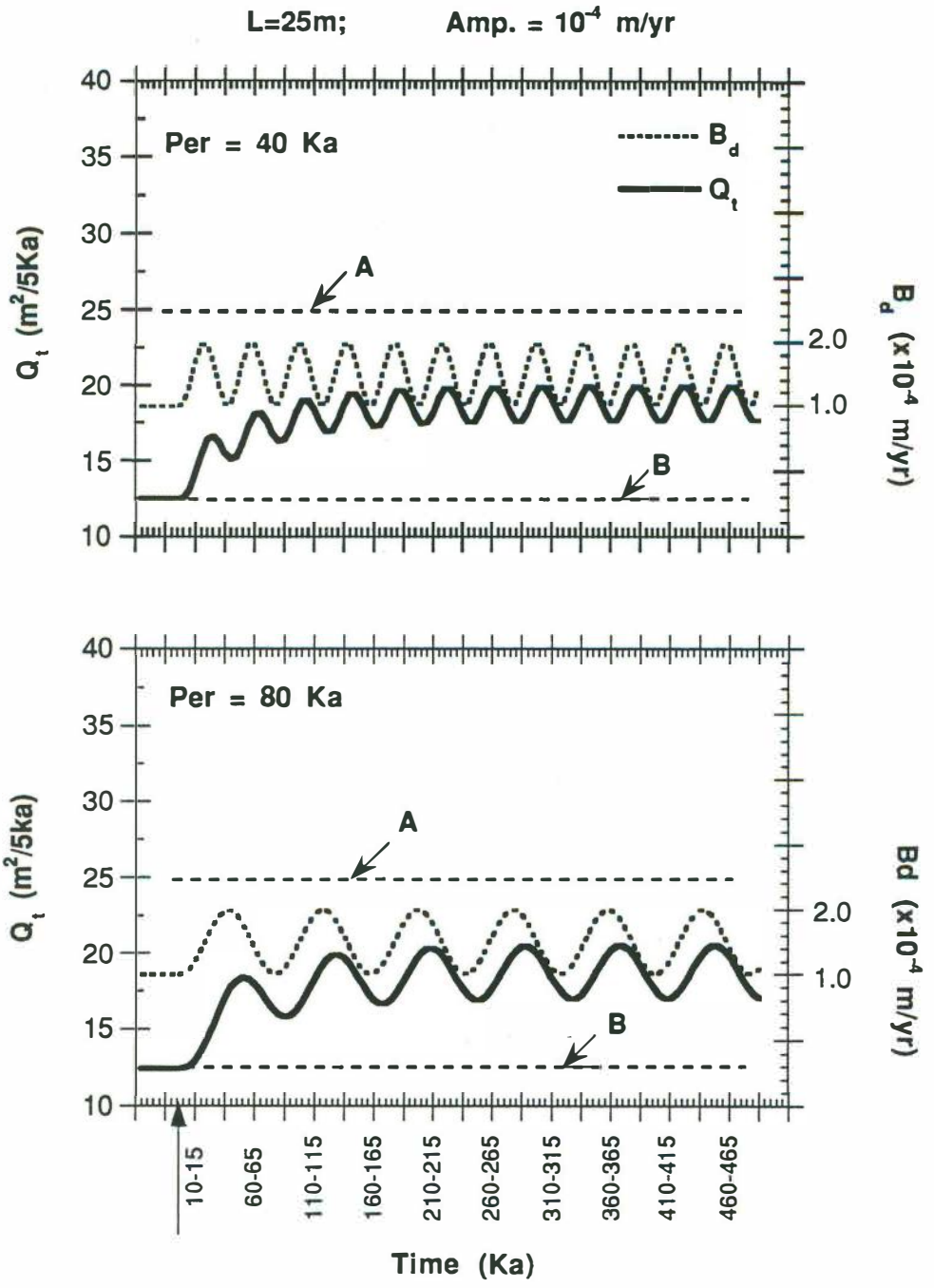

Figure 18 - Temporal response of the total sediment flux (Q_t) to sine oscillations in the downcutting rate (B_d). The hillslope profile is 25 m long and the downcutting rate oscillates between 1.0 and 2.0 ($x10^{-4}$ m/yr), resulting in an amplitude of 10^{-4} m/yr. The imposed oscillations have a periodicity of 40 ka (top) and 80 ka (bottom). The diffusion coefficient is kept constant (40 $x10^{-4}$ m^2/yr), and the horizontal lines in both plots represent the equilibrium values for the sediment flux associated with the lower (B) and upper (A) downcutting rates.

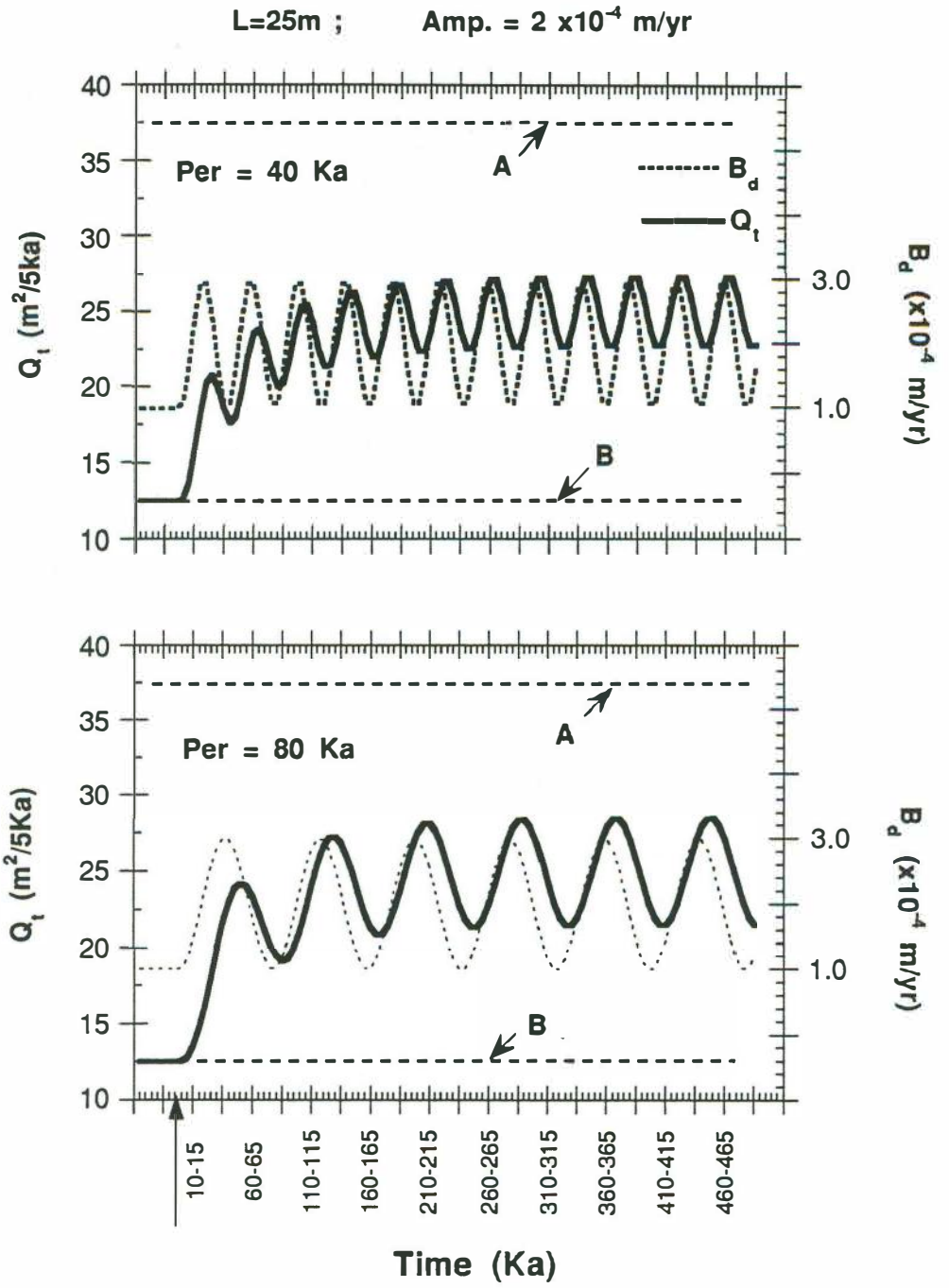

Figure 19 - Temporal response of the total sediment flux (Q_t) to sine oscillations in the downcutting rate (B_d). The hillslope profile is 25 m long and the downcutting rate oscillates between 1.0 and 3.0 ($x10^{-4}$ m/yr), resulting in an amplitude of 2.0 $x10^{-4}$ m/yr. The imposed oscillations have a periodicity of 40 ka (top) and 80 ka (bottom). The diffusion coefficient is kept constant (40 $x10^{-4}$ m^2/yr), and the horizontal lines in both plots represent the equilibrium values for the sediment flux associated with the lower (B) and upper (A) downcutting rates.

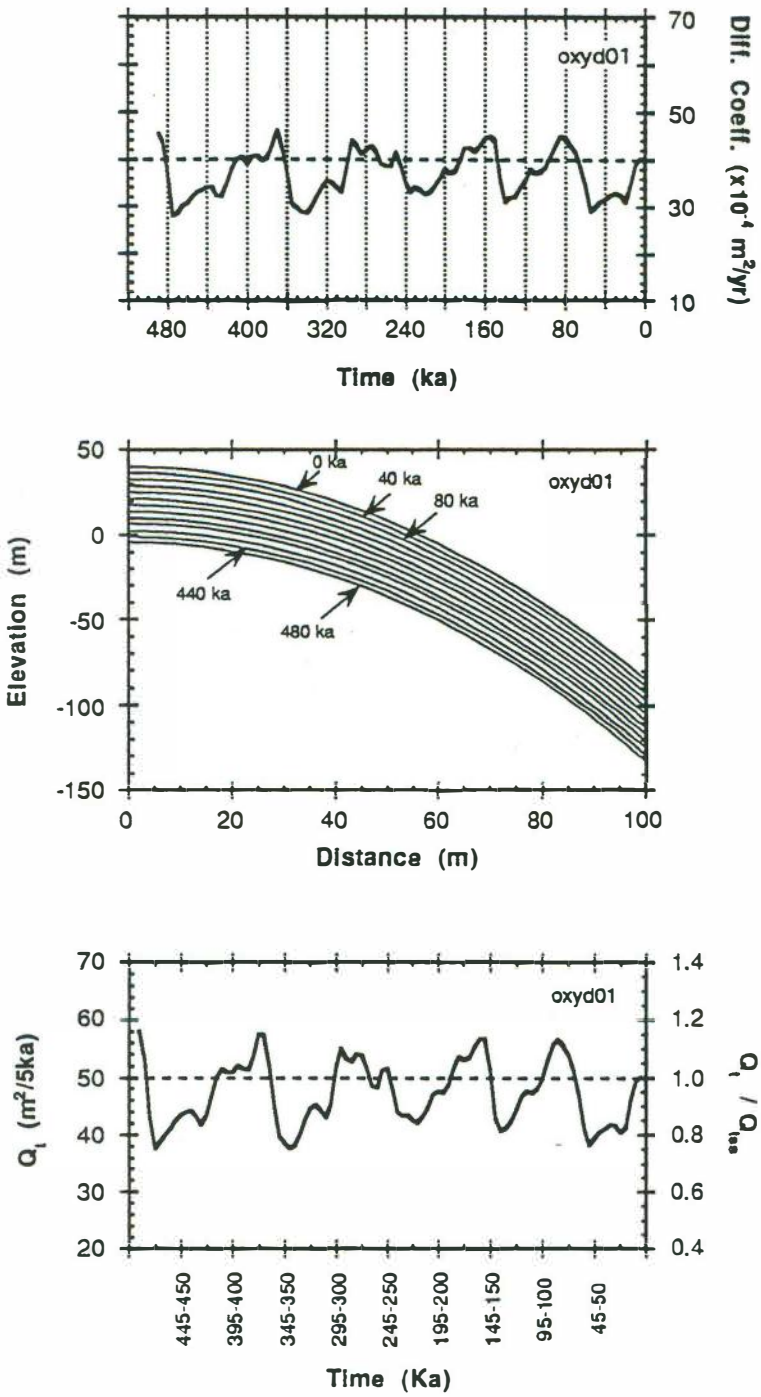

Figure 20 - Response of 100 m long hillslope profiles to the ^{18}O-based oscillations in the diffusion coefficient (Run 3.A1). Plot (a) shows the imposed changes in the diffusion coefficient against time from the beginning of the simulation. Plot (b) presents the associated morphological response for every 40 ka. Plot (c) shows the temporal variation in the total sediment flux (Q_t) - left, and in the ratio of its value over the sediment flux at equilibrium (Q_{tss}) - right.

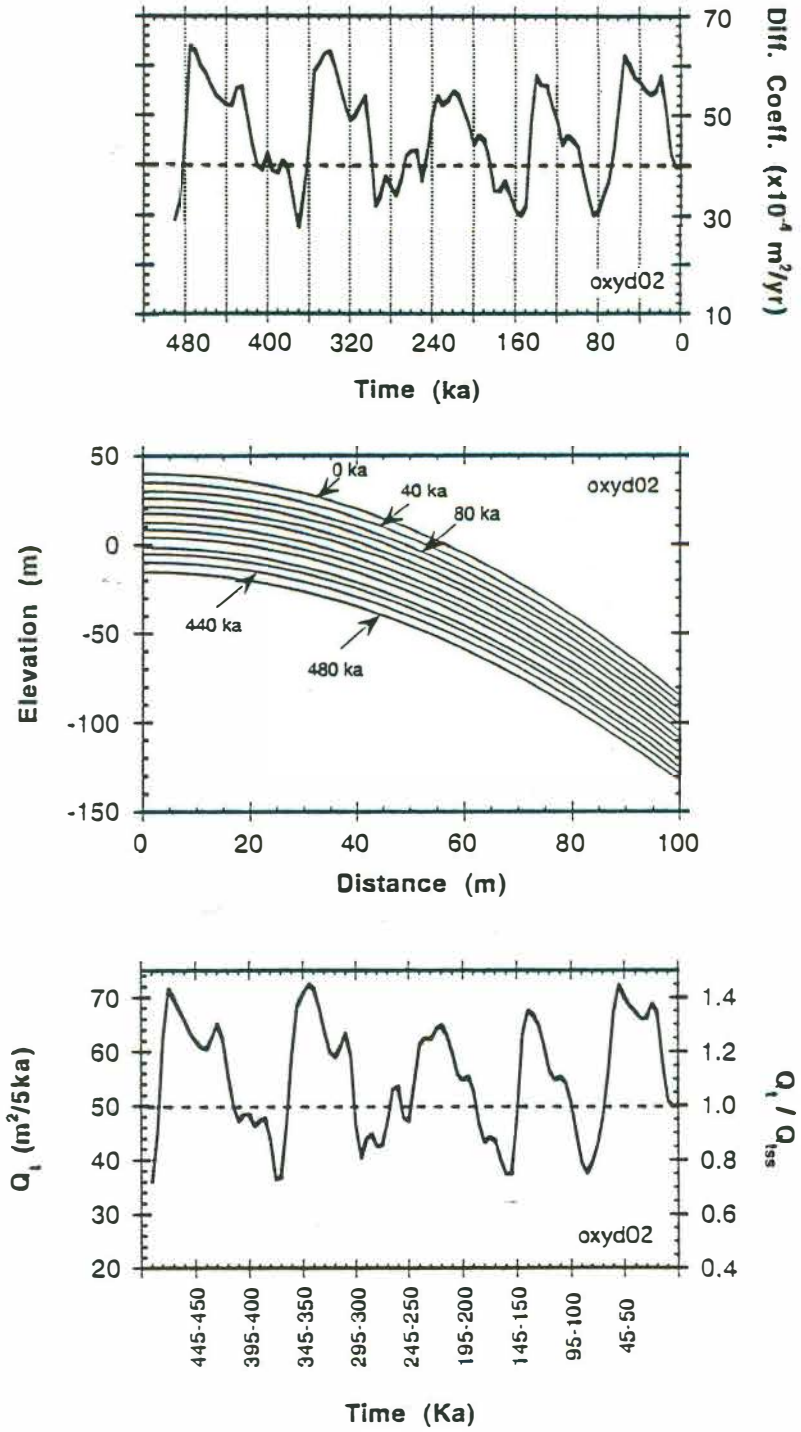

Figure 21 - Response of 100 m long hillslope profiles to the ^{18}O-based oscillations in the diffusion coefficient (Run 3.B1). Plot (a) shows the imposed changes in the diffusion coefficient against time from the beginning of the simulation. Plot (b) presents the associated morphological response for every 40 ka. Plot (c) shows the temporal variation in the total sediment flux (Q_t) - left, and in the ratio of its value over the sediment flux at equilibrium (Q_{tss}) - right.

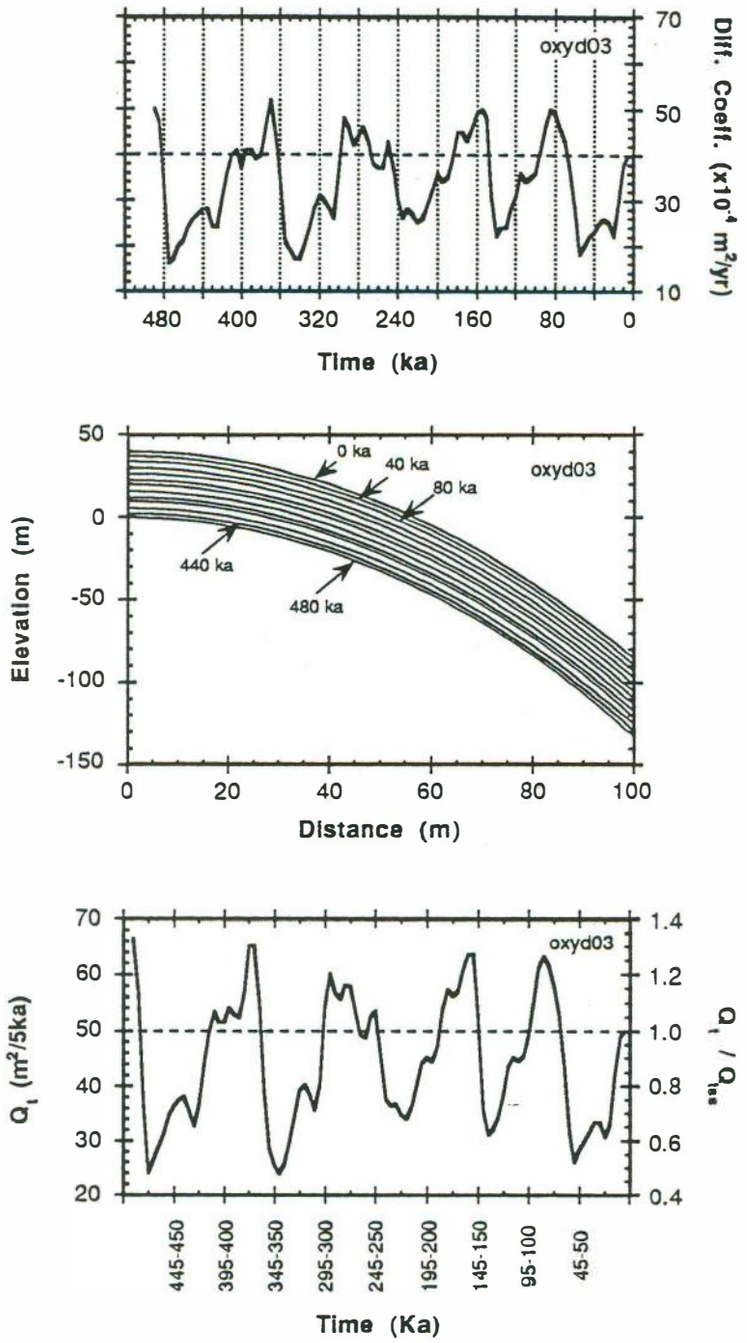

Figure 22 - Response of 100 m long hillslope profiles to the ^{18}O-based oscillations in the diffusion coefficient (Run 3.C1). Plot (a) shows the imposed changes in the diffusion coefficient against time from the beginning of the simulation. Plot (b) presents the associated morphological response for every 40 ka. Plot (c) shows the temporal variation in the total sediment flux (Q_t) - left, and in the ratio of its value over the sediment flux at equilibrium (Q_{tss}) - right.

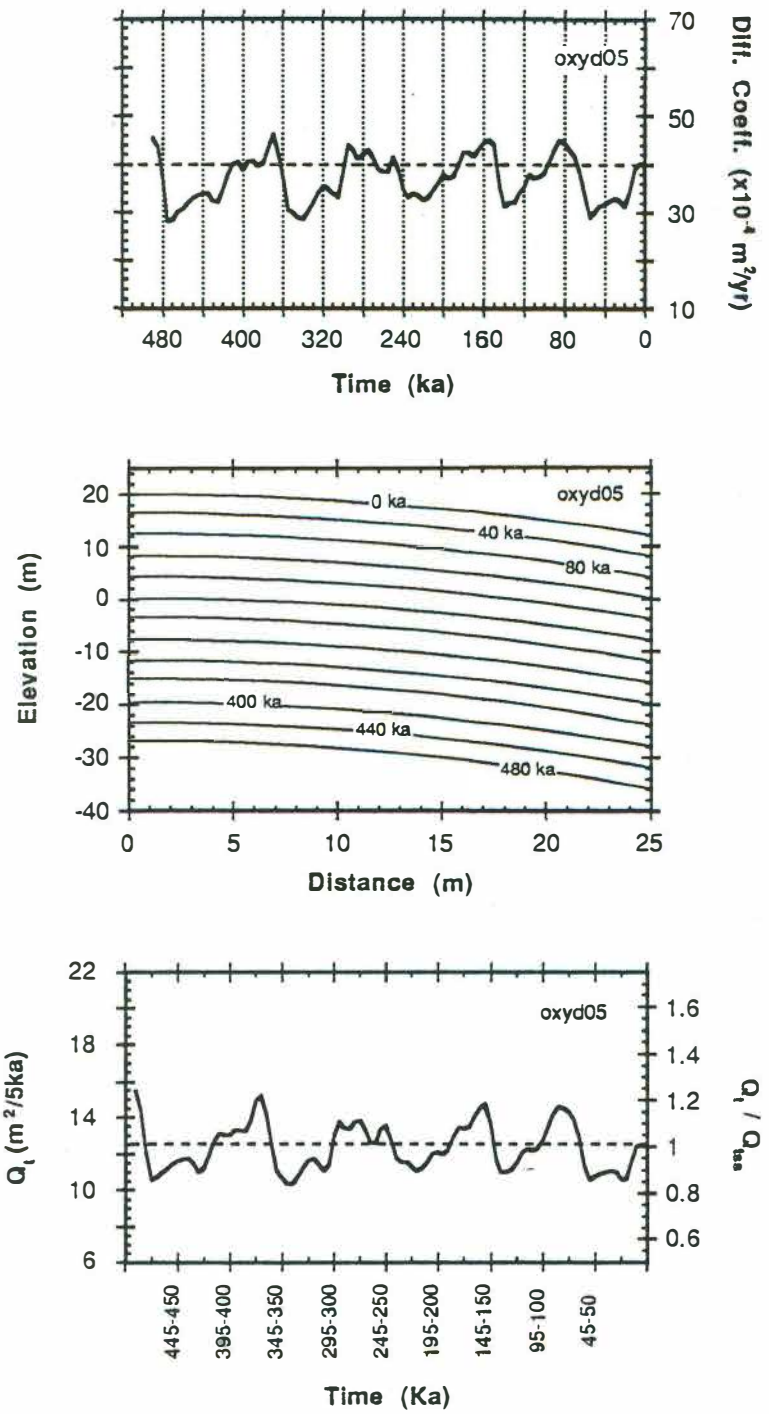

Figure 23 - Response of 25 m long hillslope profiles to the ^{18}O-based oscillations in the diffusion coefficient (Run 3.A2) Plot (a) shows the imposed changes in the diffusion coefficient against time from the beginning of the simulation. Plot (b) presents the associated morphological response for every 40 ka. Plot (c) shows the temporal variation in the total sediment flux (Q_t) - left, and in the ratio of its value over the sediment flux at equilibrium (Q_{tss}) - right.

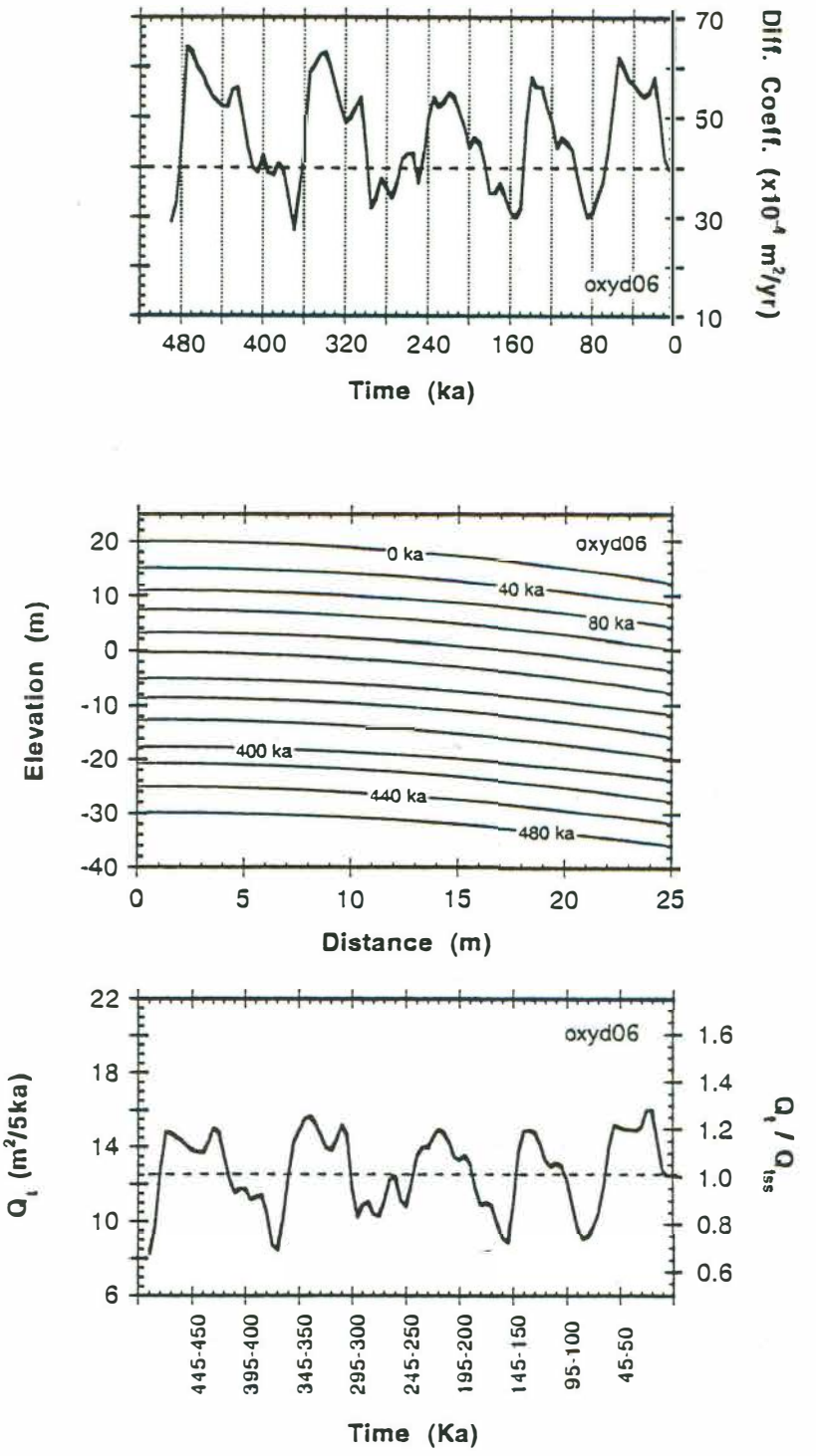

Figure 24 - Response of 25 m long hillslope profiles to the ^{18}O-based oscillations in the diffusion coefficient(Run 3.B2). Plot (a) shows the imposed changes in the diffusion coefficient against time from the beginning of the simulation. Plot (b) presents the associated morphological response for every 40 ka. Plot (c) shows the temporal variation in the total sediment flux (Q_t) - left, and in the ratio of its value over the sediment flux at equilibrium (Q_{tss}) - right.

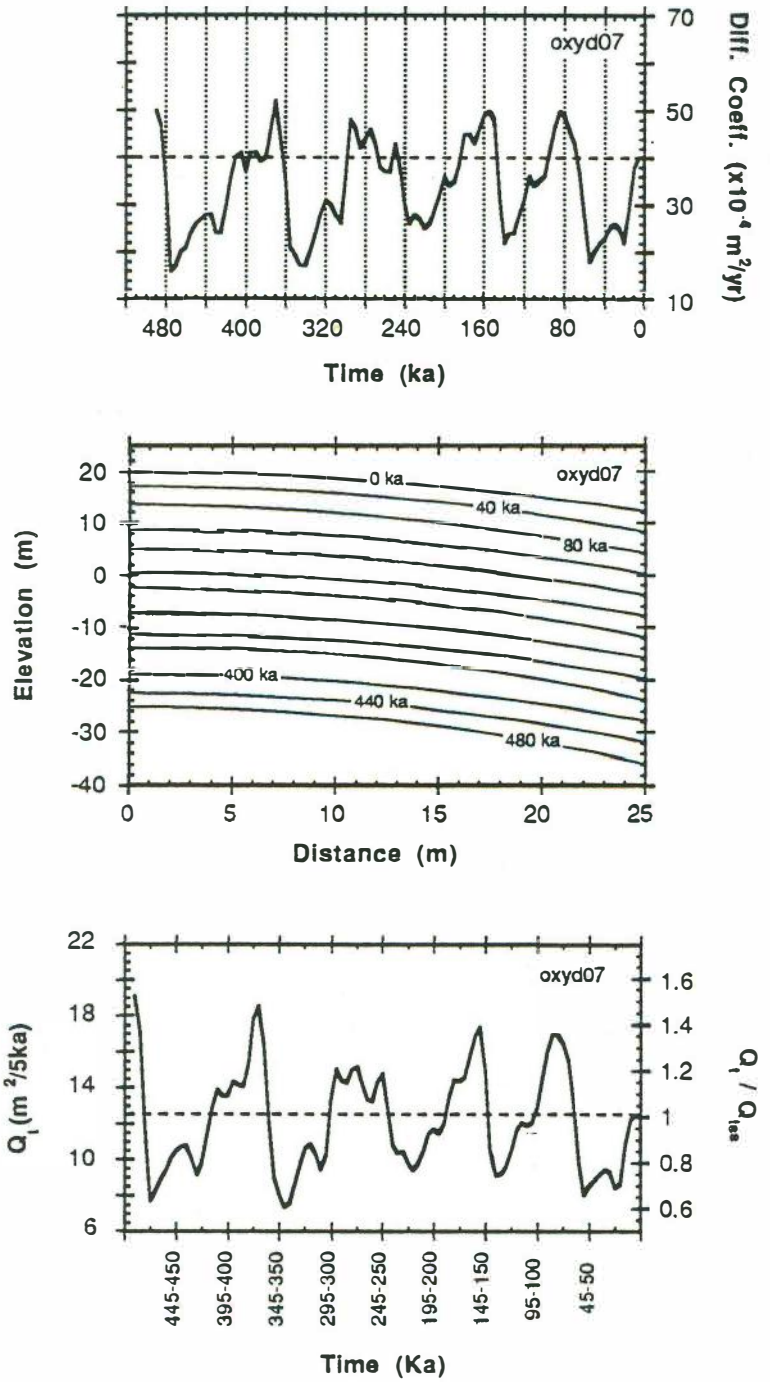

Figure 25 - Response of 25 m long hillslope profiles to the ^{18}O-based oscillations in the diffusion coefficient (Run 3.C2). Plot (a) shows the imposed changes in the diffusion coefficient against time from the beginning of the simulation. Plot (b) presents the associated morphological response for every 40 ka. Plot (c) shows the temporal variation in the total sediment flux (Q_t) - left, and in the ratio of its value over the sediment flux at equilibrium (Q_{tss}) - right.

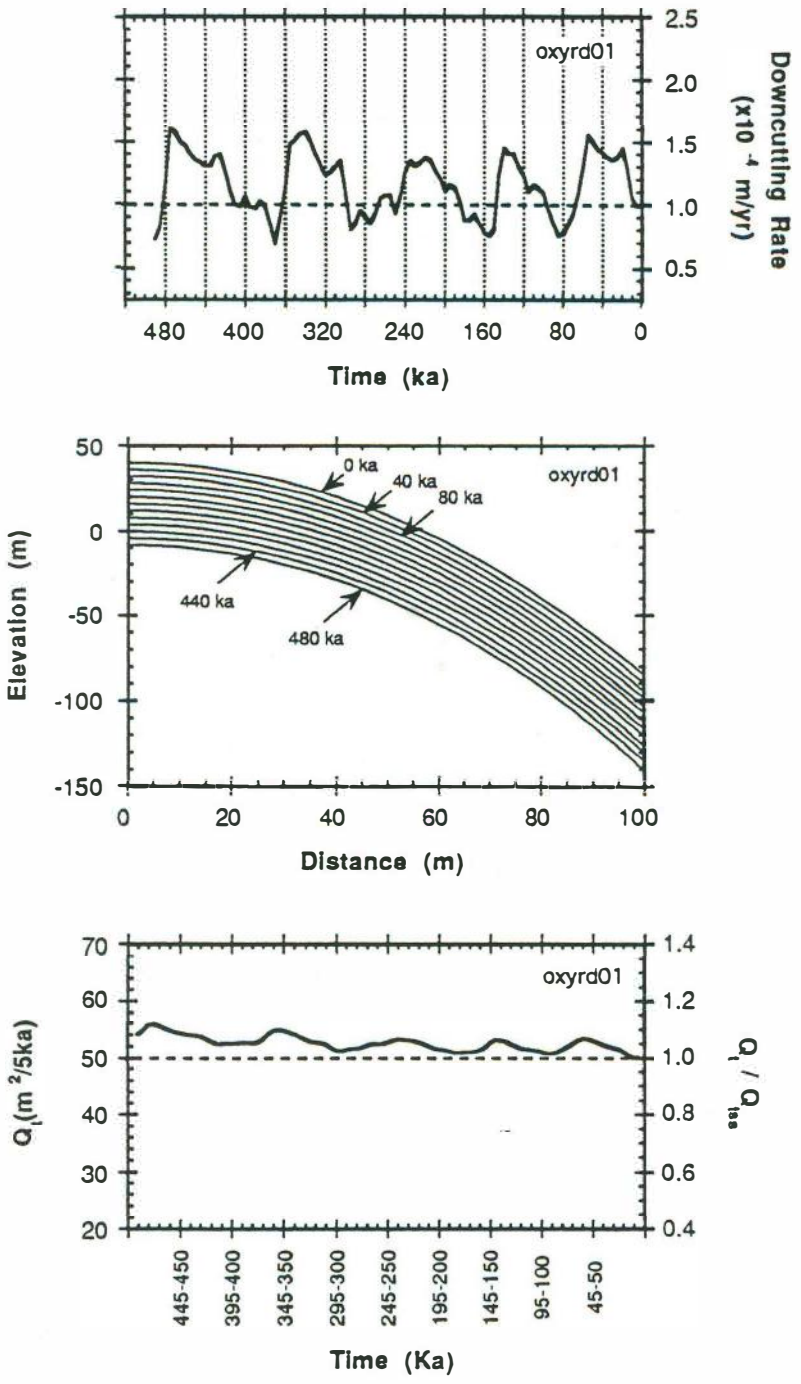

Figure 26 - Response of 100 m long hillslope profiles to the ^{18}O-based oscillations in the downcutting rate (Run 3.D1). Plot (a) shows the imposed changes in the incision rate against time from the beginning of the simulation. Plot (b) presents the associated morphological response for every 40 ka. Plot (c) shows the temporal variation in the total sediment flux (Q_t) - left, and in the ratio of its value over the sediment flux at equilibrium (Q_{tss}) - right.

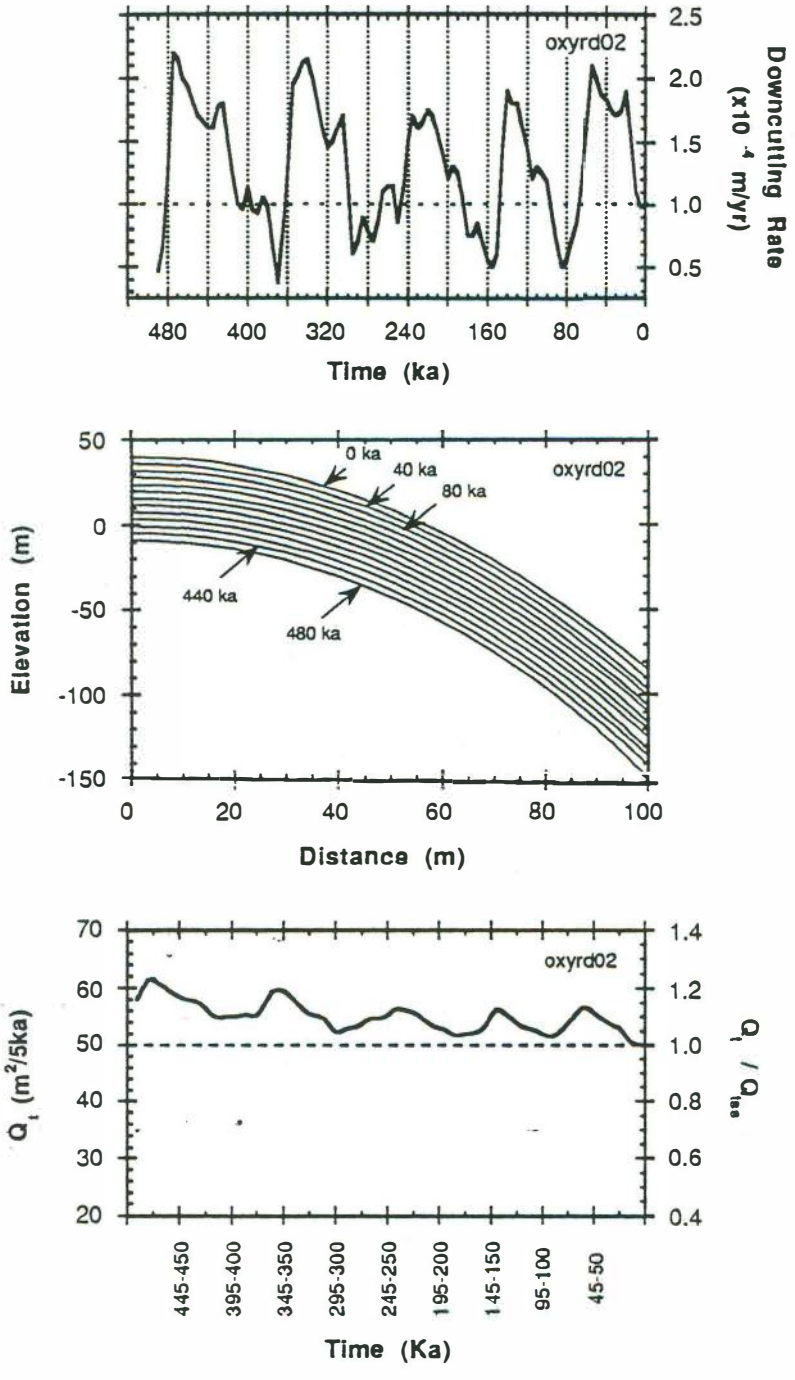

Figure 27 - Response of 100 m long hillslope profiles to the ^{18}O-based oscillations in the downcutting rate (Run 3.E1). Plot (a) shows the imposed changes in the downcutting rate against time from the beginning of the simulation. Plot (b) presents the associated morphological response for every 40 ka. Plot (c) shows the temporal variation in the total sediment flux (Q_t) - left, and in the ratio of its value over the sediment flux at equilibrium (Q_{tss}) - right.

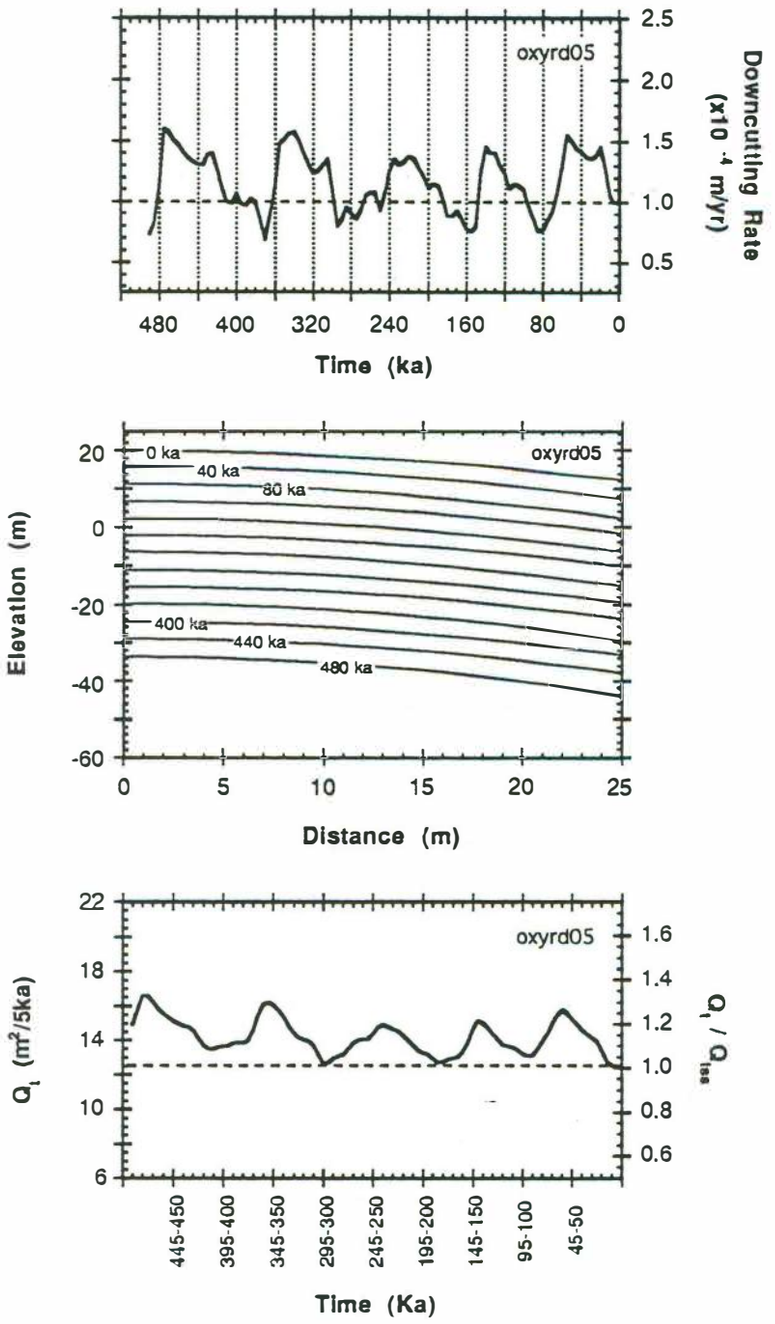

Figure 28 - Response of 25 m long hillslope profiles to the ^{18}O-based oscillations in the downcutting rate (Run 3.D2). Plot (a) shows the imposed changes in the downcutting rate against time from the beginning of the simulation. Plot (b) presents the associated morphological response for every 40 ka. Plot (c) shows the temporal variation in the total sediment flux (Q_t) - left, and in the ratio of its value over the sediment flux at equilibrium (Q_{tss}) - right.

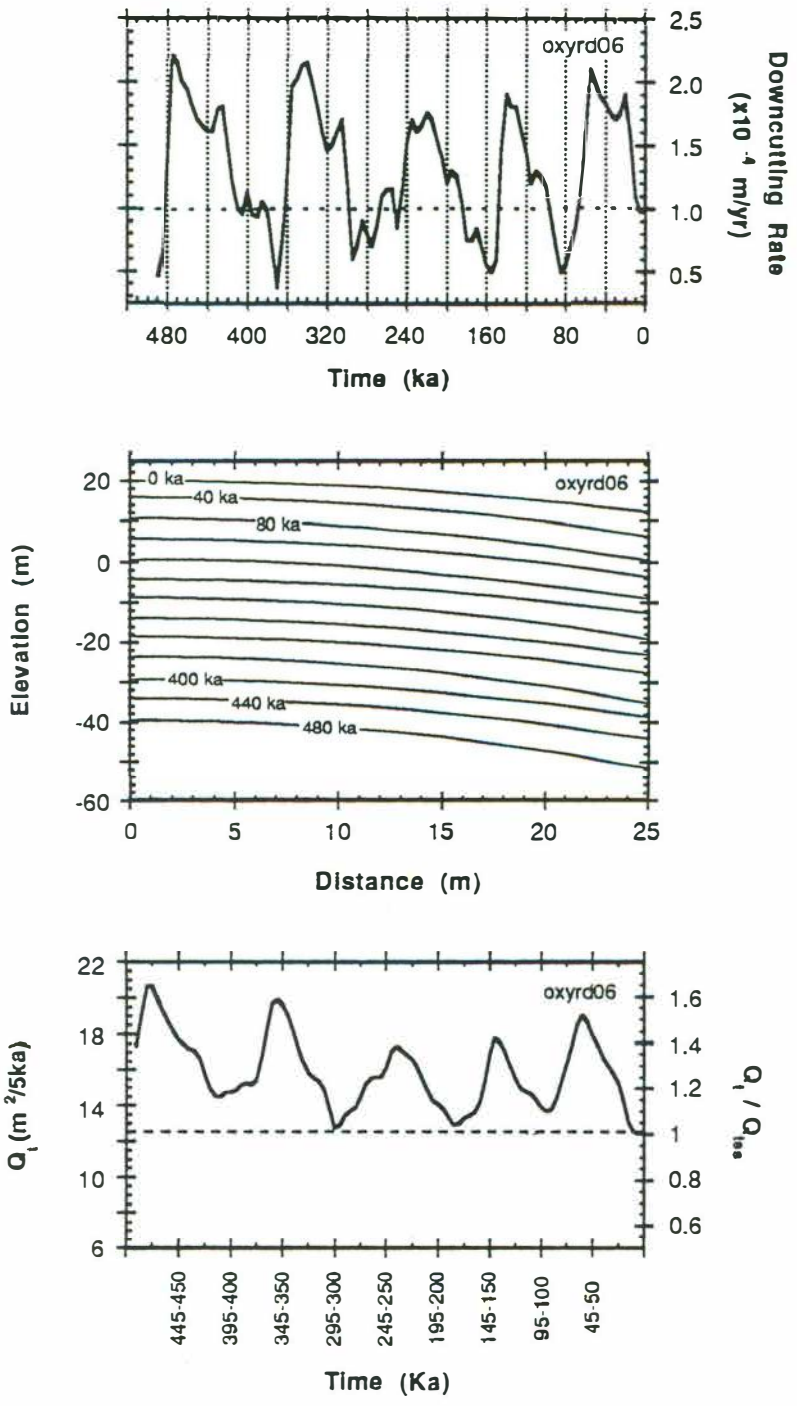

Figure 29 - Response of 25 m long hillslope profiles to the ^{18}O-based oscillations in the downcutting rate (Run 3.E2). Plot (a) shows the imposed changes in the downcutting rate against time from the beginning of the simulation. Plot (b) presents the associated morphological response for every 40 ka. Plot (c) shows the temporal variation in the total sediment flux (Q_t) - left, and in the ratio of its value over the sediment flux at equilibrium (Q_{tss}) - right.

APPENDICES

APPENDIX 1

Analytical Solution

We want to find the analytical solution of the following problem:

(1.1) $$\frac{\partial z}{\partial t} = D\frac{\partial^2 z}{\partial x^2} \qquad 0 < x < L;\ 0 < t$$

(1.2) b.c. $$\left.\frac{\partial z}{\partial x}\right|_{(0,t)} = 0$$

(1.3) $$z(L,t) = B_d t$$

(1.4) i.c. $$z(x,0) = f(x)$$

System I

where B_d and D are constants, x is distance, t is time, z is elevation, and f(x) is a polynomial.

Consider the following systems of equations:

(1.5) $$\frac{\partial u}{\partial t} = \cancel{D}\frac{\partial^2 u}{\partial x^2} \qquad 0 < x < L;\ 0 < t$$

(1.6) b.c. $$\left.\frac{\partial u}{\partial x}\right|_{(0,t)} = 0$$

(1.7) $$u(L,t) = 0$$

(1.8) i.c. $$u(x,0) = f(x)$$

System II

(1.9) $$\frac{\partial v}{\partial t} = \cancel{D}\frac{\partial^2 v}{\partial x^2} \qquad 0 < x < L;\ 0 < t$$

(1.10) b.c. $$\left.\frac{\partial v}{\partial x}\right|_{(0,t)} = 0$$

(1.11) $$v(L,t) = B_d t$$

(1.12) i.c. $$v(x,0) = 0$$

System III

Assume we can find solutions to II and III, say u and v respectively. Then, by putting

(1.13) $$z = u + v ,$$

we obtain a solution to System I.

Indeed, the formula

$$Af = \frac{\partial}{\partial t} f - D\frac{\partial^2}{\partial x^2} f$$

defines a linear operator A. Since u solves II and v solves III, with $z = u + v$, we have

$$Az = A(u + v) = Au + Av = 0 + 0 = 0.$$

Hence, Az=0 and therefore $\frac{\partial}{\partial t} z = D\frac{\partial^2}{\partial x^2} z$. Thus eq. (1.1) is satisfied. Note that

$$\left.\frac{\partial u}{\partial x}\right|_{(0,t)} = 0 \qquad \text{and}$$

$$\left.\frac{\partial v}{\partial x}\right|_{(0,t)} = 0.$$

Since $\left.\frac{\partial}{\partial x}\right|_{(0,t)}$ is linear, it follows that

$\left.\frac{\partial z}{\partial x}\right|_{(0,t)} = 0$. Hence eq. (1.2) is also satisfied.

To check that z satisfies eq. (1.3), note that since u(L,t)=0 and $v(L,t)=B_d t$, $z(L,t)=B_d t$. Similarly, one sees that eq. (1.4) is satisfied for x when t=0. Hence, the problem reduces to the determination of solutions to systems II and III.

The solution of System II will be obtained by the method of Separation of Variables. and is straightforward. One obtains the following expression for u:

(1.14) $$u(x,t) = \sum_{n=0}^{\infty} c_n \cos\left[\frac{(2n+1)\pi x}{2L}\right] e^{-Dt(2n+1)^2\pi^2/4L^2}$$

which is the unique solution of our problem when

(1.15) $$c_n = \frac{2}{L}\int_0^L f(x)\cos\frac{(2n+1)\pi x}{2L}\,dx$$

Combining eqs. (1.14) and (1.15), we get our solution for System II

(1.16) $$u(x,t) = \frac{2}{L}\sum_{n=0}^{\infty}\cos\left[\frac{(2n+1)\pi x}{2L}\right]e^{-Dt(2n+1)^2\pi^2/4L^2}\cdot\int_0^L f(x)\cos\frac{(2n+1)\pi x}{2L}\,dx$$

The problem stated by System II appears in many textbooks on PDE's (e.g. Bleecker and Csordas, 1992, p. 159) and the solution above was first presented in a geomorphological context by Culling (1963, p. 146, eq. 38).

Solution of System III

Now we need to find the solution v(x,t) of System III. Define

(1.17) $$w(x,t) = -B_d\, t\cos\frac{\pi x}{L} \quad \text{and}$$

(1.18) $$F(x,t) = -\left[D\left(\frac{\pi}{L}\right)^2 + \frac{1}{t}\right]w(x,t).$$

Suppose φ is a solution to IV:

(1.19) $$A\varphi = F \qquad 0 < x < L;\ 0 < t$$

(1.20) $$\text{b.c.}\quad \left.\frac{\partial\varphi}{\partial x}\right|_{(0,t)} = 0$$

(1.21) $$\varphi(L,t) = 0$$

(1.22) $$\text{i.c.}\quad \varphi(x,0) = 0.$$

System IV

Then

(1.23) $$v = w + \varphi$$

is a solution to III. To see this, note that an easy computation shows that

(1.24) $$Aw = -F,$$

hence

$$Av = Aw + A\varphi = -F + F = 0,$$

reducing the problem to finding the solution to IV.

We will solve System IV - and hence System III - by applying Duhamel's Principle (see for ex., Bleecker and Csordas, 1992, p.174). Essentially, Duhamel's Principle says the following:

Suppose that for each $\tau \geq 0$ we solve the following initial boundary problem

(1.25) $$\frac{\partial \psi}{\partial t} = D\frac{\partial^2 \psi}{\partial x^2} \qquad 0 < x < L;\ \tau < t$$

(1.26) b.c. $$\left.\frac{\partial \psi}{\partial x}\right|_{(0,t)} = 0$$

(1.27) $$\psi(L,t) = 0 \qquad \text{(for all t)}$$

(1.28) i.c. $$\psi(x,\tau) = F(x,\tau) \qquad (t = \tau)$$

System V.

[Note that this gives a parameterized family of functions $\psi(x,t\,;\tau)$]

Then, by putting

(1.29) $$\varphi(x,t) = \int_0^t \psi(x,t\,;\tau)\, d\tau,$$

we obtain a solution to System IV. This reduces the problem to solving System V for each $\tau \geq 0$.

To this end, put

(1.30) $$\xi = t - \tau.$$

Then,

(1.31) $$(A\psi)(t) = 0 \quad \text{for } t > \tau, \text{ if}$$

(1.32) $$(A\psi)(\xi) = 0 \quad \text{for } \xi > 0$$

and

(1.33) $$\psi(x,t)\big|_{t=\tau} = F(x,\tau) \quad \text{if}$$

(1.34) $$\psi(x,\xi)\big|_{\xi=0} = F(x,\tau).$$

Hence, we obtain as before

(1.35) $$\psi(x,\xi) = \sum_{n=0}^{\infty} F_n(\tau)\, \cos\left[\frac{(2n+1)\pi x}{2L}\right] e^{c\,\xi}$$

where

(1.36) $$F_n(\tau) = \frac{2}{L}\int_0^L F(x,\tau)\, \cos\left[\left(\frac{2n+1}{2L}\right)\pi x\right] dx \ , \text{and}$$

(1.37) $$c = -D\left[\frac{\pi}{L}\left(n+\frac{1}{2}\right)\right]^2.$$

Combining Eqs. (1.17) and (1.18) gives

(1.38) $$F(x,\tau) = \left[D\,\tau\left(\frac{\pi}{L}\right)^2 + 1\right] B_d \cos\frac{\pi x}{L} \ .$$

Then F_n, for each value of τ, becomes

(1.39) $$F_n(\tau) = \frac{2}{L}\int_0^L \left[\left[D\,\tau\left(\frac{\pi}{L}\right)^2 + 1\right] B_d\, \cos\frac{\pi x}{L}\right]\ \cos\left[\frac{\pi x}{L}\left(n+\frac{1}{2}\right)\right] dx$$

which gives

(1.40) $$F_n(\tau) = \frac{(-1)^{n+1}\, B_d}{\pi}\left[D\,\tau\left(\frac{\pi}{L}\right)^2 + 1\right]\left(\frac{1}{n-\frac{1}{2}} + \frac{1}{n+\frac{3}{2}}\right).$$

Eq. (1.35) can be written as

(1.41) $$\psi_\tau(x,\ t-\tau) = \sum_{n=0}^{\infty} e^{ct}\, e^{-c\tau}\, F_n(\tau)\, \cos\left[\frac{\pi x}{L}\left(n+\frac{1}{2}\right)\right],$$

and consequently

(1.42) $$\varphi(x,t) = \int_0^t \left[\sum_{n=0}^{\infty} e^{ct}\, e^{-c\tau}\, F_n(\tau)\, \cos\left[\frac{\pi x}{L}\left(n+\frac{1}{2}\right)\right] \right] d\tau \ , \text{or}$$

(1.43) $$\varphi(x,t) = \sum_{n=0}^{\infty} e^{ct}\, \cos\left[\frac{\pi x}{L}\left(n+\frac{1}{2}\right)\right] \int_0^t \left[e^{-c\tau}\, F_n(\tau)\right] d\tau \ , \text{or}$$

(1.44) $$\varphi(x,t) = \sum_{n=0}^{\infty} e^{ct}\, \cos\left[\frac{\pi x}{L}\left(n+\frac{1}{2}\right)\right] \frac{(-1)^{n+1}}{\pi} \left[\frac{1}{n-\frac{1}{2}} + \frac{1}{n+\frac{3}{2}}\right] *$$
$$* \int_0^t \left[e^{-c\tau}\left(1 + D\,\tau\left(\frac{\pi}{L}\right)^2\right) \right] d\tau$$

Putting

(1.45) $$\beta = D\left(\frac{\pi}{L}\right)^2, \text{ and}$$

(1.46) $$\alpha_n = \frac{(-1)^{n+1}}{\pi}\, B_d \left[\frac{1}{n-\frac{1}{2}} + \frac{1}{n+\frac{3}{2}}\right] \ , \text{we get}$$

(1.47) $$\varphi(x,t) = \sum_{n=0}^{\infty} \alpha_n\, e^{ct}\, \cos\left[\frac{\pi x}{L}\left(n+\frac{1}{2}\right)\right] \int_0^t \left[e^{-c\tau}\,(1+\beta\,\tau)\right] d\tau \ , \text{or}$$

(1.48) $$\varphi(x,t) = \sum_{n=0}^{\infty} \alpha_n\, e^{ct}\, \cos\left[\frac{\pi x}{L}\left(n+\frac{1}{2}\right)\right] *$$
$$* \left[\frac{-1}{c}\left(e^{-ct} - 1\right) - \frac{\beta t}{c}\, e^{-ct} - \frac{\beta}{c^2}\left(e^{-ct} - 1\right)\right], \text{ or}$$

$$(1.49) \qquad \varphi(x,t) = \sum_{n=0}^{\infty} \alpha_n \cos\left[\frac{\pi x}{L}\left(n+\frac{1}{2}\right)\right]\left(\frac{-1}{c}\right)\left[\beta t+\left(1-e^{ct}\right)\left(1+\frac{\beta}{c}\right)\right],$$

and this is the solution of System IV.

By putting $\varphi(x,t)$ back into Eq. (1.23), we get the solution $v(x,t)$ of System III

$$(1.50) \qquad v(x,t) = \left(-B_d\, t \cos\frac{\pi x}{L}\right) + \sum_{n=0}^{\infty} \alpha_n \cos\left[\frac{\pi x}{L}\left(n+\frac{1}{2}\right)\right] * \left(\frac{-1}{c}\right)\left[\beta t+\left(1-e^{ct}\right)\left(1+\frac{\beta}{c}\right)\right]$$

We can now use Eq. (1.13) to obtain the solution $z(x,t)$

$$(1.51) \qquad z(x,t) = \sum_{n=0}^{\infty} \cos\left[\frac{\pi x}{L}\left(n+\frac{1}{2}\right)\right]\left[c_n e^{ct}+\left[\alpha_n\left(\frac{-1}{c}\right)\left[\beta t+\left(1-e^{ct}\right)\left(1+\frac{\beta}{c}\right)\right]\right]\right] - B_d\, t \cos\frac{\pi x}{L}$$

and this is the final solution of the problem stated by System I.

References

Bleecker, D. and Csordas, G., *Basic Partial Differential Equations*, Van Nostrand Reinhold, New York, 676p., 1992.

Culling, W. E. H., Soil creep and the development of hillside slopes. *J. Geol.*, 71, 127-161, 1963.

APPENDIX 2

Numerical Analysis

We want to find a numerical solution z(x,t) of Equation 2.1

(2.1) $$\frac{\partial z}{\partial t} = D\frac{\partial^2 z}{\partial x^2},$$

an one dimension, transient, diffusion-type equation, where z is the elevation, x is the distance from the divide, D is the diffusion coefficient, and t is the time. Such solution will be obtained here by Finite Differences through a method generally known as the Explicit Method. A more careful development of this solution can be found in many books that treat numerical solutions of parabolic equations (e.g., Burden and Faires, 1989).

We can consider our domain (x,t) as shown in Figure 1. The boundary conditions are represented by $u(a,t) = u_a$ and $u(b,t) = u_b$, while the initial condition is shown as $u(x,0) = u_0$.

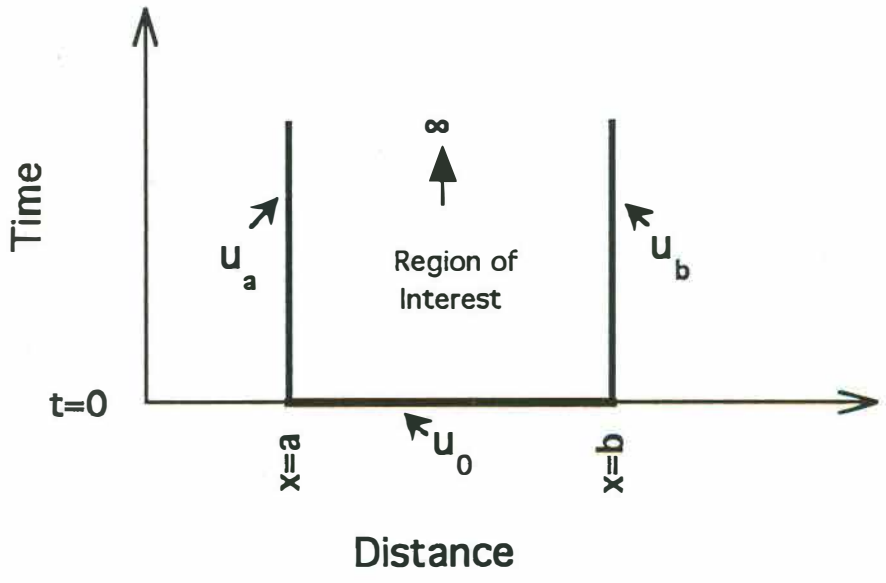

Figure 1 - General scheme of the problem.

Basically, the numerical procedure consists of starting with the initial condition (known values) and advancing the solution through time. For each increment in time, we need to take into consideration the values defined for the boundary conditions.

Suppose the solution u(x,t) was obtained until a time j and now we want to obtain the solution at the next time step, say j+1. The finite difference scheme related to this problem is represented in Figure 2. In other words, we know the values of all points at time j (for example, points B, C, and D) and we want to obtain the value of a point at time j+1 (point A, for example).

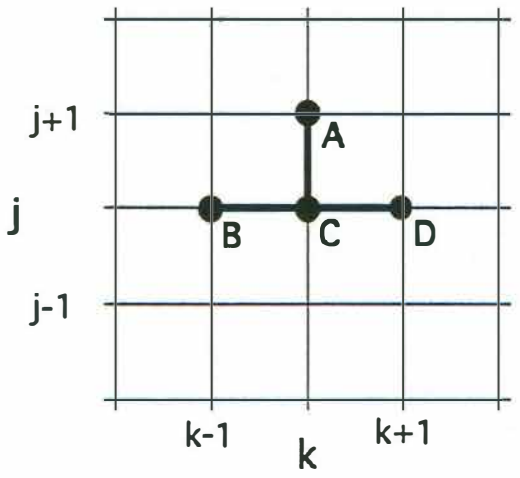

Figure 2 - Finite differences grid of the Explicit Method used here.

By representing $\frac{\partial^2 z}{\partial x^2}$, in Equation 2.1, by a central difference, and $\frac{\partial z}{\partial t}$ by a forward difference we have:

(2.2) $$\frac{\partial^2 z}{\partial x^2} = \frac{u(x+1,t) - 2u(x,t) + u(x-1,t)}{\Delta x^2}$$

(2.3) $$\frac{\partial z}{\partial t} = \frac{u(x,t+1) - u(x,t)}{\Delta t}.$$

Substituting into Equation 2.1 yields

(2.4) $$\frac{u(x,t+1) - u(x,t)}{\Delta t} = D\,\frac{u(x+1,t) - 2u(x,t) + u(x-1,t)}{\Delta x^2},$$

and writing in terms of the subscripts used in Figure 2 (k for x-steps, and j for time-steps) we get

(2.5) $$\frac{u_{k,j+1} - u_{k,j}}{\Delta t} = D\,\frac{u_{k+1,j} - 2u_{k,j} + u_{k-1,j}}{\Delta x^2}\,.$$

Since all those values of u with subscript j are known, the only unknown value in Equation 2.5 is the point u(k,j+1). Solving Equation 2.5 for this value, yields

(2.6) $$u_{k,j+1} = u_{k,j} + \frac{D(\Delta t)}{(\Delta x)^2}\left(u_{k+1,j} - 2u_{k,j} + u_{k-1,j}\right).$$

By looking carefully to Equation 2.6, we can notice that the unknown value was represented in Figure 2 by point A. In other words, Equation 2.6 uses the values of points B, C, and D, which are known, to obtain the solution at point A. This method is called Explicit because the unknowns can be explicitly determined form Equation 2.6.

If D, Δt, and Δx are constants, we can write

(2.7) $$u_{k,j+1} = u_{k,j} + R\left(u_{k+1,j} - 2u_{k,j} + u_{k-1,j}\right)$$

where

(2.8) $$R = \frac{D(\Delta t)}{(\Delta x)^2}\,.$$

Equations 2.7 and 2.8, together with the boundary conditions, can then be used in a computer program (see Appendix 3) to obtain the solution for all points in the region of interest.

The Explicit Method used here has the advantage of being fairly simple. However, to avoid instability problems, it requires that

(2.9) $$\Delta t \leq \frac{(\Delta x)^2}{2D} .$$

References

Burden, R. L. and Faires, J. D., *Numerical Analysis*. PWS-Kent Publ. Co., 729p., 1989.

APPENDIX 3

Computer Programs

The general numerical solution obtained in Appendix 2 was implemented through a series of FORTRAN programs in order to model the evolution of hillslope profiles by diffusive processes. Here, we will present only the principal programs used in the analysis presented in Chapters 1 and 2. One should notice that many small changes were introduced to these basic programs in order to accommodate the variety of hillslope lengths, diffusion coefficients, downcutting rates, boundary condition types, etc, used in all the simulations carried out. The output of these programs is a matrix in which the rows are distance from the divide and the columns are the elevation at various user-defined times.

The output of these programs was inputted into a WINGZ spreadsheet, in which a script was written to perform a variety of analysis on the data generated by the FORTRAN programs. Such analysis included the computation, for every user-defined time,of the slope, curvature, erosion rates and total sediment flux. Both the FORTRAN programming and the WINGZ calculations were carried out in a SunSparcstation.

The basic programs that will be presented here are:

Program RT40 - general program for one-step changes in the diffusion coefficient or in the downcutting rate, presented in Chapter 1. Similar programs were used to model hillslope evolution

under step oscillations (see Chapter 2) in the diffusion coefficient or in the incision rate.

Program SINED10 - general program used when sine oscillations were imposed to the diffusion coefficient (see Chapter 2).

Program SINERD26 - general program used when sine oscillations were imposed to the downcutting rate (see Chapter 2).

Program OXYD07 - general program used when ^{18}O-based oscillations were imposed to the diffusion coefficient (see Chapter 2). Notice that this program reads the file in which the change in the diffusion coefficient with time is stored.

Program OXYRD06 - general program used when ^{18}O-based oscillations were imposed to the downcutting rate (see Chapter 2). Notice that this program reads the file in which the change in the downcutting rate with time is stored.

```
      PROGRAM RT40
c
c           uses the convexity at steady state as the initial condition
c
c           this program solves the diffusion equation UT=D*UXX
c           for dynamic boundary conditions using the explicit method
c
c           L = 100m
c
c     inputs: D, diffusivity value (m2/yr)
c           N, number of x-subintervals
c           H, x-step for each iteration
c           K, time-step for each iteration
c           X1-X3, x-interval (m)
c           X2, mid-point of the interval (m)
c           P(T), left boundary condition
c           Q(T), right boundary condition
c           W, convexity at steady state (with the negative sign)
c           F(X), function expressing initial conditions at the pos. side
c           TMAXI - (20 ka)
c           TMAXF - (1960 ka)
c           DELTAT - (20 ka)
c
c     output: numerical solution at T=TMAX where TMAXI<TMAX<TMAXF, following
c           the time increment DELTAT.
c
c
c
      COMMON U(0:900), V(0:900)
      REAL D,H,K,R,X,T,P,Q,F,RD,W
      DIMENSION ARRAY(50,99)
      INTEGER N,I,TIME, TMAXI, TMAXF
      DATA T,X1,X2,X3/0,-100,0,100/
c
      P(T) = - 85  - (RD * T)
      Q(T) = - 85  - (RD * T)
      F(X) =  40 + (( W/2) * (X**2))
c
      PRINT *, 'ENTER THE CONVEXITY @ STEADY STATE WITH THE MINUS SIGN'
      READ *, W
      PRINT *, 'ENTER RIVER DOWNCUTTING VALUE IN m/yr'
      READ *, RD
      PRINT *, 'ENTER THE DIFFUSIVITY VALUE IN m2/yr'
      READ *, D
      PRINT *, 'ENTER THE NUMBER OF X-SUBINTERVALS AND TIME STEPS'
      READ *, N, K
      H = (X3 - X1) / N
c
c     testing stability condition
c
          IF (K .GT. ((H**2)/(2*D))) THEN
```

```
          PRINT *, 'STABILITY CONDITION WAS NOT SATISFIED'
          ENDIF
c
      R = D * K/(H**2)
      PRINT *, 'ENTER TMAXI, TMAXF, DELTAT'
      READ *, TMAXI, TMAXF, DELTAT
      L=1
c
c     SET INITIAL CONDITION
      DO 10 I = 0, N
          X= X1 + I * H
            V(I) = F(X)
 10   CONTINUE
c
c
c     SET THE OUTER LOOP TO DEFINE THE MAXIMUM TIME FOR WHICH THE
c     SOLUTION WILL BE OBTAINED
c
c
      DO 20 TIME = TMAXI, TMAXF, DELTAT
c
c     FINITE DIFFERENCE FUNCTION TO SOLVE THE UNKNOWNS U(I)
c     AT T=K+1 USING V(I) KNOWN AT T=K
c
 15     DO 30 I = 1, N-1
         U(I)=V(I) + R*(V(I+1) - 2*V(I) + V(I-1))
 30     CONTINUE
c
c     INCREASE TIME BY K
c
        T = T + K
c
c     OBTAIN THE VALUES OF U(0) AND U(N), USING THE BOUNDARY
c     CONDITION, TO COMPLETE THE ARRAY U(I) AT T=K+1
c
        U(0) = P(T)
        U(N) = Q(T)
c
c     WRITE U OVER V TO PREPARE FOR NEXT STEP
        DO 40 I = 0, N
          V(I) = U(I)
 40       CONTINUE
c
c     IF T IS LESS THAN TIME, TAKE A TIME STEP
c
        IF (ABS (TIME - T) .GT. K/4) GO TO 15
c
c     assign the first column
c
        IF (ABS (TIME - TMAXI) .LT. K/4) THEN
          DO 50 J = 0,N
```

```
            X=X1+J*H
            ARRAY(J,L)=X
 50         CONTINUE
          ENDIF
c
c     assigning the elevation values
c
      L=L+1
      DO 60 J=0,N
           ARRAY(J,L)=U(J)
 60   CONTINUE
 20   CONTINUE
      OPEN(1, FILE='rt40.dat')
      DO 70 J=0,N
           WRITE(1,130) (ARRAY(J,L), L=1,99)
 70   CONTINUE
130   FORMAT(99F15.6)
      END
```

```
      PROGRAM SINED10
c
c
c           uses the convexity at steady state as the initial condition
c
c           used to compute the relaxation time Rt
c
c           this program solves the diffusion equation UT=D*UXX
c           for dynamic boundary conditions using the explicit method
c
c           use sine changes in the diffusion coefficient
c
c           the user defines the period and the amplitude of
c           the oscillation
c
c           L = 25 m
c
c     inputs: D1, smaller diffusivity value (m2/yr)
c           D2, greater diffusivity value (m2/yr)
c           D(T), sine function of the diff. coeffic.; it defines
c                 the new diff. coeffic. at each time step.
c           RD baselevel downcutting (m/yr)
c           A, amplitude = (D2-D1) / 2
c           PER, period of the sine function
c           AF , angular frequency = (2*pi)/PER
c           N, number of x-subintervals
c           H, x-step for each iteration
c           K, time-step for each iteration
c           X1-X3, x-interval (m)
c           X2, mid-point of the interval (m)
c           P(T), left boundary condition
c           Q(T), right boundary condition
c           W, convexity at steady state (with the negative sign) for
c                 the initial condition
c           F(X), function expressing initial conditions at the pos. side
c           TMAXI - (user-defined)
c           TMAXF - (user-defined)
c           DELTAT - (user-defined)c
c     output: numerical solution at T=TMAX where TMAXI<TMAX<TMAXF, following
c           the time increment DELTAT.
c
c
c
      COMMON U(0:900), V(0:900)
      REAL D,H,K,R,X,T,F,D1,D2,RD,W,PER,A,AF
      DIMENSION ARRAY(50,300)
      INTEGER N,I,TIME, TMAXI, TMAXF
      DATA T,X1,X2,X3/0,-25,0,25/
c
c     function defining the boundary conditions
c
```

```
      P(T) =  12.1875  - (RD * T)
      Q(T) =  12.1875  - (RD * T)
c
c
c     function defining the oscillating diffusion coefficient
c
      D(T)= ((A*SIN((AF*T)-(PI/2)))+(D1+A))
c
c
c     function defining the initial condition
      F(X) =  20 + (( W/2) * (X**2))
c
c
c     function defining the R value for each time step
c
      R(T) = D(T) * K/(H**2)
c
c
      PRINT *, 'ENTER THE CONVEXITY @ STEADY STATE WITH THE MINUS SIGN'
      READ *, W
      PRINT *, 'ENTER THE PERIOD OF THE SINE FUNCTION, IN YEARS'
      READ *, PER
      PRINT *, 'ENTER THE SMALLER AND GREATER DIFF. COEFF. VALUES IN m2/yr'
      READ *, D1, D2
      PRINT *, 'ENTER THE RIVER DOWNCUTTING IN m/yr'
      READ *, RD
      PRINT *, 'ENTER THE NUMBER OF X-SUBINTERVALS AND TIME STEPS'
      READ *, N, K
      PI = 4 * ATAN(1.)
      H = (X3 - X1) / N
c
      AF = (2*PI) / PER
      A = (D2-D1) / 2
c
c
c     testing stability condition
c
          IF (K .GT. ((H**2)/(2*D1))) THEN
          PRINT *, 'STABILITY CONDITION WAS NOT SATISFIED WITH D1'
          ENDIF
          IF (K .GT. ((H**2)/(2*D2))) THEN
          PRINT *, 'STABILITY CONDITION WAS NOT SATISFIED WITH D2'
          ENDIF
c
c
      PRINT *, 'ENTER TMAXI, TMAXF, DELTAT'
      READ *, TMAXI, TMAXF, DELTAT
      L=1
c
c     SET INITIAL CONDITION
      DO 10 I = 0, N
```

```
          X= X1 + I * H
            V(I) = F(X)
 10   CONTINUE
c
c
c     SET THE OUTER LOOP TO DEFINE THE MAXIMUM TIME FOR WHICH THE
c     SOLUTION WILL BE OBTAINED
c
c
      DO 20 TIME = TMAXI, TMAXF, DELTAT
c
c     FINITE DIFFERENCE FUNCTION TO SOLVE THE UNKNOWNS U(I)
c     AT T=K+1 USING V(I) KNOWN AT T=K
c
 15     DO 30 I = 1, N-1
         U(I)=V(I) + R(T)*(V(I+1) - 2*V(I) + V(I-1))
 30     CONTINUE
c
c     INCREASE TIME BY K
c
        T = T + K
c
c     OBTAIN THE VALUES OF U(0) AND U(N), USING THE BOUNDARY
c     CONDITION, TO COMPLETE THE ARRAY U(I) AT T=K+1
c
        U(0) = P(T)
        U(N) = Q(T)
c
c
c     WRITE U OVER V TO PREPARE FOR NEXT STEP
          DO 40 I = 0, N
            V(I) = U(I)
 40       CONTINUE
c
c     IF T IS LESS THAN TIME, TAKE A TIME STEP
c
          IF (ABS (TIME - T) .GT. K/4) GO TO 15
c
c     assign the first column
c
          IF (ABS (TIME - TMAXI) .LT. K/4) THEN
            DO 50 J = 0,N
              X=X1+J*H
              ARRAY(J,L)=X
 50           CONTINUE
          ENDIF
c
c     assigning the elevation values
c
      L=L+1
      DO 60 J=0,N
```

```
          ARRAY(J,L)=U(J)
 60    CONTINUE
 20    CONTINUE
       OPEN(1, FILE='sineD10.dat')
       DO 70 J=0,N
          WRITE(1,130) (ARRAY(J,L), L=1,300)
 70    CONTINUE
130    FORMAT(300F15.6)
       END
```

```
      PROGRAM SINERD26
c
c
c           uses the convexity at steady state as the initial condition
c
c           used to compute the relaxation time Rt
c
c           this program solves the diffusion equation UT=D*UXX
c           for dynamic boundary conditions using the explicit method
c
c           use sine changes as boundary conditions
c
c           the user defines the period and the amplitude of
c           the oscillation
c
c           L = 25 m
c
c     inputs: D, diffusivity value (m2/yr)
c           RD1, smaller baselevel downcutting (m/yr)
c           RD2, greater baselevel downcutting (m/yr)
c           RD(T), sine function of the baselevel downcutting; it is used
c                to define the new boundary condition at each time step
c           A, amplitude = (RD2-RD1) / 2
c           PER, period of the sine function
c           AF , angular frequency = (2*pi)/PER
c           N, number of x-subintervals
c           H, x-step for each iteration
c           K, time-step for each iteration
c           X1-X3, x-interval (m)
c           X2, mid-point of the interval (m)
c           P(T), left boundary condition
c           Q(T), right boundary condition
c           W, convexity at steady state (with the negative sign)
c           F(X), function expressing initial conditions at the pos. side
c           TMAXI - (user-defined)
c           TMAXF - (user-defined)
c           DELTAT - (user-defined)
c
c     output: numerical solution at T=TMAX where TMAXI<TMAX<TMAXF, following
c           the time increment DELTAT.
c
c
c
      COMMON U(0:900), V(0:900)
      REAL D,H,K,R,X,T,F,RD1,RD2,W,PER,A,AF
      DIMENSION ARRAY(50,300)
      INTEGER N,I,TIME, TMAXI, TMAXF
      DATA T,X1,X2,X3/0,-25,0,25/
c
c     function defining the oscillating boundary condition
c
```

```
      RD(T)= ((A*SIN((AF*T)-(PI/2)))+(RD1+A))
c
c
c     function defining the initial condition                    c
      F(X) =  20 + (( W/2) * (X**2))
c
c
      PRINT *, 'ENTER THE CONVEXITY @ STEADY STATE WITH THE MINUS SIGN'
      READ *, W
      PRINT *, 'ENTER THE PERIOD OF THE SINE FUNCTION, IN YEARS'
      READ *, PER
      PRINT *, 'ENTER THE SMALLER AND GREATER DOWNCUTTING VALUE IN m/yr'
      PRINT *, 'ENTER THE DIFFUSIVITY VALUE IN m2/yr'
      READ *, D
      PRINT *, 'ENTER THE NUMBER OF X-SUBINTERVALS AND TIME STEPS'
      READ *, N, K
      PI = 4 * ATAN(1.)
      H = (X3 - X1) / N
c
      AF = (2*PI) / PER
      A = (RD2-RD1) / 2
c
c
c     testing stability condition
c
          IF (K .GT. ((H**2)/(2*D))) THEN
          PRINT *, 'STABILITY CONDITION WAS NOT SATISFIED'
          ENDIF
c
      R = D * K/(H**2)
      PRINT *, 'ENTER TMAXI, TMAXF, DELTAT'
      READ *, TMAXI, TMAXF, DELTAT
      L=1
c
c     SET INITIAL CONDITION
      DO 10 I = 0, N
           X= X1 + I * H
             V(I) = F(X)
 10   CONTINUE
c
c
c     SET THE OUTER LOOP TO DEFINE THE MAXIMUM TIME FOR WHICH THE
c     SOLUTION WILL BE OBTAINED
c
c
      DO 20 TIME = TMAXI, TMAXF, DELTAT
c
c     FINITE DIFFERENCE FUNCTION TO SOLVE THE UNKNOWNS U(I)
c     AT T=K+1 USING V(I) KNOWN AT T=K
c
 15     DO 30 I = 1, N-1
```

```
          U(I)=V(I) + R*(V(I+1) - 2*V(I) + V(I-1))
 30       CONTINUE
c
c     INCREASE TIME BY K
c
          T = T + K
c
c     OBTAIN THE VALUES OF U(0) AND U(N), USING THE BOUNDARY
c     CONDITION, TO COMPLETE THE ARRAY U(I) AT T=K+1
c
          U(0) = V(0) - (RD(T) * K)
          U(N) = V(N) - (RD(T) * K)
c
c
c     WRITE U OVER V TO PREPARE FOR NEXT STEP
          DO 40 I = 0, N
            V(I) = U(I)
 40         CONTINUE
c
c     IF T IS LESS THAN TIME, TAKE A TIME STEP
c
          IF (ABS (TIME - T) .GT. K/4) GO TO 15
c
c     assign the first column
c
          IF (ABS (TIME - TMAXI) .LT. K/4) THEN
            DO 50 J = 0,N
              X=X1+J*H
              ARRAY(J,L)=X
 50           CONTINUE
          ENDIF
c
c     assigning the elevation values
c
     L=L+1
     DO 60 J=0,N
          ARRAY(J,L)=U(J)
 60   CONTINUE
 20   CONTINUE
     OPEN(1, FILE='sinerd26.dat')
     DO 70 J=0,N
          WRITE(1,130) (ARRAY(J,L), L=1,300)
 70   CONTINUE
 130  FORMAT(300F15.6)
     END
```

```
      PROGRAM OXYD07
c
c
c           uses the convexity at steady state as the initial condition
c
c           used to compute the relaxation time Rt
c
c           this program solves the diffusion equation UT=D*UXX
c           for dynamic boundary conditions using the explicit method
c
c           uses sine oscillations in the diffusion coefficient
c           based on the 18 oxyg. curve
c
c           this run uses D=80 for today and D=40 for 15Ka BP
c
c           it reads these values from an input file
c
c           the user defines the period and the amplitude of
c           the oscillation
c
c           the boundary conditions as linearly dependent on time
c
c           hillslope length=25m
c
c     inputs: DA, diffusion coefficient value (m2/yr)
c           DI(T), sine function of the diff. coeffic.; it defines
c                the new diff. coeffic. at each time step.
c           RD baselevel downcutting (m/yr)
c           N, number of x-subintervals
c           H, x-step for each iteration
c           K, time-step for each iteration
c           X1-X3, x-interval (m)
c           X2, mid-point of the interval (m)
c           P(T), left boundary condition
c           Q(T), right boundary condition
c           W, convexity at steady state (with the negative sign) for
c                the initial condition
c           F(X), function expressing initial conditions at the pos. side
c           TMAXI - (user-defined)
c           TMAXF - (user-defined)
c           DELTAT - (user-defined)
c
c     output: numerical solution at T=TMAX where TMAXI<TMAX<TMAXF, following
c           the time increment DELTAT.
c
c
c
      REAL DA,H,K,R,X,T,F,RD,W,TI(15000),DI(15000)
      REAL ARRAY(0:50,300),U(0:100),V(0:100)
      INTEGER N,I,TIME, TMAXI, TMAXF, DELTAT
```

```
      DATA T,X1,X2,X3/0,-25,0,25/
c
c     function defining the boundary conditions
c
      P(T) = 12.1875  - (RD * T)
      Q(T) = 12.1875  - (RD * T)
c
c
c     function defining the initial condition
c
      F(X) =  20 + (( W/2) * (X**2))
c
c
c     function defining the R value for each time step
c
      R(DA) = DA * K/(H**2)
c
c
      OPEN(1,FILE='d(40-80).out')
c
c
      PRINT *, 'ENTER THE CONVEXITY @ STEADY STATE WITH THE MINUS SIGN'
      READ *, W
      PRINT *, 'ENTER THE RIVER DOWNCUTTING IN m/yr'
      READ *, RD
      PRINT *, 'ENTER THE NUMBER OF X-SUBINTERVALS AND TIME STEPS'
      READ *, N, K
      H = (X3 - X1) / FLOAT(N)
c
c
      PRINT *, 'ENTER TMAXI, TMAXF, DELTAT'
      READ *, TMAXI, TMAXF, DELTAT
      L=1
c
c     SET INITIAL CONDITION
      DO 10 I = 0, N
          X= X1 + FLOAT(I) * H
            V(I) = F(X)
 10   CONTINUE
c
c
c     SET THE OUTER LOOP TO DEFINE THE MAXIMUM TIME FOR WHICH THE
c     SOLUTION WILL BE OBTAINED
c
c
c
c     READ THE INPUT FILE
c
     DO 25 M = 1,9801
          READ(1,*) TI(M), DI(M)
 25   CONTINUE
```

```
c
c
      M=1
c
      DO 20 TIME = TMAXI, TMAXF, DELTAT
c
c     FINITE DIFFERENCE FUNCTION TO SOLVE THE UNKNOWNS U(I)
c     AT T=K+1 USING V(I) KNOWN AT T=K
c
c
 15   DA=DI(M)
c
c
        DO 30 I = 1, N-1
          U(I)=V(I) + R(DA)*(V(I+1) - 2*V(I) + V(I-1))
 30     CONTINUE
c
c     INCREASE TIME BY K
c
        T = T + K
c
        M = M + 1
c
c     OBTAIN THE VALUES OF U(0) AND U(N), USING THE BOUNDARY
c     CONDITION, TO COMPLETE THE ARRAY U(I) AT T=K+1
c
        U(0) = P(T)
        U(N) = Q(T)
c
c
c     WRITE U OVER V TO PREPARE FOR NEXT STEP
          DO 40 I = 0, N
            V(I) = U(I)
 40       CONTINUE
c
c     IF T IS LESS THAN TIME, TAKE A TIME STEP
c
          IF (ABS (FLOAT(TIME) - T) .GT. K/4.) GO TO 15
c
c     assign the first column
c
          IF (ABS (FLOAT(TIME - TMAXI)) .LT. K/4.) THEN
            DO 50 J = 0,N
              X=X1+J*H
              ARRAY(J,L)=X
 50           CONTINUE
          ENDIF
c
c     assigning the elevation values
c
     L=L+1
```

```
      DO 60 J=0,N
           ARRAY(J,L)=U(J)
60    CONTINUE
20    CONTINUE
      OPEN(2, FILE='oxyd07.dat')
      DO 70 J=0,N
           WRITE(2,130) (ARRAY(J,L), L=1,300)
70    CONTINUE
130   FORMAT(300F15.6)
      CLOSE(1)
      CLOSE(2)
      END
```

```
      PROGRAM OXYRD06
c
c
c           uses the convexity at steady state as the initial condition
c
c           used to compute the relaxation time Rt
c
c           this program solves the diffusion equation UT=D*UXX
c           for dynamic boundary conditions using the explicit method
c
c           uses the oxygen 18 curve as boundary conditions
c
c           hillslope length = 25m
c
c     inputs: D, diffusivity value (m2/yr)
c           RDI(T), oxyg. 18 derived values for the baselevel downcutting;
c           it is used to define the new boundary condition at each time st
c           N, number of x-subintervals
c           H, x-step for each iteration
c           K, time-step for each iteration
c           X1-X3, x-interval (m)
c           X2, mid-point of the interval (m)
c           P(T), left boundary condition
c           Q(T), right boundary condition
c           W, convexity at steady state (with the negative sign)
c           F(X), function expressing initial conditions at the pos. side
c           TMAXI - (user-defined)
c           TMAXF - (user-defined)
c           DELTAT - (user-defined)
c
c     output: numerical solution at T=TMAX where TMAXI<TMAX<TMAXF, following
c           the time increment DELTAT.
c
c
c
      REAL D,H,K,R,X,T,F,RD,W,TI(15000),RDI(15000)
      REAL ARRAY(0:50,300),U(0:100),V(0:100)
      INTEGER M,N,I,TIME, TMAXI, TMAXF,DELTAT
      DATA T,X1,X2,X3/0,-25,0,25/
c
c
c
c     function defining the initial condition                    c
      F(X) =  20 + (( W/2) * (X**2))
c
      OPEN(1,FILE='rd(1-3x10-4).out.new')

c
      PRINT *, 'ENTER THE CONVEXITY @ STEADY STATE WITH THE MINUS SIGN'
      READ *, W
```

```
      PRINT *, 'ENTER THE DIFFUSIVITY VALUE IN m2/yr'
      READ *, D
      PRINT *, 'ENTER THE NUMBER OF X-SUBINTERVALS AND TIME STEPS'
      READ *, N, K
      H = (X3 - X1) / N
c
c
c
c     testing stability condition
c
           IF (K .GT. ((H**2)/(2*D))) THEN
           PRINT *, 'STABILITY CONDITION WAS NOT SATISFIED'
           ENDIF
c


      R = D * K/(H**2)



      PRINT *, 'ENTER TMAXI, TMAXF, DELTAT'
      READ *, TMAXI, TMAXF, DELTAT
      L=1
c
c     SET INITIAL CONDITION
      DO 10 I = 0, N
           X= X1 + I* H
             V(I) = F(X)
 10    CONTINUE
c
c
c
c     READ THE INPUT FILE
c
      DO 25 M = 1,9801
           READ(1,*) TI(M), RDI(M)
 25    CONTINUE


      M=1

c
c


      V(0)= 12.1875
      V(N)= 12.1875


c     SET THE OUTER LOOP TO DEFINE THE MAXIMUM TIME FOR WHICH THE
c     SOLUTION WILL BE OBTAINED
c
```

```
c
      DO 20 TIME = TMAXI, TMAXF, DELTAT
c
c     FINITE DIFFERENCE FUNCTION TO SOLVE THE UNKNOWNS U(I)
c     AT T=K+1 USING V(I) KNOWN AT T=K


c
 15     DO 30 I = 1, N-1
        U(I)=V(I) + R*(V(I+1) - 2*V(I) + V(I-1))
 30     CONTINUE
c
c     INCREASE TIME BY K
c
       T = T + K

       M = M + 1
c
c     OBTAIN THE VALUES OF U(0) AND U(N), USING THE BOUNDARY
c     CONDITION, TO COMPLETE THE ARRAY U(I) AT T=K+1


      RD=RDI(M)

c
       U(0) = V(0) - (RD * K)
       U(N) = V(N) - (RD * K)
c
c
c     WRITE U OVER V TO PREPARE FOR NEXT STEP
         DO 40 I = 0, N
           V(I) = U(I)
 40        CONTINUE
c
c     IF T IS LESS THAN TIME, TAKE A TIME STEP
c
         IF (ABS (TIME - T) .GT. K/4) GO TO 15
c
c     assign the first column
c
         IF (ABS (TIME - TMAXI) .LT. K/4) THEN
           DO 50 J = 0,N
             X=X1+J*H
             ARRAY(J,L)=X
 50          CONTINUE
         ENDIF
c
c     assigning the elevation values
c
      L=L+1
      DO 60 J=0,N
```

```
          ARRAY(J,L)=U(J)
 60    CONTINUE
 20    CONTINUE
       OPEN(2, FILE='oxyrd06.dat')
       DO 70 J=0,N
          WRITE(2,130) (ARRAY(J,L), L=1,300)
 70    CONTINUE
130    FORMAT(300F15.6)
       CLOSE(1)
       CLOSE(2)
       END
```

APPENDIX 4

Dimensional Analysis

The dimensional analysis carried out in this study was based on a technique known as the Buckingham's Pi Theorem (see for ex., Dim and Ivey, 1980). The variables and fundamental dimensions in our problem are:

VARIABLE	SYMBOL	DIMENSION
Hillslope length	L	L
Diffusion coefficient	D	L^2/T
Baselevel downcutting rate	B_d	L/T
Initial curvature	W_i	1/L
Relaxation time	R_t	T

[where L is length and T is time].

Because we have 5 variables and 2 dimensions we need 3 dimensionless parameters to fully describe the problem. When we choose D and L among the derived variables, and permute the remaining 3 variables (W_i, R_t, and B_d) we get the following 3 dimensionless groups:

$$(4.1) \qquad \prod_1 = D^{a1} L^{b1} W_i = \left(\frac{\mathcal{L}^2}{\mathcal{T}}\right)^{a1} \mathcal{L}^{b1} \frac{1}{\mathcal{L}}$$

$$(4.2) \qquad \prod_2 = D^{a2}\, L^{b2}\, R_t = \left(\frac{\mathcal{L}^2}{\mathcal{T}}\right)^{a2} \mathcal{L}^{b2}\, \mathcal{T}$$

$$(4.3) \qquad \prod_3 = D^{a3}\, L^{b3}\, B_d = \left(\frac{\mathcal{L}^2}{\mathcal{T}}\right)^{a3} \mathcal{L}^{b3}\, \frac{\mathcal{L}}{\mathcal{T}}.$$

Solving for the exponents, yields:

$$(4.4) \qquad \prod_1 \Rightarrow \begin{Bmatrix} \mathcal{L} \rightarrow 2a_1 + b_1 - 1 = 0 \\ \mathcal{T} \rightarrow -a_1 \qquad\quad = 0 \end{Bmatrix} \Rightarrow a_1 = 0;\ b_1 = 1\,,$$

$$(4.5) \qquad \prod_2 \Rightarrow \begin{Bmatrix} \mathcal{L} \rightarrow 2a_2 + b_2 = 0 \\ \mathcal{T} \rightarrow -a_2 + 1 = 0 \end{Bmatrix} \Rightarrow a_2 = 1;\ b_2 = -2\,,$$

$$(4.6) \qquad \prod_3 \Rightarrow \begin{Bmatrix} \mathcal{L} \rightarrow 2a_3 + b_3 + 1 = 0 \\ \mathcal{T} \rightarrow -a_3 - 1 \qquad = 0 \end{Bmatrix} \Rightarrow a_3 = -1;\ b_3 = 1.$$

Putting the exponents back into Eqs. (4.1 - 4.3) yields the following dimensionless parameters:

$$(4.7) \qquad \prod_1 = D^0\, L^1\, W_i = W_i\, L\,,$$

$$(4.8) \qquad \prod_2 = D^1\, L^{-2}\, R_t = \frac{D\, R_t}{L^2}\,,$$

$$(4.9) \qquad \prod_3 = D^{-1}\, L^1\, B_d = \frac{B_d}{D} L = W_f\, L$$

(where W_f is the final hillslope curvature, or the hillslope curvature at the equilibrium condition).

References

Dym, C. L. and Ivey, E. S., *Principles of Mathematical Modeling*. Academic Press, New York, 260p., 1980.